Network Factors for Idiosyncratic Volatility Spillover *

Belinda (Chen) Chen†

March 8, 2025

Abstract

I develop a dynamic production-based network model to examine the economic and asset pricing implications of inter-sector idiosyncratic volatility spillovers. I introduce two time-series factors to capture time-varying structural changes in idiosyncratic volatility spillovers and show that they shape the persistent dynamics of aggregate volatility in equilibrium and are priced as volatility risk factors. Empirically, I construct these factors using stock data and show that they predict future aggregate volatility in the direction implied by the model. Consistent with the model, long-short portfolios formed on these factors generate return spreads unexplained by existing factor models.

Keywords: Idiosyncratic Volatility Spillover, Contagion Risk, Supplier Customer Network

*I would like to express my deepest gratitude to Professors Tim Johnson and Dana Kiku. I am also grateful for the insightful comments and suggestions from Bernard Herskovic, Mahyar Kargar, Neil Pearson, George Pennacchi, Sébastien Planté, John Shim, Collin Ward, Dacheng Xiu, Jun Pan, Adlai Fisher, Hengjie Ai, Serhiy Kozak, Pete Kyle and Vojislav Maksimovic. Additionally, I have greatly benefited from feedback received at seminars and conferences, including UIUC, AFA, NFA, FMA, UChicago MFR, LBS TADC, USC, UBC, UCSD, UW-Madison, UMD, UAlberta, NUS, SMU, SAIF, Fudan, and Tsinghua SEM. All errors are my own.

†Gies College of Business, University of Illinois at Urbana-Champaign; Email: chenc16@illinois.edu

1 Introduction

Volatility is central to finance, as it is a key component in determining how risk is priced in financial markets. Financial market volatility can be categorized into two types: aggregate volatility, which reflects overall uncertainty, and idiosyncratic volatility, which reflects firm-specific risks. There are unresolved questions regarding both types of volatility. Aggregate volatility has significant economic implications,[1] yet its origins remain largely unexplored. Much of the existing literature either treats it as a given or attributes it to aggregate shocks without addressing its microfoundations.[2] Idiosyncratic volatility, often measured by the volatility of benchmark-adjusted stock returns, presents its own empirical puzzle. Herskovic, Kelly, Lustig, and Van Nieuwerburgh (2016) show that firms' idiosyncratic volatilities exhibit persistent co-movement, which is priced—a surprising result given that most theories suggest firm-specific risks should be diversifiable and unpriced. Although Herskovic et al. (2016) attribute this common factor to household income risk, their explanation does not fully account for the observed comovement, suggesting the presence of additional channels.

Therefore, this paper aims to provide a unified model that not only clarifies the microfoundations of aggregate volatility but also offers an alternative explanation for the comovement in idiosyncratic volatilities. The approach to establishing such a unified model is to link aggregate and idiosyncratic volatility through a network perspective. Specifically, it investigates how the dynamic evolution of pairwise idiosyncratic volatility spillovers, stemming from a time-varying input-output network, shapes the persistent dynamics of aggregate volatility.

The network literature has shown that under certain network distribution assumptions, idiosyncratic risks may not be fully diversified away and can instead accumulate into aggregate risk. For

[1] For example, Bloom, Bond, and Van Reenen (2007) demonstrate that aggregate volatility influences firms' investment decisions.

[2] However, one exception is Gabaix (2011), who shows that aggregate volatility can arise from firm-specific shocks when the firm size distribution has a heavy tail and large firms suffer from extremely large firm-specific shocks.

example, Acemoglu, Carvalho, Ozdaglar, and Tahbaz-Salehi (2012) show that the real-world input-output network exhibits an asymmetric structure, hindering the quick diversification of idiosyncratic risks. However, two key elements have been overlooked in prior network research.

First, the supplier-customer chain links all aspects of firm fundamentals—not only first-moment fundamentals like cash flows and stock returns but also second-moment fundamentals such as idiosyncratic volatilities, which are a function of the first moment. Second-moment connections are crucial for understanding risk transmission and how risk is priced. However, no study has examined firms' networks from a second-moment perspective, specifically through the lens of idiosyncratic volatility spillovers.

Second, the dynamic evolution of firms' networks and the implications of idiosyncratic risks for the dynamics of aggregate volatility—and therefore for asset prices—have been largely overlooked. For example, Acemoglu et al. (2012) examine a static production-based network and analyze how the cross-sectional distribution of a network structure affects the speed of risk diversification. However, without considering the time-series dynamics of network structure changes, there are no testable model implications and, consequently, no empirical evidence on how network might influence the time-series behavior of aggregate volatility and, in turn, asset prices.

Moreover, the dynamics of network themselves warrant further study. Firms' trade network not only relies heavily on past relationships but can also be fundamentally altered by technological shocks or other factors. For instance, in recent years, semiconductors have replaced silicon-based materials as more important inputs to the electronics sector. These network changes can reflect technological shocks or shifts in market fundamentals. Therefore, it is essential to study network within a dynamic setting.[3]

Building on these insights, this paper provides the first analysis of firms' network from both a

[3]Herskovic (2018) explore a dynamic input-output network structure, assuming i.i.d. structural changes with no temporal dependency and focusing mainly on first-moment implications.

second-moment perspective and as a dynamic system. It demonstrates how the dynamic evolution of idiosyncratic volatility spillovers drives long-run aggregate volatility and affects the cross-section of assets. This paper derives testable network implications from a model and is the first to empirically demonstrate both the predictability of idiosyncratic risks for future aggregate volatility and their pricing due to spillover effects through the network.

I begin by developing a dynamic production-based multi-sector model. Each sector is modeled as a representative firm, and I use the terms 'sector' and 'firm' interchangeably.[4] At every time t, each sector uses outputs from other sectors as inputs, with input weights determined exogenously. A representative household consumes final goods from all sectors. Sectors experience independent, normally distributed productivity shocks, which are referred to as idiosyncratic shocks. These shocks initially affect the final output of each product and subsequently spill over to influence other sectors' investment decisions or propagate through the common household.

In equilibrium, after sectors and the household behave optimally, the interconnections among all sectors are determined. These interconnections exist not only at the first moment—i.e., stock prices—but also at the second moment—i.e., idiosyncratic volatilities. Over time, the network weights follow a stochastic process (which aligns with the data), where shocks reflect exogenous technological changes. Consequently, the interconnections between sectors evolve over time.

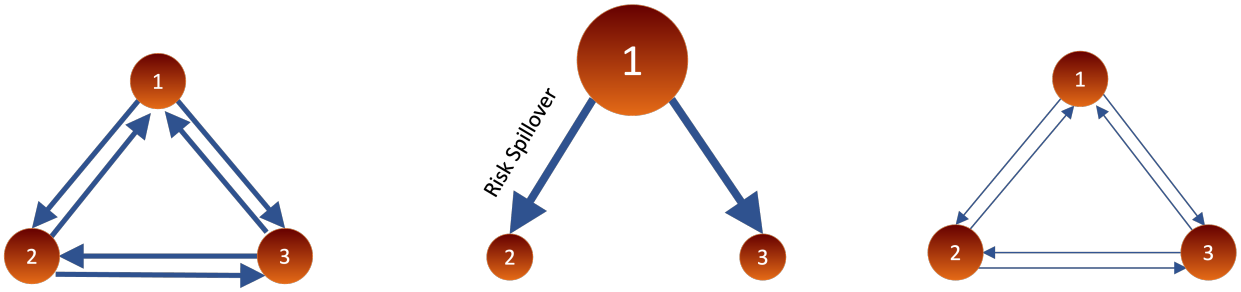
My main focus is on changes in the second-moment connection structure. Since this structure is complex, characterized by an $n \times n \times T$ matrix, I perform a dimension reduction exercise. Specifically, I introduce two well-defined factors, *Risk-Intensity* (*INT*) and *Risk-Dominance* (*DOM*), to summarize the dynamic changes in pairwise idiosyncratic volatility spillovers. In equilibrium, I show that both factors influence the speed of risk diversification at each cross-section and exert long-term effects on the dynamics of aggregate volatility. Additionally, I demonstrate that both

[4] A sector can be interpreted as the value-weighted average of multiple homogeneous firms producing the same product. When the number of sectors, n, becomes sufficiently large, each sector effectively represents a single firm.

time-series factors are priced as volatility risk factors.

To illustrate the definition and key implications of these network factors, I use a three-sector economy as an example. (The risk diversification idea should be examined under infinitely many sectors; therefore, these figures are intended to illustrate the basic intuition, which should be applied in the limit as $n \to \infty$.) Figure 1 visualizes three different patterns of idiosyncratic volatility spillovers, with each panel representing a different economic state.

Figure 1. Illustrative Examples of Inter-Sector Idiosyncratic Volatility Spillovers
This figure presents three panels illustrating inter-sector idiosyncratic volatility spillovers within the economy across three states. Panel A represents a state with high *Risk-Intensity* and low *Risk-Dominance*. Panel B depicts a state with both high *Risk-Intensity* and high *Risk-Dominance*. Panel C represents a state with low *Risk-Intensity* and low *Risk-Dominance*.



High *Risk-Intensity*
Low *Risk-Dominance*
Panel A

High *Risk-Intensity*
High *Risk-Dominance*
Panel B

Low *Risk-Intensity*
Low *Risk-Dominance*
Panel C

In these panels, each node represents a sector, and each directional linkage represents an idiosyncratic volatility spillover. A thicker linkage indicates greater spillover intensity (i.e., an idiosyncratic shock in one sector has a larger spillover effect on another sector), while a larger node size represents greater overall spillover intensity from that sector to all others (i.e., an idiosyncratic shock in one sector has a broader impact across the entire economy).

The *DOM* and *INT* factors describe the distribution of node sizes and linkage thicknesses, respectively. The *INT* factor captures the average thickness of all linkages, representing the mean

pairwise risk spillover magnitude. The *DOM* factor measures the concentration of node sizes, indicating the extent to which a few selected sectors dominate risk spillovers.

In Figure 1, Panels A and C represent two states where the *DOM* factor is the same (i.e., the node size concentrations are equal), but the *INT* factor differs (i.e., Panel A has thicker linkages on average than Panel C). In contrast, Panels A and B depict states with the same *INT* factor (i.e., equivalent average linkage thicknesses), but the *DOM* factor varies (i.e., Panel B has a higher *DOM* due to a greater concentration of node sizes).

When *DOM* is held constant (comparing Panel A with Panel C), the model predicts that higher *INT* leads to an increase in aggregate volatility. Intuitively, *INT* reflects the overall connection strength across sectors—it is low when the market is relatively segmented and high when sectors are tightly linked. For example, during the late 1990s, when the internet first became widely accessible to the public, connections between sectors grew stronger, potentially leading to an increase in the *INT* factor. When *INT* is high, all sectors exert a strong influence on one another. As a result, idiosyncratic shocks to any one sector propagate fully to another, then to the next, and quickly become amplified through the network, ultimately adding up to greater aggregate volatility.

When *INT* is constant (comparing Panel A with Panel B), the model predicts that an increase in *DOM* leads to a decline in aggregate volatility. Intuitively, *DOM* captures the differences between normal times and recessions. During normal times, certain central sectors, such as the financial or information sector, serve as the primary risk propagators in the economy, while peripheral sectors exert minimal influence on others, resulting in a state where *DOM* is high. In contrast, during downturns, all sectors experience distress. Risk spillovers from struggling peripheral sectors back to the financial sector and other sectors become amplified, making all sectors equally effective at propagating risks, leading to a state where *DOM* is low.

The implication is that when *DOM* is low, i.e., when everyone is equally effective at propagating

risks, idiosyncratic shocks in any sector can keep transmitting from one sector to another, then to the next, and may even return to the originating sector itself and propagate outward again, falling into an infinite loop of transmission. Therefore, idiosyncratic risks can keep accumulating through this infinite loop and ultimately add up to larger aggregate volatility.

In contrast, when *DOM* is high, i.e., in good times, only a few sectors are capable of propagating idiosyncratic risks, so the shock transmission path is limited. Shocks can only propagate from the financial sector to others, after which the transmission quickly stops. As a result, idiosyncratic risks can only accumulate through these limited paths, leading to lower aggregate volatility.

Empirically, I construct the two network factors using stock return data from the Center for Research in Security Prices (CRSP) and assess their predictability for aggregate volatility. I measure sectoral idiosyncratic volatilities[5] as the volatility of benchmark-adjusted stock returns. I then estimate idiosyncratic volatility spillovers using the approach of Diebold and Yilmaz (2014), first estimating a vector autoregression (VAR) model for the idiosyncratic volatility panel and then performing a generalized variance decomposition (GVD) of the forecast error. The GVD provides the proportion of a sector's future uncertainty that is explained by shocks originating from another sector. This pairwise measure serves as the empirical counterpart to the idiosyncratic volatility spillover measure in the model.

Based on this spillover structure, I construct two factors, *INT* and *DOM*, using network distribution measures as outlined in Robert (1990). I find that both factors have predictive power for future aggregate volatility, measured as the volatility of aggregate consumption growth, which aligns with the definition of aggregate volatility in the model. Specifically, *DOM* predicts a decrease in volatility, while *INT* predicts an increase, with both predictive effects being statistically significant. This not only confirms that the two network factors predict volatility in the direction implied by

[5] A data limitation prevents measurement of firm-level idiosyncratic volatility spillovers, but I demonstrate robustness using various industry classifications.

the model but also demonstrates that, empirically, idiosyncratic risk spillovers play a critical role in shaping aggregate volatility.

From an asset pricing perspective, when investors are averse to volatility risk and prefer an early resolution of uncertainty, an increase in *INT* raises marginal utility, while an increase in *DOM* reduces it. As a result, in the model, innovations in *INT* carry a negative price of risk, whereas innovations in *DOM* carry a positive price of risk.

Empirically, I estimate Fama-MacBeth regressions using the two-factor innovations as explanatory variables and confirm that *INT* has a significantly negative price of risk, while *DOM* has a significantly positive price of risk, even when controlling for the Fama-French five factors (FF5).

Additionally, I sort all CRSP-listed stocks into portfolios based on their exposures to the factor innovations and find that a long-short portfolio formed on exposure to *INT* generates an annual return spread of -4%, while a long-short portfolio formed on exposure to *DOM* produces an annual return spread of 5%. Neither spread is explained by existing risk factor models. These findings suggest that stocks with higher exposure to *INT* serve as hedges against rising marginal utility, earning lower risk premiums, while stocks with higher exposure to *DOM* are riskier and earn higher risk premiums as compensation for bearing this risk.

Finally, to test whether the model can quantitatively match the asset pricing moments observed in the empirical portfolio sorting, I calibrate a reduced-form structural model. The general equilibrium model is simplified into a long-run risk framework (see Bansal and Yaron (2004)), where consumption growth is assumed to have a small persistent component with stochastic volatility, and the volatility is further modeled as a linear function of the two network factors, with *INT* increasing it and *DOM* decreasing it. I solve for the Stochastic Discount Factor (SDF) and verify that the prices of risk for the two factors implied by the model quantitatively match those observed in the data. In addition, I calibrate the cross-section, demonstrating that the model's predicted risk premiums and

volatilities for individual portfolios quantitatively align with those observed in the data.

Related Literature

My paper contributes to the growing literature on firms' networks. For example, Ahern (2013) demonstrates that sectors occupying more central positions within the input-output network tend to earn higher returns. Herskovic (2018) captures changes in the input-output structure using two network factors and shows that they influence aggregate output. The key distinction between his factors and mine lies in their respective implications. His factors capture first-moment network changes, such as output concentration and input allocation efficiency, with implications for first-moment outcomes, namely GDP. However, his framework does not account for risk. Building on this important work, I focus on second-moment network changes, where my factors have implications for second-moment outcomes, specifically the volatility of GDP. One advantage of examining the network from a second-moment perspective is that it allows us to overcome data limitations and derive higher-frequency network dynamics. While Herskovic (2018) constructs two annual factors using input-output tables, my approach examines volatility connections, leveraging high-frequency stock data to construct high-frequency asset pricing factors. Moreover, my paper is the first to demonstrate that network dynamics constitute a distinct source of risk—volatility risk.

Additionally, my paper builds on the work of Gabaix (2011) and Acemoglu et al. (2012), who show that under different assumptions, idiosyncratic risks can contribute to aggregate risk. Both studies primarily examine static systems and do not provide direct empirical evidence. My paper extends their works by developing a dynamic network framework and demonstrating the predictability of idiosyncratic risks for aggregate risk. More importantly, I empirically show both the predictability and the pricing implications. In other words, my paper is the first to provide micro-foundations for aggregate volatility, explaining not only its origins but also its persistent

dynamics, both theoretically and empirically.[6]

My paper also contributes to the literature on idiosyncratic volatility. Herskovic et al. (2016) document that firms' idiosyncratic volatilities exhibit co-movement, which is priced through its correlation with household labor income dispersion. In this paper, I provide an alternative explanation—namely, a network-based mechanism to account for the puzzling co-movement. Ang, Hodrick, Xing, and Zhang (2009) demonstrate that firms with higher idiosyncratic volatility earn lower risk premiums. My paper sheds light on why idiosyncratic volatility is priced—idiosyncratic volatility has spillover effects through the network, and the aggregate impact of these spillovers is both nonnegligible and persistent at the market-wide level.

Furthermore, my paper extends the broader literature on aggregate volatility. Ang, Hodrick, Xing, and Zhang (2006), Adrian and Rosenberg (2008) and Boguth and Kuehn (2013)show that different measures of aggregate volatility are priced. Long-run risk studies by Bansal and Yaron (2004) and Bansal, Kiku, and Yaron (2010) assume that the volatility of the long-run component of consumption growth is stochastic. My paper contributes to this literature by clarifying the origins and components of this volatility, demonstrating that it arises from the dynamic evolution of idiosyncratic risk spillovers.

This paper also relates to the standard production-based asset pricing literature, particularly studies on long-run productivity growth. Kung and Schmid (2015) examine a production economy in which long-run growth is endogenously driven by innovation and R&D. In my paper, the innovations of the two network factors can be interpreted as capturing technological shocks. Similar to Kung and Schmid (2015), I adopt recursive preferences to ensure that these innovations are priced.

[6]Further contributions to the network literature include studies by Carvalho (2008), Cohen and Frazzini (2008), Menzly and Ozbas (2010), Ahern (2013), Carvalho and Gabaix (2013), Ahern and Harford (2014), Elliott, Golub, and Jackson (2014), Acemoglu, Akcigit, and Kerr (2016), Acemoglu, Ozdaglar, and Tahbaz-Salehi (2017), Grant and Yung (2019), Gofman, Segal, and Wu (2020), Herskovic, Kelly, Lustig, and Van Nieuwerburgh (2020), Branger, Konermann, Meinerding, and Schlag (2021), Grigoris and Segal (2021), Jackson and Pernoud (2021), Farboodi and Kondor (2022), Smirnyagin and Tsyvinski (2022), Dew-Becker (2023) and Grigoris, Hu, and Segal (2023).

The key distinction is that, in my model, the network factors represent the volatility of long-run growth and, consequently, serve as volatility risk factors.[7]

Finally, this study bridges the gap between the risk measurement literature and asset pricing. Previous research has established empirical risk measurements, including pairwise risk spillover measures by Diebold and Yilmaz (2014). However, a crucial question remains: which elements of risk spillovers constitute genuinely systematic and persistent risk, and are therefore priced? This paper addresses this question by analyzing risk spillovers through a network perspective.[8]

The paper is structured as follows: Section 2 presents the theoretical framework, Section 3 discusses the empirical results, Section 4 details the model calibration, and Section 5 concludes.

2 Theoretical Framework

To explore the dynamics of idiosyncratic volatility spillovers, I develop a multi-sector model that traces these spillovers back to input-output relationships. I introduce network factors to characterize the distribution of volatility spillovers and demonstrate their economic and asset pricing implications.

2.1 Model Setting

I develop a model based on the framework of Herskovic (2018). Consider a multi-sectoral production framework within a perfectly competitive economy comprising n sectors. Each sector

[7]Related literature also includes works by Long Jr and Plosser (1983), Jermann (1998), Jermann (2010), Jermann (2013), Gomes, Kogan, and Yogo (2009), Kogan, Papanikolaou, and Stoffman (2013), Corhay, Kung, and Schmid (2020), Yogo (2006), Binsbergen (2016), Kuehn (2009), Kuehn and Schmid (2014), Lochstoer (2009), Belo (2010), Gomes and Schmid (2012) and Croce (2014).

[8]More studies about volatility include papers by Ang et al. (2009), Irvine and Pontiff (2009), Adrian and Brunnermeier (2011), Acharya, Engle, and Richardson (2012), Brownlees, Engle, et al. (2012), Diebold and Yilmaz (2012), Engle and Kelly (2012), Bansal, Kiku, Shaliastovich, and Yaron (2014), Bloom, Floetotto, Jaimovich, Saporta-Eksten, and Terry (2018) and Demirer, Diebold, Liu, and Yilmaz (2018).

produces a unique good that serves as an intermediate input for other sectors. Each sector's production function is specified as follows:

$$y_{i,t} = e^{z_{i,t}} \zeta_i l_{i,t}^{\eta} \prod_{j=1}^{n} x_{ij,t}^{(1-\eta)\omega_{ij,t}}, \tag{1}$$

where $y_{i,t}$ represents sector i's output, $z_{i,t}$ denotes sector i's productivity level, and ζ_i is a normalization constant. The parameter $\eta \in (0, 1)$ represents decreasing returns to investment. The variable $l_{i,t}$ indicates labor input, with the market assumed to have unit labor supply. $x_{ij,t}$ refers to the amount of sector j's good purchased by sector i, while $\omega_{ij,t}$ represents the weight or importance of input j.

The intersectoral trade network is characterized by the matrix $\mathbf{W}_t \equiv [\omega_{ij}]_t$. Each row i of $\mathbf{W}_t$ represents the input proportions that sector i sources from other sectors, reflecting the relative importance of various inputs to its production process. Conversely, each column i depicts the output proportions, indicating the importance of sector i's good as inputs for other sectors in the economy. Each $\omega_{ij,t}$ is nonnegative, and each row of the matrix sums to 1, that is,

$$\sum_{j=1}^{n} \omega_{ij,t} = 1, \quad \omega_{ij,t} \geq 0. \tag{2}$$

To establish a dynamic network structure, I assume that $\omega_{ij,t}$ follows the process outlined below:

Assumption 1. *The log of weight* $\ln \omega_{ij,t}$ *follows proportional random growth in a drift-neutral random walk:*

$$\ln(\omega_{ij,t}) = \ln(\omega_{ij,t-1}) + \left(-\frac{\sigma_{ij,t-1}^2}{2} \right) \cdot \Delta t + \sigma_{ij,t-1} \cdot \varepsilon_{ij,t}, \tag{3}$$

where $\varepsilon_{ij,t}$ *is a standard normal variable,* $\sigma_{ij,t-1} = c\omega_{ij,t-1}$ *represents size-dependent volatility. The initialization condition is that, at* $t = 0$*, each row of* W *follows a power-law distribution, with the largest suppliers for each sector (i.e., the largest components in each row) being the same.*

This assumption is a novel addition to the framework presented in Herskovic (2018). This implies two key ideas: first, that the shocks are exogenous; and second, that as the system reaches a steady state, the cross-sectional distribution of sectors' output importance follows a power-law distribution, with a few sectors providing critically important inputs to the economy. I will elaborate on both points below.

First, the shocks are considered exogenous to reflect the evolution of input-output relationships due to technological shocks or shifts in market fundamentals. This paper takes network dynamics as given and explores their implications.[9]

Second, based on Gabaix (2009), proportional random growth with reflecting barriers is sufficient to generate a power-law distribution for cross-sectional quantities at steady state.[10] To illustrate, suppose sector i heavily relies on a few sectors for inputs at $t = 0$. The proportional growth process ensures that the volatility of large suppliers is greater, while that of smaller suppliers remains low. Over time, larger suppliers tend to stay large, while smaller suppliers remain small, and the dampening effect from the drift term ensures that large suppliers do not grow too quickly. At steady state, their weights follow a power-law distribution. When we initialize the weight matrix by assigning the largest suppliers to be the same for each sector, these large suppliers will continue to serve as major inputs to all sectors over time. This assumption is supported by data: sectors such as manufacturing, finance, and insurance consistently produce goods that are more essential to other sectors. Acemoglu et al. (2012) provides empirical evidence showing that the cross-sectional distribution of sectors' output importance follows a power-law distribution consistently across years.

For analytical purposes, I formally describe the steady-state distribution of sectors' output

[9] Similarly, Herskovic (2018) adopts an i.i.d. assumption for the weights to reflect the same idea of exogenous technological shocks.

[10] Under proportional random growth models, even though individual time series may be non-stationary, the cross-sectional distribution of values (e.g., weights) can converge to a power law. Larger firms tend to remain large and evolve with higher volatility, while smaller firms tend to remain small and evolve with lower volatility. See detailed discussions in Gabaix (1999), Gabaix, Gopikrishnan, Plerou, and Stanley (2003) and Gabaix (2009).

importance to the economy in the following assumption:

Assumption 2. *Conditional on time t, the cross-sectional distribution of sectors' output importance follows a power-law distribution, where the output importance of each sector i is defined as:*

$$d_{i,t} \equiv \sum_{j=1, j\neq i}^{n} \omega_{ji,t}.$$

$d_{i,t}$ measures the importance of sector i's output to all other sectors. This assumption embodies the same underlying principles as Assumption 1. It describes the steady-state distribution that naturally results from the proportional random growth process outlined in Assumption 1. Acemoglu et al. (2012) directly imposes a similar distribution assumption in a static multi-sector model. This paper extends that assumption to a dynamic framework.

For analytical purposes, I formally define the power-law distribution as follows:

Definition 1. *Let $\mathcal{E}_t^n$ represent the economy with n representative sectors at time t.*[11] *Let $d_{i,t}^n$ represent the output importance of sector i, and let $d_{\max,t}^n$ denote the maximum output importance in this economy. Conditional on time t, the economy $\mathcal{E}_t^n$ has a power law $d_{i,t}^n$ sequence if there exist a constant $\beta > 1$, a slowly varying function $\mathcal{F}_t(k)$ satisfying $\lim_{k\to\infty} \mathcal{F}_t(k)k^{\delta} = \infty$ and $\lim_{k\to\infty} \mathcal{F}_t(k)k^{-\delta} = 0$ for all $\delta > 0$, and a sequence of positive numbers $c_{n,t} = \Theta(1)$ such that, for all $n \in \mathbb{N}$ and all $k < d_{\max,t}^n = \Theta\left(n^{1/\beta}\right)$, we have*

$$P_{n,t}(k) = c_{n,t}k^{-\beta}\mathcal{F}_t(k), \tag{4}$$

where $P_{n,t}(k) \equiv \frac{1}{n}\left|\left\{i \in \mathcal{I}_{n,t} : d_{i,t}^n > k\right\}\right|$ is the empirical counter-cumulative distribution function of $d_{i,t}^n$. The parameter β is greater than 1.

The shape parameter β in Equation (4) represents the scaling behavior of the tail of the output

[11] The economy can be examined at varying levels of disaggregation. As n increases from 1 to ∞, the economy is viewed at increasingly disaggregated levels.

importance distribution. Specifically, lower values of β indicate heavier tails[12], which in turn suggest greater variability in the sequence $d_{i,t}^n$. This definition provides a detailed characterization of the power-law distribution referenced in Assumption 2.

Assumption 2 is crucial in this model. It implies that sectors do not operate in a completely symmetric network—meaning they do not play identical roles in the economy. This network asymmetry hinders risk diversification and ensures that part of sector-specific shocks contribute to aggregate volatility. Specifically, when both central and peripheral sectors are present, shocks to central sectors propagate more widely across the network, leading to highly correlated outcomes among many other sectors. This breaks the independence or weak independence assumption of the Central Limit Theorem (CLT) when there are sufficiently many entities (i.e., as $n \to \infty$). Consequently, idiosyncratic risks cannot be fully averaged out across all those entities, and part of these risks will constitute aggregate risk.

Following Bloom et al. (2018), I assume an AR(1) process for the productivity levels:

$$z_{i,t} = \rho_z z_{i,t-1} + \sigma_z \epsilon_{i,t}^z, \tag{5}$$

where ρ_z is the AR(1) coefficient, σ_z is the constant volatility,[13] and $\epsilon_{i,t}^z$ is the firm-specific productivity shock following a standard normal distribution.

All sectors maximize their time-separable profits. These profits are derived from the revenues of selling final goods, minus the costs of purchasing intermediate inputs and labor:

[12] Acemoglu et al. (2012) estimate the tail parameter β using the commodity-to-commodity data sourced from the U.S. Bureau of Economic Analysis (BEA), and show that β is stable from year to year, with values around 1.1.

[13] The volatility σ_z could be extended to be time-varying $\sigma_{z,t}$ without altering the main results. However, introducing sectoral heterogeneity adds complexity that lies outside the scope of the paper.

$$D_{i,t} = \max_{\{x_{ij,t}\},\{l_{i,t}\}} \left[P_{i,t} y_{i,t} - \sum_{j=1}^{n} P_{j,t} x_{ij,t} - h_t l_{i,t} \right], \tag{6}$$

where $D_{i,t}$ denotes the dividend and $P_{i,t}$ is the spot market price of good i. h_t is the market wage and it is determined exogenously.[14]

The cum-dividend value of sector i, denoted as $V_{i,t}$, is computed recursively by

$$V_{i,t} = D_{i,t} + \mathbb{E}_t \left[M_{t+1} V_{i,t+1} \right], \tag{7}$$

where M_{t+1} is the SDF and $D_{i,t}$ is sector i's dividend.

I assume that the representative household has Epstein-Zin recursive preferences:

$$U_t = \left[(1-\psi) C_t^{1-\rho} + \psi \left(\mathbb{E}_t \left(U_{t+1}^{1-\gamma} \right) \right)^{\frac{1-\rho}{1-\gamma}} \right]^{\frac{1}{1-\rho}},$$

where ψ is the discount rate, γ is the risk aversion parameter, and ρ is the inverse of the elasticity of intertemporal substitution. C_t is a Cobb-Douglas consumption aggregator, which is defined as:

$$C_t = \prod_{i=1}^{n} c_{i,t}^{\alpha_i}, \tag{8}$$

where $c_{i,t}$ is the consumption of final good i at time t, and α_i represents the taste preference for good i. The taste preferences sum to one.

The recursive utility assumption is crucial for the model. Under recursive utility, volatility risk is priced, and my network factors will be priced, as investors fear that persistent economic downturns are accompanied by low asset valuations.

[14] Labor plays a peripheral role in this model and is not a key focus of the analysis.

Under the recursive utility framework, the household's maximization problem is:

$$J_t\left(P_t, s_t, Q_t, h_t\right) = \max_{\{c_{i,t}, s_{i,t+1}\}} \left[(1-\psi)\, C_t^{1-\rho} + \psi \left(\mathbb{E}_t \left(J_{t+1}^{1-\gamma} \right) \right)^{\frac{1-\rho}{1-\gamma}} \right]^{\frac{1}{1-\rho}}, \tag{9}$$

where $Q_{i,t} = V_{i,t} - D_{i,t}$ is the pre-dividend value of sector i, and $s_{i,t}$ is the share of sector i at time t.

The intertemporal budget constraint is given by

$$\sum_{i=1}^{n} P_{i,t} c_{i,t} + \sum_{i=1}^{n} \left(V_{i,t} - D_{i,t} \right) s_{i,t+1} = \sum_{i=1}^{n} V_{i,t} s_{i,t} + h_t. \tag{10}$$

This constraint implies that the total expenditure on consumption goods and the cost of adjusting shareholdings (calculated using pre-dividend sector values) must equal the sum of gains from previous share values and labor income.

2.2 Competitive Equilibrium

A competitive equilibrium consists of spot market prices $\{P_{i,t}\}$, household's consumption of different goods $\{c_{i,t}\}$, shareholdings $\{s_{i,t}\}$, and sector input choices $\{x_{ij,t}\}$. For each period t, sectors maximize their profit function (6) subject to the production function (1), while households maximize the utility function (9) subject to the intertemporal budget constraint (10). The market clearing conditions are as follows:

$$\begin{cases} y_{i,t} = c_{i,t} + \sum_{j=1}^{n} x_{ji,t} \\ \sum_{i=1}^{n} s_{i,t} = 1, \quad \sum_{i=1}^{n} l_{i,t} = 1. \end{cases} \tag{11}$$

The conditions in Equation (11) stipulate three points: (1) the output of each good i is either

consumed by the household or used as intermediate inputs by other sectors; (2) total stock shares sum to 1; and (3) total labor shares sum to 1.[15]

Prices are normalized as follows:

$$\prod_{j=1}^{n} P_{j,t}^{\alpha_j} = \prod_{j=1}^{n} \alpha_{j,t}^{\alpha_j}. \tag{12}$$

This normalization makes the risk-free rate of return the return on a claim to the consumption aggregator, and considerably simplifies the expression for the SDF.[16]

Let ξ_t denote the aggregate output, $v_{i,t} \equiv \frac{P_{i,t} y_{i,t}}{\xi_t}$ denote the sales share of each sector i, and $\mathbf{v}_t$ be the vector form of $v_{i,t}$.[17]

Under the price normalization in Equation (12) and the consumption aggregator in Equation (8), the equilibrium yields

$$\mathbf{v}_t = \tilde{\mathbf{L}}_\mathbf{t} \alpha, \tag{13}$$

where $\tilde{\mathbf{L}}_\mathbf{t} \equiv \left[\tilde{l}_{ij}\right]_t = \left(\mathbf{I} - (1-\eta)\,\mathbf{W}_\mathbf{t}'\right)^{-1}$. Equation (13) indicates that sales shares $\mathbf{v}_t$ are influenced by both taste preferences and the input demands through the trade network. $\tilde{\mathbf{L}}_\mathbf{t}$ represents the Leontief inverse (Burres, 1994). Given that all eigenvalues of $(1-\eta)\mathbf{W}_\mathbf{t}'$ lie within the unit circle, the Leontief inverse can be expanded as follows:

$$\left(\mathbf{I} - (1-\eta)\,\mathbf{W}_\mathbf{t}'\right)^{-1} = \mathbf{I} + (1-\eta)\,\mathbf{W}_\mathbf{t}' + (1-\eta)^2\,\mathbf{W}_\mathbf{t}'^\mathbf{2} + (1-\eta)^3\,\mathbf{W}_\mathbf{t}'^\mathbf{3} + \ldots \tag{14}$$

In Equation (14), the identity matrix $\mathbf{I}$ represents the direct consumption preference from the household. The matrix $\mathbf{W}_\mathbf{t}'$ describes first-order interdependencies (e.g., good i is needed by sector

[15] Detailed derivations for the equilibrium are provided in the Online Appendix A.

[16] A risk-free claim is well-defined under this price normalization. See the Online Appendix A.4 for details. Herskovic (2018) adopts the same price normalization.

[17] $v_{i,t}$ is also known as the 'Domar weight' in Acemoglu et al. (2012).

j), while higher-order terms capture higher-order demands (e.g., good i is needed by sector j, whose product j is needed by sector k, and so on).

In this economy, the aggregate output is determined by both the sector-level productivity and the intersectoral network of the economy, summarized by the Leontief inverse. Specifically, the aggregate output, ξ_t, can be expressed as follows:

$$\ln \xi_t = \alpha' \ln \alpha + \alpha' \tilde{\mathbf{L}}_\mathbf{t} \mathbf{z}_\mathbf{t}, \tag{15}$$

where α is the vector of good preferences. Equation (15) states that the log of aggregate output is a linear combination of sectoral productivity levels, with coefficients determined by both the network structure (i.e., the Leontief inverse) and the household's consumption preferences.

2.3 Model Implications

Proposition 1. *The vector of prices is given by*

$$\ln \mathbf{P}_t = \tilde{\mathbf{L}}_t \left[\underbrace{-ln\eta^{\eta} (1-\eta)^{1-\eta}}_{constant} \quad \underbrace{-\mathbf{z}_t}_{sector-specific} \quad \underbrace{-(1-\eta) \sum_{i=1}^{n} v_{i,t} \sum_{j=1}^{n} \omega_{ij,t} \ln \omega_{ij,t} + \eta \ln h_t}_{common} \right]. \tag{16}$$

Let $\ln \mathbf{P}_t^* \equiv -\tilde{\mathbf{L}}_t \mathbf{z}_t$ *denote the vector of sector-specific components of prices. Under the first-order approximation of the Leontief inverse, the idiosyncratic volatility of each sector i, defined as the conditional variance of the common-component-adjusted log return from t to* $t+1$[18]*, can be*

[18]Given that the stock price is linearly related to the spot price of goods, the stock volatility spillover inherits the same structure. In equilibrium, there is no exact solution for the SDF or for individual stock prices. Therefore, I calibrate a structural framework to simulate the cross-section and demonstrate that consistent implications exist.

expressed as follows:

$$Var_t\left(r^*_{i,t\to t+1}\right) = \sigma_z^2\left[\left(1+(1-\eta)\,\omega_{ii,t}\right)^2 + \sum_{k\neq i}\left((1-\eta)\,\omega_{ik,t}\right)^2\right]. \tag{17}$$

This proposition establishes the determinants of sectoral idiosyncratic volatility. Equation (16) reveals that prices are determined by both the Leontief inverse $\tilde{\mathbf{L}}_t$ and time-series shocks, including a firm-specific shock and a common component. The firm-specific shock is the productivity shock ($\mathbf{z}_t$), while the common component includes two elements: the sales-share weighted average of input concentration ($\sum_{i=1}^{n} v_{i,t} \sum_{j=1}^{n} \omega_{ij,t} \ln \omega_{ij,t}$) and the aggregate market wage ($\ln h_t$).[19]

Equation (17) states that the idiosyncratic volatility of each sector i can be decomposed into two parts: the first is its own self-effect, represented by $\sigma_z^2\left(1+(1-\eta)\,\omega_{ii,t}\right)^2$, and the second is the risk spillover effects from other sectors, denoted by $\sigma_z^2\left((1-\eta)\,\omega_{ik,t}\right)^2$. The spillover effect encompasses (1) all first-order and higher-order impacts from k to i—such as when sector k's product is needed by sector i, or when sector k's product is required by other sectors whose products are needed by i; and (2) the impact from k to i through the household. The household cannot perfectly negate the idiosyncratic shock spillover from one sector by substituting between all goods, as all sectors are interconnected. For the self-effect term, the additional '1' emphasizes the crucial role of households: if sector i experiences an idiosyncratic shock, it directly impacts household consumption, as households purchase the final good i. If the shock transmits to another sector j, it also affects household consumption. This process continues, ultimately influencing aggregate consumption, which then has a feedback effect on sector i.

This decomposition highlights the dual sources of volatility within a sector: the self-effect from idiosyncratic shocks and the risk spillover effects arising from inter-sectoral dependencies.

[19]The first element in the common component, i.e., the sales-share weighted average of input concentration, is referred to as the Sparsity Factor in Herskovic (2018). When it is high, it indicates more efficient input reallocation in the economy.

Based on Equation (17), I define an n by n matrix Δ_t to describe the dynamics of idiosyncratic volatility spillovers. Δ_t is also referred to as the adjacency matrix in the following context.

Definition 2. *Δ_t is defined as follows:*

$$\Delta_t \equiv \left[\delta_{ij}\right]_t \equiv \begin{bmatrix} \frac{\left(1+(1-\eta)\,\omega_{11,t}\right)^2}{norm_{1t}} & \frac{\left((1-\eta)\,\omega_{12,t}\right)^2}{norm_{1t}} \cdots & \frac{\left((1-\eta)\,\omega_{1n,t}\right)^2}{norm_{1t}} \\ \frac{\left((1-\eta)\,\omega_{21.t}\right)^2}{norm_{2t}} & \frac{\left(1+(1-\eta)\,\omega_{22,t}\right)^2}{norm_{2t}} \cdots & \frac{\left((1-\eta)\,\omega_{2n,t}\right)^2}{norm_{2t}} \\ & \cdots & \\ & \cdots & \\ \frac{\left((1-\eta)\,\omega_{n1,t}\right)^2}{norm_{nt}} & \frac{\left((1-\eta)\,\omega_{n2,t}\right)^2}{norm_{nt}} \cdots & \frac{\left(1+(1-\eta)\,\omega_{nn,t}\right)^2}{norm_{nt}} \end{bmatrix}, \tag{18}$$

where $norm_{it} \equiv \left(1+(1-\eta)\,\omega_{ii,t}\right)^2 + \sum_{k\neq i}\left((1-\eta)\,\omega_{ik,t}\right)^2$ *is a normalization constant.*

In the adjacency matrix Δ_t, the diagonal elements reflect the self-effect proportion: $\left(1+(1-\eta)\,\omega_{ii,t}\right)^2$, while the off-diagonal elements capture the spillover effect proportion: $\left((1-\eta)\,\omega_{ik,t}\right)^2$. Each row is normalized to sum to 1. Thus, each element $\delta_{ij,t}$ quantifies the proportion of sector i's volatility attributable to the shock arising from sector j at time t.[20] Further, I define two factors: *Risk-Dominance* (*DOM*) and *Risk-Intensity* (*INT*) to characterize two dimensions of Δ_t.

Definition 3. *The two network factors are defined as follows:*

$$\begin{cases} DOM_t \equiv \sum_{i=1}^{n} Out_{i,t} \ln\left(Out_{i,t}\right) \\ INT_t \equiv \frac{1}{n}\sum_{i=1}^{n}\sum_{j=1}^{n} \delta_{ij,t} \ln\left(\delta_{ij,t}\right), \end{cases} \tag{19}$$

[20] Although idiosyncratic volatility spillovers stem from the input-output relationship, $\mathbf{W}_t$ and Δ_t are fundamentally distinct due to the role of the household. I elaborate on this distinction in the Online Appendix E.2.

where $Out_{i,t} \equiv \sum_{j=1, j\neq i}^{n} \delta_{ji,t}$ *is the spillover outdegree of sector* i.

$Out_{i,t}$, defined as the off-diagonal sum of column i of Δ_t, measures the total risk spillovers from sector i to the rest of the economy. If a sector, when shocked, has a larger risk spillover to the whole economy, then it will have a higher $Out_{i,t}$.

DOM is defined as the negative entropy (i.e., the function $\sum x \ln x$) of the spillover outdegree $Out_{i,t}$. Based on Robert (1990), negative entropy serves as a sufficient statistic to measure the overall concentration degree of the cross-sectional degree distribution within a network graph.[21] The *DOM* factor measures the concentration of cross-sectional risk spillover capability. When *DOM* is high, it indicates that only a few key sectors can spill over their idiosyncratic risks to the rest of the economy when shocked. When *DOM* is low, it means that all sectors have equal risk spillover capabilities, so both central and peripheral sectors will equally impact the entire economy when shocked.

INT is defined as the cross-sectional average of the concentration of each sector's shock-receiving distribution. To clarify, let's consider an economy with 10 sectors. For sector 1, we examine the following two cases of its shock-receiving distribution:

$$\text{Case 1: } [0.1, 0.1, ..., 0.1] \text{ vs. Case 2: } [0.05, \mathbf{0.3}, \mathbf{0.3}, ..., 0.05]\,. \tag{20}$$

In Case 1 of Equation (20), sector 1 experiences uniform shock spillover from all other sectors. These shocks are easily diversified. Conversely, in Case 2, sector 1 is impacted primarily by shocks from two key sectors, leading to exposure to larger and less diversifiable shocks, thereby encountering a greater intensity of risk spillover. The *INT* factor, defined as the cross-sectional

[21] More references include Bianconi (2007) and Bianconi (2009). For a detailed elaboration on negative entropy, refer to the Online Appendix E.1. Additionally, in robustness tests, I provide alternative measurements for the two factors. See the Online Appendix C.5 for details.

average of this concentration, measures the average magnitude of pairwise risk spillovers across the entire economy.

Next, I explore the economic implications of these factors, with a focus on their relationship with aggregate volatility. This relationship can be analyzed from two perspectives. First, conditional on time t, we can examine how network factors influence the speed of risk diversification across all entities as the economy is viewed from a highly aggregated level to a highly disaggregated level, i.e., $n \to \infty$. Second, given the dynamic nature of the network structure, we can analyze the time-series effects of network factors on aggregate volatility.

To examine the implication for risk diversification speed, let's briefly recall the Lucas diversification argument (Lucas, 1995). Under the diversification argument, suppose all sectors operate independently (i.e., without a network) or within a perfectly symmetric network (where all sectors take the same input-output amount from one another) and sectoral shocks are identically distributed. Then, according to the CLT, the aggregate effect of these shocks tends to average out as $n \to \infty$. Specifically, under the Law of Large Numbers (LLN), idiosyncratic risks completely average out, leading to a rapid decay of aggregate volatility toward its mean, with the decay rate proportional to $\sqrt{n}$:

$$\sqrt{Var_t\left(\Delta \ln \xi_{t\to t+1}\right)} = \Omega\left(\frac{1}{\sqrt{n}}\right), \tag{21}$$

where $\sqrt{Var_t\left(\Delta \ln \xi_{t\to t+1}\right)}$ denotes the aggregate volatility and Ω is a limit infimum symbol.[22]

However, in the model, the input-output network is asymmetric, as stated in Assumption 2, and thus the CLT does not apply. Idiosyncratic risks cannot be fully averaged out across sufficiently

[22]The definition of the limit infimum symbol is as follows. Given two sequences of positive real numbers $\{f_n\}_{n\in\mathbb{N}}$ and $\{g_n\}_{n\in\mathbb{N}}$, we have:

$$f_n = \Omega\left(g_n\right) \text{ iff there exists } C > 0 \text{ and } k \geq 1 \text{ such that } f_n \geq C \times g_n \text{ for every } n \geq k.$$

many entities, leading aggregate volatility to decay more slowly toward its mean.

Moreover, the exact decay rate of aggregate volatility depends on the network. In the following proposition, I elucidate the relationship between the decay rate and the two network factors.

Proposition 2. *Conditional on time t, consider the economy $\mathcal{E}_t^n$ at different aggregation levels. As n increases from 1 to ∞, the sequence $\left\{\mathcal{E}_t^n\right\}_{n\in\mathbb{N}}$ represents the economy viewed from a highly aggregated level to an extensively disaggregated level. Assume the shape parameter of the power-law output distribution $\beta \in (1, \frac{6}{5}]$. Then, the aggregate volatility satisfies the following:*

$$\sqrt{Var_t\left(\Delta \ln \xi_{t\to t+1}\right)} = \Omega\left(\frac{1}{\sqrt{\frac{\sqrt{n}INT_t}{DOM_t}}}\right). \tag{22}$$

This proposition establishes the effect of the network factors on the decay rate of aggregate volatility, conditional on time t. The limit infimum of aggregate volatility is a function of network factors and the number of representative sectors. *INT* and *DOM* are inherently negative (i.e., 'negative entropy' by design). A larger *INT* value implies a higher limit infimum, i.e., a higher lower bound, of aggregate volatility, indicating a slower decay of aggregate volatility. Contrastingly, a larger *DOM* value indicates a quicker decay of aggregate volatility.

Conditional on a given level of *DOM*, when *INT* is high, the average magnitude of risk spillover is elevated. This implies that all sectors are more tightly interconnected, and a shock to any sector can rapidly largely impact one over another and transform into economy-wide contagion. Consequently, idiosyncratic risks become more difficult to diversify, impeding the rapid decay of aggregate volatility to its mean. Conversely, in the absence of pairwise spillover effects among sectors, aggregate volatility would remain unaffected. Households can perfectly substitute one good with another if a sector is shocked, so aggregate output doesn't need to be affected. As a result, aggregate volatility, which is the volatility of output growth, does not have to be impacted.

When *INT* is held constant, a high *DOM* indicates that only a few key sectors have the ability to spill over idiosyncratic risks to the entire economy when shocked. In this case, only shocks to these few sectors can propagate to the rest of the economy, while the other sectors lack risk propagation capability. As a result, there is only one potential path for risk spillovers: shocks originate in the key sectors and spread to the rest, and once they reach the peripheral sectors, the propagation stops. These sectors do not propagate the shock back or to others. Consequently, aggregate volatility forms quickly after this one round of spillover, allowing for risk diversification across sectors and enabling aggregate volatility to return to its mean relatively quickly.

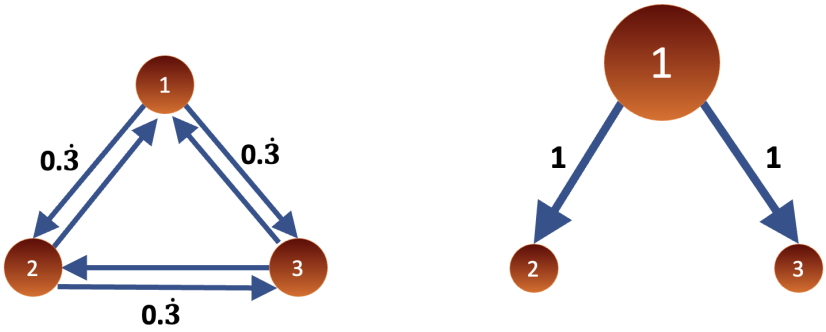
However, when *DOM* is low, all sectors are equally capable of propagating their idiosyncratic risks across the entire market when shocked. In this scenario, an idiosyncratic shock in one sector can spread to another, and then to the next, continuing in an infinite loop. This happens with every sector's idiosyncratic shock, meaning that aggregate volatility constantly accumulates and cannot quickly revert to its mean.

To better illustrate the intuition, I provide a numerical example. Figure 2 shows a simplified example with three sectors, but the numerical calculation can be applied to a sufficiently large number of sectors, n. Suppose in the second panel, if sector 1 is shocked, it can propagate 100% of its idiosyncratic risk to both sector 2 and sector 3, but sectors 2 and 3 only absorb the shock and do not have any spillover capability. In contrast, in the left panel, each sector can cause $\frac{1}{3}$ of another sector's volatility when shocked. In both cases, the average spillover magnitude is the same, so the difference in aggregate volatility arises solely from the different *DOM* values.

Suppose all three sectors experience a normal shock with volatility σ^2. In the second panel, sector 1 propagates its idiosyncratic risk to sectors 2 and 3, so the total volatility caused by sector 1 is the sum of its own volatility σ^2 and the volatilities transmitted to sectors 2 and 3. Since sectors 2 and 3 do not propagate their own idiosyncratic risks, the total volatility in this economy is $5\sigma^2$.

However, in the first panel, a shock to sector 1 will spread to both of the other sectors, and each of those will further spread the shock. The same applies to the shock arising from sectors 2 or 3. In total, the aggregate volatility in this economy is $6\sigma^2$. This numerical example illustrates how the infinite loop of risk propagation leads to the accumulation of idiosyncratic risks, resulting in larger aggregate volatility.

Figure 2. Numerical Example for *DOM* Factor
This figure presents a numerical example illustrating the implications of *DOM*. Both panels exhibit the same *INT*, but the second panel has a higher *DOM*.



Low *Risk-Dominance* **High** *Risk-Dominance*

$$6\sigma^2 = \begin{cases} \sigma^2 + \begin{cases} 0.\dot{3}\sigma^2 + 0.\dot{3}^2\sigma^2 + 0.\dot{3}^3\sigma^2 + \ldots \\ 0.\dot{3}\sigma^2 + 0.\dot{3}^2\sigma^2 + 0.\dot{3}^3\sigma^2 + \ldots \end{cases} \\ \sigma^2 + \begin{cases} 0.\dot{3}\sigma^2 + 0.\dot{3}^2\sigma^2 + 0.\dot{3}^3\sigma^2 + \ldots \\ 0.\dot{3}\sigma^2 + 0.\dot{3}^2\sigma^2 + 0.\dot{3}^3\sigma^2 + \ldots \end{cases} \\ \sigma^2 + \begin{cases} 0.\dot{3}\sigma^2 + 0.\dot{3}^2\sigma^2 + 0.\dot{3}^3\sigma^2 + \ldots \\ 0.\dot{3}\sigma^2 + 0.\dot{3}^2\sigma^2 + 0.\dot{3}^3\sigma^2 + \ldots \end{cases} \end{cases} \qquad 5\sigma^2 = \begin{cases} \sigma^2 + \begin{cases} \sigma^2 \\ \sigma^2 \end{cases} \\ \sigma^2 \\ \sigma^2 \end{cases}$$

Given that the network structure changes over time, I proceed with the second analysis, illustrating the time-series effect of network factors on aggregate volatility. I begin with a simple case involving two representative sectors and then generalize to a broader case.

Proposition 3. *Consider an economy with two representative sectors ($n = 2$). Assume that from t to $t + 1$, the change in the network matrix is infinitesimal, i.e., $\Delta L_{t+1} \to 0$, and assume equal*

consumption preferences, i.e., $\alpha = \left[\frac{1}{2}, \frac{1}{2}\right]'$. *Under the first-order approximation of the Leontief inverse, the aggregate volatility can be approximated as follows:*

$$Var_t(\Delta \ln \xi_{t+1}) = \frac{1}{2}\sigma_z^2 \left[1 + (1-\eta) INT_t - \frac{1}{2}(1-\eta)^2 DOM_t\right]. \tag{23}$$

Equation (23) demonstrates that aggregate volatility is a linear function of the network factors, where *INT* increases aggregate volatility while *DOM* decreases it. This proposition extends Proposition 2 by considering the unconditional time-series effects.

When *INT* is high, the pairwise risk spillover is stronger and of higher magnitude, preventing idiosyncratic risks from being quickly averaged out. Consequently, aggregate volatility cannot rapidly decay to its mean. This is reflected in the time series as an increase in aggregate volatility.

In contrast, when *DOM* is high, the state more closely resembles normal times. Not every sector can propagate idiosyncratic shocks to the rest of the economy when shocked. The limited potential for spillovers facilitates risk diversification, causing aggregate volatility to quickly decay to its mean. As a result, aggregate volatility decreases over time.

This analytical result relies on the assumption that there are two representative sectors. When the economy is viewed at a more disaggregated level and represented by more than two sectors, analytical results are not available. To demonstrate that the result holds more generally, I confirm it through simulations.

2.4 Model Simulations

I simulate the model (without approximations) to demonstrate how aggregate volatility responds to network factors over time. Consider an economy with 48 representative sectors and simulate time

series over 504 months (42 years), including a 500-month burn-in period.[23]

First, I simulate the weight matrix $\mathbf{W}_t = \left[\omega_{ij}\right]_t$ following Assumption 1. I begin by initializing $\mathbf{W}_0$. For each row of the weight matrix, I draw a series of 48 values from a power-law distribution with a tail parameter $\beta = 1.1$,[24] which is empirically estimated by Acemoglu et al. (2012). Without loss of generality, I rank the series from largest to smallest, assuming the first sector dominates the most output, followed by the second, and so on. I normalize each row based on Equation (2). Next, I simulate W_t following the proportional random growth in Assumption 1 where the volatility is proportional to each pairwise weight at each time point. As per Equation (3), $\sigma_{ij,t-1} = c\omega_{ij,t-1}$. I select c to reflect the average volatility of input-output weights in the data. Specifically, I construct annual input-output matrices for the Fama-French 48 industries using Compustat Customer Segment data from 1984 to 2019, following Herskovic (2018), and estimate weight volatility for each sector pair. The median volatility is 0.015 per year, implying a monthly volatility of 0.004. Since input-output data is typically noisy and sensitive to how it is segmented, I choose c to be slightly smaller than the estimated volatility, setting it at 0.001.

Next I simulate sectoral productivity processes following Equation (5). The AR(1) coefficient ρ_z is set to be 0.95, as estimated by Khan and Thomas (2008). The monthly volatility σ_z is set at 0.029 to be consistent with the 0.05 quarterly volatility estimated in Bloom et al. (2018). The consumption preferences are assumed to be the same, i.e., $\alpha_i = \frac{1}{48}$, consistent with the condition in Proposition 3. Aggregate consumption $\ln \xi_t$ is then constructed following Equation (15), and network factors are constructed following Equation (19).

To estimate the conditional mean of consumption growth, I regress consumption growth onto lagged consumption growth, lagged *INT*, and lagged *DOM*:[25]

[23] The sector number and time periods are chosen to match those in the empirical sample.

[24] The result is robust for other β values in $(1, \frac{6}{5}]$ as per the condition in Proposition 2.

[25] The two network factors are persistent in the data. In case they affect the conditional mean of the consumption growth, I include them in the regression. They do not have significant coefficients, however, indicating that the network

$$\Delta \ln \xi_{t+1} \sim \Delta \ln \xi_t + DOM_t + INT_t + u_{t+1}. \tag{24}$$

The residual u_{t+1} in Equation (24) represents the demeaned consumption growth. Aggregate volatility is then calculated either as the absolute residual $|u_{t+1}|$ or as the squared residual $|u_{t+1}|^2$.[26] To maintain consistency with the empirical analysis, all variables are aggregated from monthly to quarterly frequency. Quarterly aggregate volatility is the sum of monthly volatility, i.e., $\sum |u_{t+1}|^{1 \text{ or } 2}$, and the quarterly network factors are taken at the end of the month.

Following this, I run a VAR(1) model for the network factors and aggregate volatility and plot the impulse response of aggregate volatility to the network factors. In the VAR framework, the variables are ordered as *DOM*, *INT*, and aggregate volatility.[27] Figure 3 below shows the impulse response of the absolute residual $|u_{t+1}|$ to two network factors.[28]

The left plot shows that an initial surge in *INT* raises aggregate volatility, with this effect persisting for 150 quarters. Intuitively, when *INT* is high, the average risk spillover intensity is high in the economy. Idiosyncratic risks cannot be quickly averaged out, and aggregate volatility persists. The right plot demonstrates that an initial increase in *DOM* reduces aggregate volatility, with this impact lasting around 150 quarters. When *DOM* is high, fewer sectors propagate shocks, and the shocks can be rapidly dissipated through risk-sharing, causing aggregate volatility to decrease.

These findings are consistent with the analytical result in Proposition 3, both qualitatively and quantitatively. Moreover, the findings suggest that both network factors have a long-run impact on aggregate volatility, which can be linked to the existing long-run risk literature. Bansal and Yaron

factors do not affect the first moment but are volatility risk factors.

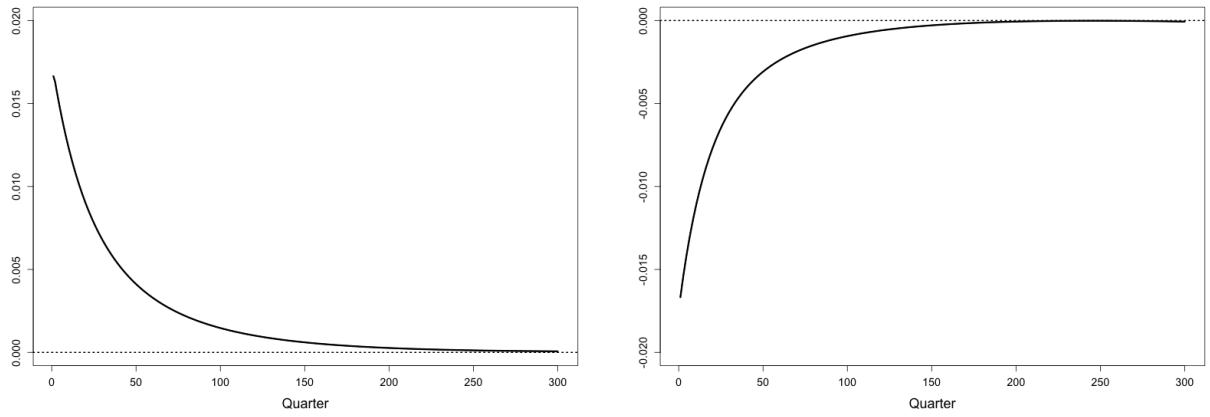
[26] In standard literature, aggregate volatility is computed using either conditional standard deviation $|u_{t+1}|$ or conditional variance $|u_{t+1}|^2$ of consumption growth. I test both to ensure the results are not subject to the nonlinearity of the measure.

[27] Changing the order of the factors or analyzing each factor separately with aggregate volatility does not alter the results.

[28] The squared residual case yields similar patterns.

(2004) and Bansal, Kiku, and Yaron (2010) assume a long-run component of consumption growth, with time-varying volatility in this component. My simulation results shed light on the origins of this volatility, showing that the network factors function as the stochastic volatility of the long-run risk component.

Figure 3. Model-implied Impulse Response to the Network Factors.
This figure presents the impulse response of aggregate volatility to network factors in the model. The left plot illustrates the response to the Risk-Intensity factor, while the right plot shows the response to the Risk-Dominance factor. Details of the simulation procedures are provided in Section 2.4.



(a) IRF to Risk-Intensity Factor

(b) IRF to Risk-Dominance Factor

Collectively, the economic implication of this model is that *INT* increases aggregate volatility, while *DOM* reduces it, with both effects persisting over the long term. From an asset pricing perspective, when investors are averse to volatility risk and prefer an early resolution of uncertainty, an increase in *INT* is associated with an increase in marginal utility, while an increase in *DOM* is associated with a decrease in marginal utility. Therefore, innovations in *INT* should carry a negative price of risk, whereas innovations in *DOM* should carry a positive price of risk. In the next section, I will empirically construct the network factors and examine both the economic and asset pricing implications.

3 Empirical Evidence

In this section, I construct the network factors using stock data and analyze the implications of idiosyncratic volatility spillovers. I demonstrate that the network factors hinder risk diversification through an extrapolation exercise, and show they have predictability for aggregate volatility. In addition, I test the asset pricing implications of these factors through cross-sectional portfolio sorting and Fama-MacBeth regressions. I show that the signs of their prices of risk are consistent with the model's predictions.

3.1 Construction of Idiosyncratic Volatility Spillover

I estimate the idiosyncratic volatility spillovers for sectors[29] where each sector can be viewed as a value-weighted average of homogeneous firms producing the same good.

I compute daily industry portfolio returns using all CRSP stocks[30] with share codes 10, 11, and 12 from January 1, 1969, to December 31, 2019. The Fama-French 48 industry classification is used, and daily industry returns are calculated as the value-weighted average of firm-level returns.

Following Herskovic et al. (2016), I estimate a common factor model for the daily return observations within each month, taking the residual return as the idiosyncratic return. The common factors are the Fama-French three factors, but the results are robust to other factor models.[31] Monthly idiosyncratic volatility is then calculated as the standard deviation of daily idiosyncratic returns. Log volatility (*logvol*) is used in the subsequent analyses.[32]

[29] A data limitation prevents the estimation at the firm level, as the estimation method, which will be described below, requires non-missing idiosyncratic volatility values for all sectors throughout the entire sample period.

[30] Penny stocks with absolute prices below \$5 are excluded, and delisting returns are accounted for. CRSP data is sourced from WRDS.

[31] The results are robust under various conditions: (1) after including penny stocks; (2) using different sector classifications; and (3) when removing common factors using PC5 factors, the CAPM factor, or even without removing common factors. For further details, refer to the Online Appendix C.5.

[32] The serial correlation of volatility is accounted for in the following empirical procedures using a VAR model.

Subsequently, I measure idiosyncratic volatility spillovers following the methods of Diebold and Yilmaz (2014) and Demirer et al. (2018). For each rolling window of 90 months, I estimate a LASSO Vector Autoregression (VAR) model of the volatility panel and then perform a Generalized Variance Decomposition (GVD) for the 6-month-ahead forecasting error.[33]

The VAR(1) model is estimated for the 48×90 volatility panel:

$$\begin{bmatrix} logvol_{1,t} \\ logvol_{2,t} \\ logvol_{3,t} \\ \vdots \\ logvol_{48,t} \end{bmatrix} = \begin{bmatrix} \phi^0_{1,t} \\ \phi^0_{2,t} \\ \phi^0_{3,t} \\ \vdots \\ \phi^0_{48,t} \end{bmatrix} + \begin{bmatrix} \phi_{1,1,t} & \cdots & \phi_{1,48,t} \\ \phi_{2,1,t} & \cdots & \phi_{2,48,t} \\ \phi_{3,1,t} & \cdots & \phi_{3,48,t} \\ \vdots & \ddots & \vdots \\ \phi_{48,1,t} & \cdots & \phi_{48,48,t} \end{bmatrix} \begin{bmatrix} logvol_{1,t-1} \\ logvol_{2,t-1} \\ logvol_{3,t-1} \\ \vdots \\ logvol_{48,t-1} \end{bmatrix} + \begin{bmatrix} \varepsilon^{VAR}_{1,t} \\ \varepsilon^{VAR}_{2,t} \\ \varepsilon^{VAR}_{3,t} \\ \vdots \\ \varepsilon^{VAR}_{48,t} \end{bmatrix}, \tag{25}$$

where $\phi_{i,j,t}$'s represent the coefficients of the VAR model, and $\varepsilon^{VAR}_{i,t}$'s are the forecasting errors.

This VAR model needs to be estimated in a high-dimensional setting. Following Demirer et al. (2018), I use LASSO to estimate the parameters. LASSO automatically imposes sparsity in the coefficients and is a computationally efficient method for both shrinkage and selection. The regularization parameter is selected equation by equation using 10-fold cross-validation.[34] Then, I perform a GVD for the forecasting error, to derive the pairwise directional risk spillover measure.[35] GVD gives us the elements $\{\delta_{ij}\}$'s where each δ_{ij} represents the proportion of sector i's future

Based on Andersen, Bollerslev, Diebold, and Labys (2003) and Diebold and Yilmaz (2014), the log of realized volatilities approximates normality.

[33]Following Demirer et al. (2018), the rolling window length is chosen to be approximately 1.5 to 2 times the number of sectors. I demonstrate that the empirical results are robust across rolling window lengths ranging from 80 to 100 months. Additionally, results remain robust across forecasting periods ranging from 6 to 10 months. See details in the Online Appendix C.6.

[34]While traditional methods like informative-prior Bayesian VAR and ridge regression offer pure shrinkage, and criteria such as Akaike Information Criterion provide pure selection, LASSO offers a compelling blend of both. The estimate uses a penalty term consisting of 0.5 L^1 penalty plus 0.5 L^2 penalty, and the regularization parameter is selected equation by equation through cross-validation. See details in Demirer et al. (2018).

[35]Generalized variance decomposition offers greater stability compared to the standard Cholesky-based variance decomposition as it is invariant to variable ordering.

uncertainty explained by shock spillover from sector j. Mechanically, the δ_{ij} from GVD is derived as follows:

$$\delta_{ij} = \frac{\Sigma_{jj}^{-1} \sum_{h=0}^{H-1} \left(e_i' \Theta_h \Sigma e_j\right)^2}{\sum_{h=0}^{H-1} \left(e_i' \Theta_h \Sigma \Theta_h' e_i\right)}, \tag{26}$$

where $H = 6$, e_i is the unit vector with the ith element as 1 and all others zero, Σ is the variance-covariance matrix of the residual $\varepsilon_{i,t}^{VAR}$, and Σ_{jj} is the jth diagonal element of Σ. Θ_h represents the VAR coefficients in Equation (25) multiplied by the h-lagged shock vector in the infinite MA representation.

The elements δ_{ij} from GVD provide the empirical counterpart to the shock spillover measure in Equation (18). Although LASSO induces sparsity in the coefficients, the volatility spillovers, δ_{ij}, derived from the GVD—which is a nonlinear function of the coefficients—are not sparse. This aligns with our intuition that risk spillovers should not be sparse.

I then construct the dynamic adjacency matrices. At each time t, the matrix Δ_t is formed by collecting the $\{\delta_{ij}\}$'s estimated from a rolling window spanning from month $t - 90$ to t.

Adjacency matrix Δ_t

	IND_1	IND_2	$\cdots$	IND_{48}
IND_1	$\delta_{1,1,t}$	$\delta_{1,2,t}$	$\cdots$	$\delta_{1,48,t}$
IND_2	$\delta_{2,1,t}$	$\delta_{2,2,t}$	$\cdots$	$\delta_{2,48,t}$
$\vdots$	$\vdots$	$\vdots$	$\ddots$	$\vdots$
IND_{48}	$\delta_{48,1,t}$	$\delta_{48,2,t}$	$\cdots$	$\delta_{48,48,t}$

Finally, the two network factors DOM_t and INT_t are constructed according to the definitions in Equation (19).

3.2 Time Series of Network Factors

Figure 4 presents the time series of network factors covering the period from June 1976 to December 2019 at a monthly frequency,[36] with the upper panel showing factor levels and the lower panel displaying factor innovations, measured as the AR(1) residuals of the factor levels.

In Figure 4, the *DOM* factor (blue dotted line) exhibits procyclical behavior, dropping during each recession.[37] To better understand the procyclicality, I compare the state of the economy before and during the 2008 recession. Figure 5 presents the average adjacency matrices for two periods: (1) the year prior to the 2008 recession and (2) the period during the 2008 recession. Nodes represent sectors and edges denote idiosyncratic risk spillovers. Node size indicates spillover outdegree $Out_{i,t}$. The 48 sectors maintain fixed positions in both figures.

The left panel appears very "concentrated". In normal times (left panel), financial sectors (e.g., banking, trading, insurance) appear to dominate idiosyncratic volatility spillover, while sectors like real estate, transportation, and utilities seem peripheral. During the recession (right panel), the distribution appears more "even", with peripheral sectors seemingly gaining importance and overall dominance degree within the economy decreasing. One possible explanation for this shift could be that during recessions, distress in peripheral sectors might lead to stronger risk spillovers back to central sectors. For example, in 2008, failures in the real estate sector may have impacted the broader market due to banks' presumed extensive holdings of mortgage-backed securities. Additionally, the poor financial health of peripheral sectors might render them ineligible for loans, amplifying their risk spillover to core financial sectors and the broader market. Other mechanisms could also contribute to the procyclicality of the *DOM* factor, though they fall beyond the scope of this paper.

[36] This period is derived after accounting for a 90-month LASSO VAR rolling window based on an initial dataset starting in January 1969.

[37] The *DOM* innovation shows a 0.15 (p=0.00) correlation with the PD ratio, confirming its procyclicality.

Figure 4. Time Series Plots of the Network Factors.
This figure shows the time series of *INT* (red solid line) and *DOM* (blue dotted line), covering the period from June 1976 to December 2019 at monthly frequency. The upper panel presents the time series for factor levels, while the lower panel illustrates the time series for factor innovations, measured as the AR(1) residuals of the factor levels. The shaded areas represent NBER recession periods.

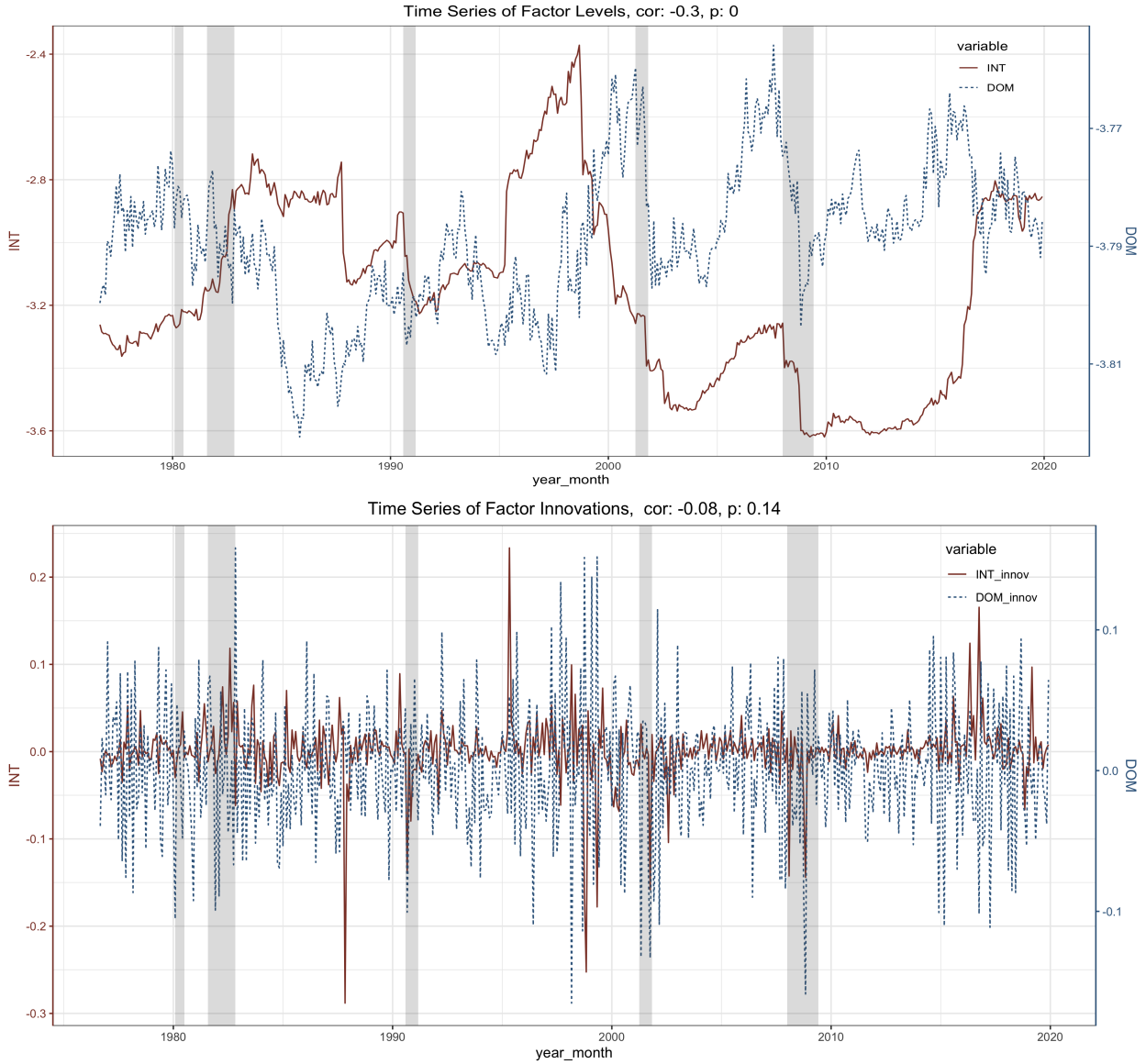
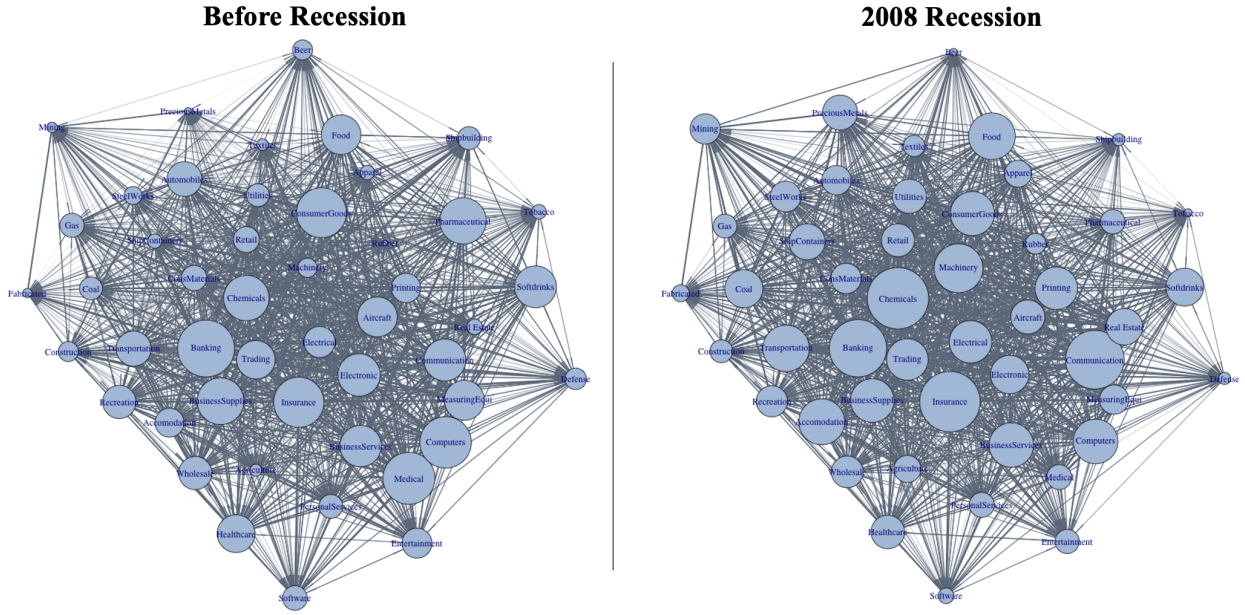


Figure 5. Network Plots Among Fama-French 48 Industries.
This figure presents the average adjacency matrices across Fama-French 48 industries for two periods: (1) the year prior to the 2008 recession and (2) the period during the 2008 recession. The monthly adjacency matrix is constructed based on Equation (26), with matrices averaged over the respective periods. The edges represent $\delta_{ij,t}$, indicating idiosyncratic risk spillover, with the thickness of each edge corresponding to the magnitude of $\delta_{ij,t}$. The nodes represent sectors, with their size determined by the spillover outdegree $Out_{i,t}$. The industries are plotted at fixed positions for consistency across periods.



The *INT* factor (red solid line) exhibits complex dynamics, with an upward shift in the late 1990s, a downward shift around 2000, and another upward shift after 2015. Various factors could drive these dynamics. For example, the rise in *INT* might be attributed to technological shocks introducing new firm-specific risks that firms struggle to diversify, as the late 1990s saw the rise of the internet, and the post-2015 period marked the advent of AI and business digitization. The decline in *INT* around 2000 might be due to increasing market power or other reasons, as firms possibly became more efficient at mitigating product-specific shocks.[38]

[38] As noted by Clara, Corhay, and Kung (2021), post-2004 saw a rise in industry HHI alongside a decrease in firms' Product Concentration Measure. Gaspar and Massa (2006) suggest that market power might buffer against idiosyncratic fluctuations and reduce investor information uncertainty, potentially explaining the reduced spillover effects.

Overall, this figure suggests that the *DOM* factor seems to reflect the business cycle, while the *INT* factor is likely to reflect market structure changes. Other mechanisms may drive these dynamics, but they are beyond the scope of this paper. The goal of this paper is to take these dynamics as given (as outlined in model Assumption 1) and explore their implications. Although beyond the scope of this paper, I provide more discussions of potential drivers behind the network dynamics in the Online Appendix D.2. Idiosyncratic volatility is not yet well understood, and these dynamics could be subjects for future studies.

3.3 Network Factors and Aggregate Volatility

Given the dynamics of idiosyncratic risk spillover, I explore its implications by examining: (1) how network factors affect diversification speed; and (2) how network factors affect aggregate volatility.

3.3.1 Risk Diversification Speed

I investigate how network factors affect risk diversification and the decay rate of aggregate volatility. The Lucas diversification argument posits that when the network is completely symmetric, idiosyncratic risks are quickly averaged out under the CLT. According to Equation (21), aggregate volatility decays rapidly to its mean, with a speed proportional to $\sqrt{n}$. Specifically, assuming an economy with 2000 firms and an average sectoral idiosyncratic volatility of 0.06, as estimated by Acemoglu et al. (2012), we would expect idiosyncratic volatility to cause approximately $0.06 \times \frac{1}{\sqrt{2000}} = 0.1\%$ aggregate volatility. This is negligible. It indicates that idiosyncratic shocks tend to be diversified and do not translate into significant aggregate volatility under the diversification argument.

However, under an asymmetric input-output network, aggregate volatility decays more slowly. Proposition 2 posits that the decay rate of aggregate volatility depends on two network factors. Based on Equation (22), aggregate volatility has a limit infimum, i.e., lower bound, of $\frac{1}{\sqrt[4]{n}}\sqrt{\frac{DOM_t}{INT_t}}$. I

examine the distribution of this lower bound across various sector classifications, including Fama-French 48 sectors, Fama-French 12 sectors, NAICS 2-digit, NAICS 3-digit, SIC 3-digit, and SIC 4-digit. For each sector classification, I repeat the entire empirical process to construct the time series of *DOM* and *INT*. I then calculate the factor ratio $\sqrt{\frac{DOM_t}{INT_t}}$ and report the corresponding summary statistics.

Table 1. Summary Statistics for Lower Bound.

This table reports the time series mean, minimum, maximum, and standard deviation for $\sqrt{\frac{DOM_t}{INT_t}}$ under different sector specifications. For each sector specification, the network factors are constructed at a monthly frequency by following the procedures outlined in section 3.1. The results are presented row by row, from the most aggregate level of 12 sectors (FF12 sectors) to the most disaggregated level of 153 sectors (SIC 3-digit).

Sector Specification	Mean	Min	Max	Std
12 sectors (FF12 sectors)	1.15	1.07	1.32	0.05
15 sectors (NAICS 2-digit)	1.17	1.03	1.50	0.12
48 sectors (FF48 sectors)	1.10	1.02	1.26	0.05
59 sectors (NAICS 3-digit)	1.15	1.04	1.37	0.09
139 sectors (SIC 4-digit)	1.08	1.04	1.15	0.03
153 sectors (SIC 3-digit)	1.07	1.03	1.14	0.03

Table 1 displays the time-series mean, minimum, maximum, and standard deviation for the ratio $\sqrt{\frac{DOM_t}{INT_t}}$ across various sector specifications. Under the most granular SIC 3-digit classification, the time-series mean of $\sqrt{\frac{DOM_t}{INT_t}}$ is 1.07, with a standard deviation of 0.03.[39] Using the mean value from the SIC 3-digit specification as an example, a sectoral idiosyncratic volatility of 0.06 will translate to $0.06 \times \frac{1}{\sqrt[4]{2000}} \times 1.07 = 1\%$ aggregate volatility. This magnitude is ten times that in the Lucas diversification argument.

[39] Due to methodological constraints, only sectors with non-missing idiosyncratic volatility values throughout the period are included. The maximum number of sectors achievable is 153, as per the SIC 3-digit classification.

This result highlights the crucial role of an asymmetric input-output network in impeding risk diversification and moderating the decay of aggregate volatility. Throughout the entire sample period, as shown in Table 1, the network factors consistently exert a significant effect on hindering the decay of aggregate volatility.

3.3.2 Time Series Prediction

I further investigate whether dynamic network factors can predict aggregate volatility. Monthly real consumption data (including nondurables and services) are sourced from the Federal Reserve Economic Data (FRED), spanning from 1983 to 2019.[40][41] Consumption growth, $\Delta \ln \xi_t$, is calculated as the first difference of the logarithm of consumption. Following Equation (24), I estimate the conditional mean of consumption growth by regressing consumption growth on lagged consumption growth and lagged network factors. I then take the residual, u_{t+1}, as the demeaned consumption growth. Monthly aggregate volatility is computed using either the absolute residual $|u_{t+1}|$ or the squared residual u_{t+1}^2. Variables are aggregated to quarterly frequency to smooth out noise in consumption data, with quarterly volatility calculated as the sum of monthly volatility values and quarterly factors taken at the end of the month.

I test the predictability of the network factors for consumption-based volatility by regressing the aggregate volatility (moving averaged across quarter t to quarter $t+m$) onto lagged *DOM* (at t) and lagged *INT* (at t), controlling for lagged volatility (at t). Table 2 reports the results using 2-quarter, 8-quarter, and 12-quarter moving averages. The standard errors are adjusted for autocorrelation using the Newey-West method with lag m.

The first column shows that *DOM* predicts negative volatility, moving averaged across 2 quarters. Across the second and third columns, the effect from *DOM* diminishes, while the effect from *INT*

[40] For more details, see https://fred.stlouisfed.org/tags/series?t=consumption.

[41] Analysis using quarterly consumption data from BEA NIPA tables yields similar findings.

gradually emerges and becomes more significant, and we can see *INT* predicts positive volatility significantly. This indicates that *DOM*'s effect is more pronounced at shorter horizons, while *INT* predicts aggregate volatility over longer horizons. This is consistent with the time series observation that *INT* is very slow-moving. More importantly, this result verifies the model prediction in Equation (23) where aggregate volatility is a linear function of both factors, with *DOM* decreasing it while *INT* increases it.

Table 2. Network Factors and Consumption-based Volatility.
This table presents the predictive regressions of network factors for consumption-based aggregate volatility over the sample period from April 1983 to December 2019. The aggregate volatility is at quarterly frequency and is computed as the sum of monthly volatilities, where the monthly volatility is calculated as the conditional standard deviation of monthly aggregate consumption growth. The dependent variable is the aggregate volatility moving averaged across t to $t+m$ quarters. The independent variables include lagged DOM at t, and lagged INT at t. The control variable is lagged volatility at t. Columns (1), (2), and (3) display the regression results for 2-quarter, 8-quarter, and 12-quarter moving averages, respectively. Standard errors, reported in parentheses, are adjusted for autocorrelation using the Newey-West method with lag m. *, **, and *** denote statistical significance at the 10%, 5%, and 1% levels, respectively.

Dep. Var:	(Moving Averaged) Consumption-based Volatility		
	(1) 2 quarters	(2) 8 quarters	(3) 12 quarters
Lagged DOM (×100)	-1.371*	-0.076	0.735
	(0.801)	(0.824)	(0.826)
Lagged INT (×100)	1.127	2.035***	2.590***
	(0.825)	(0.942)	(1.035)
Controls	x	x	x
R^2	0.152	0.232	0.253

Since the consumption data is very noisy, which could influence the significance of the factors, I also use alternative volatility measures to conduct predictability tests. I employ three monthly volatility measures: realized market volatility (computed as the monthly volatility of daily market returns), financial uncertainty, and macro uncertainty, with the latter two from Jurado, Ludvigson, and Ng (2015). I regress volatility (moving averaged across month t to month $t+24$) onto lagged

DOM (at t) and lagged *INT* (at t), controlling for lagged volatility (at t). Table 3 reports the results, with standard errors adjusted for autocorrelation using the Newey-West method with lag m.

Table 3. Network Factors and Alternative Volatility Measures.
This table presents the predictive regressions of network factors for alternative volatility measures over the sample period from April 1983 to December 2019, at a monthly frequency. The volatility measures are the realized market volatility (computed as the monthly volatility of daily market returns), financial uncertainty, and macro uncertainty, with the latter two from Jurado, Ludvigson, and Ng (2015). The dependent variable is the volatility moving averaged across t to $t+24$ months. The independent variables include lagged DOM at t, and lagged INT at t. The control variable is lagged volatility at t. Standard errors, reported in parentheses, are adjusted for autocorrelation using the Newey-West method with lag m. *, **, and *** denote statistical significance at the 10%, 5%, and 1% levels, respectively.

Dep. Var:	(MA24m) Market Volatility	(MA24m) JLN's Uncertainty	
	Realized Volatility	Financial Uncertainty	Macro Uncertainty
Lagged DOM	-2.196**	-0.230**	-0.238**
	(0.958)	(0.112)	(0.125)
Lagged INT	1.676**	0.302***	0.071
	(0.744)	(0.060)	(0.087)
Controls	x	x	x
R^2	0.293	0.550	0.598

From Table 3, we can see that *DOM* predicts a negative volatility, significantly, across different volatility measures. *INT* predicts a positive volatility significantly. These results further confirm the predictability of the network factors for aggregate volatility, confirming the story: when *INT* is high, idiosyncratic risks are less easily washed out and more likely to raise aggregate volatility. When *DOM* is high, the state mimics a normal time where fewer sectors serve as potential risk propagators; idiosyncratic risks are more easily averaged out, and aggregate volatility drops.

3.4 Network Factors in Asset Pricing

I further take these network factors to the cross-section and test the asset pricing implications.

3.4.1 Network Factor-beta Sorted Portfolios

I sort all CRSP stocks based on their exposures to the network factors and form value-weighted or equal-weighted portfolios accordingly. Stock excess returns $R^e_{i,t}$ are regressed against network innovations ΔINT_t and ΔDOM_t, while controlling for market, size, value, lagged *INT* level, and lagged *DOM* level:[42]

$$R^e_{i,t} = \alpha^{sort}_{i,t} + \beta^{INT}_t \times \Delta INT_t + \beta^{DOM}_t \times \Delta DOM_t + Controls_t + \epsilon^{sort}_{i,t}, \tag{27}$$

where β^{INT}_t and β^{DOM}_t measure stocks' exposures to the two factor innovations, respectively.

For each month t, stocks' factor exposures are computed using the regression in Equation (27) over an 80-month trailing window from $t-80$ to t.[43] Stocks are then sorted into terciles based on each beta separately (single sort), and value-weighted or equal-weighted portfolios are formed for the subsequent month $t+1$. This procedure is repeated as a trailing window until the last month of the sample. The average returns of the single-sorted portfolios are reported in Table 4, along with return volatilities, Sharpe ratios, and post-sample alphas from the CAPM model, the Fama-French three-factor (FF3) model, the FF3+Momentum (4 factor) model, and the FF3+Momentum+Liquidity (5 factor) model.[44] For portfolios constructed based on the high-minus-low (*H-L*) strategy, GRS test statistics and GRS p-values for the alphas are also reported.

[42]The controls are not crucial for the outcomes. Omitting these controls or adding additional ones, such as market volatility innovations, does not affect the results. For detailed analysis, refer to the Online Appendix C.5.

[43]The selection of an 80-month trailing window serves to differentiate from the previously utilized 90-month rolling window in the LASSO VAR analysis. The portfolio sorting outcomes are robust to varying trailing window lengths from 60 to 100 months. The benchmark analysis incorporates all CRSP firm-level stocks without penny stocks. The results are robust to the inclusion of penny stocks. For further details, refer to the Online Appendix C.6.

[44]Factor models include the CAPM from Sharpe (1964), Fama-French 3 factors from Fama and French (1993), FF3 + Momentum, and FF3 + Momentum + Liquidity from Pástor and Stambaugh (2003). The market return, FF3 factors, momentum factor, risk-free rate, and definitions of Fama-French 12 sectors and Fama-French 48 sectors are sourced from Kenneth French's website: https://mba.tuck.dartmouth.edu/pages/faculty/ken.french/data_library.html. The liquidity factor is sourced from Lubos Pastor's website: https://faculty.chicagobooth.edu/lubos-pastor/data.

Table 4. Single Sorted Portfolios.
This table reports annualized average excess returns, volatilities, and Sharpe ratios for portfolios sorted by monthly *INT* beta and *DOM* beta, along with post-sample alphas from the CAPM, Fama-French three-factor (FF3) model, FF3 + Momentum (4-factor) model, and FF3 + Momentum + Liquidity (5-factor) model. For alphas from *H-L* portfolios, GRS test statistics and GRS p-values are also provided. Panel A presents the value-weighted portfolio results, while Panel B presents the equal-weighted results.

Panel A: Value-weighted

	Risk-Intensity Factor							Risk-Dominance Factor						
	1	2	3	H-L	t	grs stat	grs p	1	2	3	H-L	t	grs stat	grs p
Ave.Exc.Ret	0.129	0.107	0.091	-0.038	-2.558			0.089	0.103	0.135	0.046	2.023		
Volatility	0.166	0.139	0.159	0.092				0.155	0.141	0.167	0.090			
Sharpe ratio	0.779	0.767	0.569	-0.419				0.571	0.728	0.807	0.513			
α_{CAPM}	0.005	0.004	0.002	-0.003	-2.139	4.576	0.033	0.002	0.003	0.005	0.003	2.533	6.414	0.012
α_{FF3}	0.003	0.002	0.000	-0.003	-2.389	5.710	0.017	0.000	0.001	0.003	0.003	2.296	5.273	0.022
$\alpha_{4factor}$	0.004	0.002	0.000	-0.004	-2.900	8.412	0.004	0.001	0.002	0.005	0.004	3.014	9.087	0.003
$\alpha_{5factor}$	0.004	0.002	0.001	-0.004	-2.765	7.645	0.006	0.001	0.002	0.005	0.004	2.988	8.933	0.003

Panel B: Equal-weighted

	Risk-Intensity Factor							Risk-Dominance Factor						
	1	2	3	H-L	t	grs stat	grs p	1	2	3	H-L	t	grs stat	grs p
Ave.Exc.Ret	0.132	0.103	0.092	-0.040	-2.539			0.091	0.101	0.134	0.043	2.001		
Volatility	0.164	0.137	0.163	0.093				0.153	0.141	0.171	0.096			
Sharpe ratio	0.804	0.748	0.563	-0.434				0.595	0.715	0.786	0.447			
α_{CAPM}	0.005	0.003	0.002	-0.003	-2.382	5.672	0.018	0.002	0.003	0.005	0.003	2.093	4.380	0.037
α_{FF3}	0.004	0.002	0.000	-0.004	-2.721	7.406	0.007	0.001	0.001	0.003	0.003	1.968	3.925	0.038
$\alpha_{4factor}$	0.005	0.002	0.000	-0.004	-3.158	9.974	0.002	0.001	0.002	0.004	0.003	2.076	4.310	0.039
$\alpha_{5factor}$	0.005	0.002	0.000	-0.004	-2.899	8.407	0.004	0.001	0.002	0.004	0.003	2.198	4.831	0.029

Panels A and B report these moments for the value-weighted and equal-weighted portfolios, respectively. In Panel A, stocks with higher exposure to *INT* earn lower risk premiums, with the *H-L* strategy yielding an annual return spread of -0.038 with a t-statistic of -2.558. This implies that stocks with higher *INT*-beta serve as hedges against increases in marginal utility and are expected to earn lower risk premiums. The GRS statistics for the *H-L* alphas are significant, suggesting that

the *H-L* portfolio cannot be explained by the existing factor models. On the right side of Panel A, stocks with higher exposure to *DOM* earn higher risk premiums, with the *H-L* strategy yielding an annual return spread of 0.046 with a t-statistic of 2.023. This suggests that stocks with a high β_t^{DOM} are perceived as riskier, thus commanding a higher risk premium. The significant GRS statistics for the *H-L* alphas indicate that these *H-L* portfolios cannot be explained by the existing factor models.[45]

3.4.2 Prices of Risk

To assess the prices of risk associated with these factors, I conduct a Fama-MacBeth analysis (Fama and MacBeth, 1973). The first stage involves estimating the factor betas for each test asset by regressing their monthly excess returns on a constant and the selected asset pricing factors. In the second stage, a cross-sectional regression is performed, where the excess returns of the test assets are regressed on the previously estimated factor betas and a constant. The time-series average of the coefficients from the second stage represents the prices of risk (λ) associated with the factors.

The test assets are chosen based on the model mechanism. According to Propositions 2 and 3, the two network factors affect the aggregate market by influencing aggregate volatility, which in turn impacts firms' investment behavior. Therefore, I mainly consider volatility-related and investment-related anomaly portfolios as test assets. The following four groups of test assets are considered: (1) 60 volatility-related test assets (VOL60) including aggregate volatility, market-beta, idiosyncratic volatility, realized volatility, idiosyncratic skewness, and trading volume; (2) VOL60 plus 10 *INT*-beta sorted portfolios and 10 *DOM*-beta sorted portfolios (VOL80); (3) 70 investment-related test assets (INV70) including size, investment, profitability, cash flow, dividend,

[45]Results are robust for double sorting. See the Online Appendix C.4. Results are robust when removing the intermediary sectors. See the Online Appendix D.4. For firms that are more exposed to network factors, see the Online Appendix D.3.

earnings, and accruals; and (4) all test assets combined (ALL150). Detailed specifications of the test portfolios are provided in the Online Appendix C.1.

For the asset pricing factors, both a benchmark model (Fama-French 5 factor (FF5) model) and a comparison model (FF5+*INT*+*DOM*) are considered.[46] *INT* and *DOM* are the High-minus-Low (H-L) mimicking factors from the tercile sorting.[47]

For each factor model, the two stages are estimated concurrently using the Generalized Method of Moments (GMM) framework, with standard errors adjusted for autocorrelation and heteroskedasticity using Newey-West lag 1 corrections (Newey and West, 1987). Table 5 presents the estimated prices of risk (λ), along with their t-statistics.

Columns 1 and 2 in Table 5 report the results using the comprehensive set of all 150 test portfolios. The comparison between these two columns shows that incorporating *DOM* and *INT* into the factor model enhances the cross-sectional R^2 from 0.37 to 0.45. The price of risk for *DOM* is estimated to be 0.41, with a t-statistic of 2.25. The price of risk for *INT* is -0.49, with a t-statistic of -2.49. Both estimates are statistically significant, implying that these network factors are priced in volatility- or investment-related anomalies. The signs of the prices of risk align with the asset pricing implications of the model. Specifically, when investors are averse to volatility risk and prefer an early resolution of uncertainty, an increase in *INT* raises marginal utility, resulting in a negative price of risk for *INT* innovations. In contrast, an increase in *DOM* lowers marginal utility, leading to a positive price of risk for *DOM* innovations. Similar outcomes are observed for other test assets, such as VOL80, INV70, and INV90. Additionally, the estimates of the prices of risks for the network factors are consistent across different test assets, underscoring the robustness of the

[46]The FF5 model is used as a benchmark because pricing investment- or volatility-related anomalies requires investment-related factors like RMW and CMA.

[47]Both factors cover the period from April 1983 to December 2019. This period is derived after accounting for a 90-month LASSO VAR rolling window and an 80-month portfolio sorting window, based on an initial dataset starting in January 1969.

network factors.

Table 5. Fama-MacBeth for FF5+DOM+INT
This table presents the estimated price of risk (λ) for the factors, with t-statistics adjusted using Newey-West standard errors reported in parentheses. VOL80 represents 80 volatility-related test assets (detailed in Section 3.4.2), INV70 consists of 70 investment-related test assets (also detailed in that section), and INV90 includes INV70 along with 10 *INT*-beta sorted portfolios and 10 *DOM*-beta sorted portfolios. ALL150 encompasses all 150 test assets. For each test assets, two factor models are considered. One is FF5 and another is FF5 +*DOM*+*INT*. The last row reports the cross-sectional R^2 and the second to last row reports the mean absolute pricing error in percentage values. The time range spans from April 1983 to December 2019, at a monthly frequency. The sample period is derived after accounting for a 90-month LASSO VAR rolling window and an 80-month portfolio sorting window, based on an initial dataset starting in January 1969.

	ALL150		VOL80		INV70		INV90	
Const	0.54	0.69	0.36	0.48	0.60	0.85	0.51	0.71
t	(2.37)	(3.13)	(1.08)	(1.64)	(2.72)	(3.90)	(2.22)	(3.40)
Mkt.Rf	0.37	0.22	0.49	0.37	0.33	0.07	0.39	0.19
t	(1.20)	(0.72)	(1.22)	(1.00)	(1.09)	(0.25)	(1.29)	(0.65)
SMB	0.18	0.15	0.30	0.28	0.12	0.11	0.20	0.16
t	(1.27)	(1.11)	(2.07)	(1.97)	(0.90)	(0.76)	(1.39)	(1.19)
HML	-0.02	0.01	-0.55	-0.55	0.05	0.09	0.03	0.07
t	(-0.16)	(0.07)	(-2.48)	(-2.71)	(0.29)	(0.59)	(0.18)	(0.44)
RMW	0.43	0.39	0.59	0.58	0.33	0.28	0.33	0.27
t	(3.18)	(2.85)	(3.06)	(3.02)	(2.47)	(2.04)	(2.54)	(2.04)
CMA	0.16	0.12	0.19	0.13	0.14	0.11	0.16	0.12
t	(1.45)	(1.14)	(0.78)	(0.56)	(1.26)	(1.06)	(1.52)	(1.18)
DOM		**0.41**		**0.38**		**0.47**		**0.39**
t		**(2.25)**		**(2.06)**		**(2.14)**		**(2.12)**
INT		**-0.49**		**-0.52**		**-0.47**		**-0.46**
t		**(-2.49)**		**(-2.59)**		**(-2.35)**		**(-2.34)**
MAPE%	0.11	0.10	0.11	0.10	0.10	0.10	0.12	0.11
R^2	0.37	0.45	0.57	0.59	0.24	0.34	0.22	0.31

To examine whether the network factors retain their pricing power when additional factors are

included, the asset pricing models are augmented with the *CIV* factor documented in Herskovic et al. (2016).[48] I then conduct the Fama-MacBeth analysis by considering the following two factor models: (1) FF5 + *CIV*; and (2) FF5 + *CIV* + *DOM* + *INT*.

Table 6 summarizes the findings. Columns 1 and 2 report the results using the comprehensive set of all 150 test portfolios. Column 2 shows that the addition of *DOM* and *INT* to the six-factor model increases the cross-sectional R^2 from 0.39 to 0.44. Both *DOM* and *INT* are significantly priced, even in the presence of *CIV*, suggesting that the network factors are robust in asset pricing models.

The Online Appendix (section C) includes additional tests confirming the robustness of the network factors *DOM* and *INT*. These tests demonstrate the following: (1) The factors are priced in other double-sorted anomaly portfolios (section C.2); (2) The factors remain priced when including the annual input-output network factors documented in Herskovic (2018) (section C.3); (3) The factors produce consistent return spreads in double-sorting (section C.4); (4) Factor betas effectively capture firms' importance within the network and thus serve as other ways to measure systemic risk (section D.1); (5) The robustness of portfolio sorting is validated across various parameters (e.g., rolling window lengths for LASSO VAR, forecasting periods for GVD, and trailing windows for portfolio sorting), control variables, and alternative network factor measurements, reinforcing the reliability of *DOM* and *INT* in asset pricing (section C.6 and section C.5); (6) The portfolio sorting outcomes remain consistent even after excluding financial sectors (i.e., banking, trading, and insurance), indicating that the empirical results are not solely driven by the intermediary sector (section D.4); and (7) A comparison between volatility spillover factors and return spillover factors reveals that the market efficiently absorbs return spillover information, but volatility spillovers contain additional systematic risk (section D.6).

[48]The *CIV* factor, representing a common factor in firms' idiosyncratic volatility as identified by Herskovic et al. (2016), has significant asset pricing implications. The data is sourced from Herskovic's website.

Table 6. Fama-MacBeth for FF5+DOM+INT+CIV

This table presents the estimated price of risk (λ) for the factors, with t-statistics adjusted using Newey-West standard errors reported in parentheses. VOL80 represents 80 volatility-related test assets (detailed in Section 3.4.2), INV70 consists of 70 investment-related test assets (also detailed in that section), and INV90 includes INV70 along with 10 *INT*-beta sorted portfolios and 10 *DOM*-beta sorted portfolios. ALL150 encompasses all 150 test assets. For each test assets, two factor models are considered. One is FF5+*CIV* and another is FF5 +*CIV*+*DOM*+*INT*. The last row reports the cross-sectional R^2 and the second to last row reports the mean absolute pricing error in percentage values. The time range spans from April 1983 to December 2019, at a monthly frequency. The sample period is derived after accounting for a 90-month LASSO VAR rolling window and an 80-month portfolio sorting window, based on an initial dataset starting in January 1969.

	ALL150		VOL80		INV70		INV90	
Const	0.58	0.71	0.39	0.49	0.63	0.86	0.52	0.71
t	(2.56)	(3.27)	(1.21)	(1.73)	(2.83)	(3.91)	(2.27)	(3.40)
Mkt.RF	0.32	0.19	0.46	0.35	0.29	0.06	0.37	0.19
t	(1.10)	(0.65)	(1.19)	(1.01)	(0.97)	(0.20)	(1.23)	(0.65)
SMB	0.16	0.14	0.27	0.24	0.11	0.10	0.19	0.16
t	(1.11)	(0.99)	(1.87)	(1.68)	(0.81)	(0.73)	(1.35)	(1.18)
HML	0.00	0.02	-0.49	-0.51	0.07	0.10	0.04	0.07
t	(0.00)	(0.14)	(-2.43)	(-2.63)	(0.41)	(0.60)	(0.25)	(0.44)
RMW	0.42	0.38	0.55	0.52	0.36	0.30	0.36	0.28
t	(3.11)	(2.81)	(2.99)	(2.90)	(2.64)	(2.24)	(2.67)	(2.14)
CMA	0.15	0.12	0.21	0.18	0.13	0.12	0.16	0.13
t	(1.43)	(1.20)	(0.96)	(0.94)	(1.20)	(1.12)	(1.51)	(1.21)
CIV	**-2.15**	**-1.84**	**-1.64**	**-2.19**	**-2.66**	**-1.45**	**-1.77**	**-0.85**
t	**(-2.02)**	**(-1.83)**	**(-1.33)**	**(-2.01)**	**(-1.93)**	**(-1.23)**	**(-1.37)**	**(-0.77)**
DOM		**0.41**		**0.37**		**0.43**		**0.39**
t		**(2.23)**		**(2.02)**		**(2.25)**		**(2.13)**
INT		**-0.49**		**-0.52**		**-0.47**		**-0.47**
t		**(-2.45)**		**(-2.61)**		**(-2.40)**		**(-2.37)**
MAPE%	0.10	0.09	0.11	0.10	0.10	0.10	0.12	0.11
R^2	0.39	0.44	0.58	0.60	0.28	0.35	0.24	0.31

4 Calibration

In this section, to assess whether the model can quantitatively match the asset pricing moments from the portfolio sorting, I calibrate a reduced-form structural model of the general equilibrium framework, where I solve for the SDF and calibrate the cross-section.

4.1 Setup

The general equilibrium model builds upon the framework developed by Herskovic (2018), who demonstrates that the consumption growth process can be decomposed into three components: the Concentration Factor, the Sparsity Factor, and a Total Factor Productivity (TFP) shock, with innovations to all of these being exogenous. Therefore, while the consumption growth process arises endogenously in the general equilibrium model, it still contains exogenous components. By assuming some persistence in the TFP shock (or in the Concentration or Sparsity Factors), a long-run risk component in consumption growth emerges. In this paper, the novel contribution lies in the second moment: I demonstrate that the volatility of the long-run risk component is a linear function of the network factors—*INT* and *DOM*—as shown in Proposition 3. Consequently, the consumption growth process can be framed within a long-run risk framework (see Bansal and Yaron (2004)):

$$\begin{aligned} \Delta \ln \xi_{t+1} &= x_t + \sigma_t \vartheta_{t+1} \\ x_{t+1} &= \rho^x x_t + \rho^e \sigma_t e^x_{t+1} \\ \sigma_t^2 &= \nu_0 + \nu_1 \mathcal{N}_t^{INT} + \nu_2 \mathcal{N}_t^{DOM}, \end{aligned} \tag{28}$$

where ϑ_{t+1} and e^x_{t+1} are independent standard normal variables.

The network factors follow an AR(1) process:

$$\begin{aligned} \mathcal{N}_{t+1}^{INT} &= \rho^{INT}\mathcal{N}_t^{INT} + \sigma^{INT}e_{t+1}^{INT} \\ \mathcal{N}_{t+1}^{DOM} &= \rho^{DOM}\mathcal{N}_t^{DOM} + \sigma^{DOM}e_{t+1}^{DOM}, \end{aligned} \tag{29}$$

where e_{t+1}^{INT} and e_{t+1}^{DOM} are independent standard normal variables.

In the consumption growth process described in Equation (28), x_t represents the long-run risk, summarizing the persistent components in TFP shocks or Concentration and Sparsity Factors. ϑ_{t+1} captures temporary shocks. The long-run risk component x_t follows an AR(1) process characterized by an autoregressive coefficient ρ^x, stochastic volatility σ_t, and a loading ρ^e on the volatility component, as per Bansal and Yaron (2004).

Following Proposition 3, I model volatility as a linear function of *INT* and *DOM*. The loading ν_1 is assumed to be positive to reflect the positive impact of *INT* on volatility, while ν_2 is assumed to be negative to capture the inverse effect of *DOM*. I further specify the processes for *INT* and *DOM* as AR(1) processes in Equation (29). The AR(1) coefficients are denoted by ρ^{INT} and ρ^{DOM}, with volatilities denoted by σ^{INT} and σ^{DOM}, respectively.

This setup serves as a structural counterpart to the general equilibrium model. While the long-run risk component x_t is necessary to generate a high risk premium, it is not the focus of this study. The primary focus is on the volatility process, wherein the aggregate volatility emerges from the dynamics of idiosyncratic risk spillover.

The specification of the unlevered consumption claim follows.

Return on Total Wealth: The first-order approximation of the return on total wealth is given by

$$r_{t+1}^{w} = \kappa_0^c + \Delta \ln \xi_{t+1} + \kappa_1^c wc_{t+1} - wc_t, \tag{30}$$

where $\kappa_0^c = \ln(\exp(\mu_{wc}) + 1) - \frac{\exp(\mu_{wc})}{\exp(\mu_{wc})+1}\mu_{wc}$, $\kappa_1^c = \frac{\exp(\mu_{wc})}{\exp(\mu_{wc})+1} < 1$ and μ_{wc} is the unconditional average of the wealth-consumption ratio (wc_t). I guess and verify that the wealth-consumption ratio in Equation (30) is linear on the long-run risk component and the two network factors:

$$wc_t = \mu_{wc} + A_0 x_t + A_1 \mathcal{N}_t^{INT} + A_2 \mathcal{N}_t^{DOM}. \tag{31}$$

Substituting the wealth-consumption ratio in the unlevered return approximation yields:

$$r_{t+1}^w = r_0^c + \beta_x x_t + \beta_I \mathcal{N}_t^{INT} + \beta_D \mathcal{N}_t^{DOM} + \beta_{\varepsilon,e}\sigma_t e_{t+1}^x + \beta_{\varepsilon,\vartheta}\sigma_t \vartheta_{t+1} + \beta_{\varepsilon,I}\sigma^{INT} e_{t+1}^{INT} + \beta_{\varepsilon,D}\sigma^{DOM} e_{t+1}^{DOM}. \tag{32}$$

Parameters in Equation (31) and (32) are specified in the Online Appendix B.1.

Stochastic Discount Factor: Let $\theta \equiv \frac{1-\gamma}{1-\rho}$. The SDF is derived as follows:

$$m_{t+1} = \lambda_0 + \lambda_x x_t + \lambda_I \mathcal{N}_t^{INT} + \lambda_D \mathcal{N}_t^{DOM} + \lambda_{\varepsilon,e}\sigma_t e_{t+1}^x + \lambda_{\varepsilon,\vartheta}\sigma_t \vartheta_{t+1} + \lambda_{\varepsilon,I}\sigma^{INT} e_{t+1}^{INT} + \lambda_{\varepsilon,D}\sigma^{DOM} e_{t+1}^{DOM}, \tag{33}$$

where

$$\begin{aligned}
\lambda_0 &= \theta \ln d + (\theta - 1) r_0^c \\
\lambda_x &= -\rho\theta + (\theta - 1)\beta_x \\
\lambda_I &= (\theta - 1)\beta_I \\
\lambda_D &= (\theta - 1)\beta_D \\
\lambda_{\varepsilon,e} &= (\theta - 1)\beta_{\varepsilon,e} \\
\lambda_{\varepsilon,\vartheta} &= (\theta - 1)\beta_{\varepsilon,\vartheta} - \rho\theta \\
\lambda_{\varepsilon,I} &= (\theta - 1)\beta_{\varepsilon,I} \\
\lambda_{\varepsilon,D} &= (\theta - 1)\beta_{\varepsilon,D}.
\end{aligned} \tag{34}$$

The Euler equation for the return on total wealth is given by

$$\mathbb{E}_t\left[m_{t+1} + r_{t+1}^w\right] + \frac{1}{2} Var_t\left(m_{t+1} + r_{t+1}^w\right) = 0. \tag{35}$$

In Equation (35), setting the constant and coefficients before x_t, $\mathcal{N}_t^{INT}$ and $\mathcal{N}_t^{DOM}$ to zero yields the solution to μ_{wc}, A_0, A_1 and A_2, which further leads to the solution for the parameters in Equations (32) and (33). All solutions are specified in the Online Appendix B.1.

The Signs of the λ's: Here I analyze the signs of the prices of risks to demonstrate the consistency of this structural framework with the model. According to Equation (34), the expressions for the solutions of λ_I and λ_D are given by

$$\begin{aligned}\lambda_I &= \frac{1}{2}\nu_1\theta(1-\theta)\left[(\kappa_1^c A_0\rho^e)^2 + (1-\rho)^2\right] \\ \lambda_D &= \frac{1}{2}\nu_2\theta(1-\theta)\left[(\kappa_1^c A_0\rho^e)^2 + (1-\rho)^2\right],\end{aligned} \tag{36}$$

where ν_1 is assumed to be positive and ν_2 is assumed to be negative. To obtain the correct signs of the λ coefficients in Equation (36), it must be assumed that the representative household has a preference for the early resolution of uncertainty. This assumption ensures that $\rho < \gamma$, resulting in a negative θ. As a result, λ_I is negative and λ_D is positive. Thus, the early preference assumption is crucial to ensure that *INT* is priced as a negative risk and *DOM* is priced as a positive risk.

The processes for the levered market dividend and individual portfolio dividend are specified in the Online Appendix B.1.

4.2 Parameters and Calibrated Model

Table 7 presents the calibrated parameter values. The majority of parameters are calibrated based on existing literature, while factor-related parameters, including autocorrelation and volatility, are calibrated using empirical data. All parameters align precisely with the data, except for the persistence of the *DOM* factor, which I adjust to make it more persistent. This calibration produces a negative price of risk for *INT* ($\lambda_I = -0.547$) and a positive price of risk for *DOM* ($\lambda_D = 0.478$) in

the SDF. These results align with the signs of the prices of risk observed in the empirical findings.

Table 7. Calibration Parameters.
This table presents the calibrated parameter values. The parameters for risk aversion, EIS, discount rate, labor proportion to scale, and long-run risk are calibrated based on the literature. All factor-related parameters, such as factor ACF, standard deviations of innovations, and volatility loadings on factors, are calibrated using data.

Parameters		Value	Target
γ	Risk aversion	10	Bansal and Yaron (2004)
$\frac{1}{\rho}$	EIS	1.5	Bansal and Yaron (2004)
ψ	Discount (monthly)	1.02	Average risk-free rate
η	Labor proportion to scale	0.65	Herskovic (2018)
ν_0	unconditional mean of volatility	0.0078^2	Bansal and Yaron (2004)
ν_1	Volatility loading on *INT* (monthly)	0.0026	Empirical OLS estimate
ν_2	Volatility loading on *DOM* (monthly)	-0.0023	Empirical OLS estimate
ρ^{INT}	ACF(1) of *INT*	0.99	Sample ACF(1): 0.99
ρ^{DOM}	ACF(1) of *DOM*	0.99	Sample ACF(1): 0.93
σ^{INT}	Standard deviation of *INT* innovation	0.006	Sample standard deviation:0.006
σ^{DOM}	Standard deviation of *DOM* innovation	0.002	Sample standard deviation:0.002
ρ^x	ACF(1) of long-run risk	0.979	Bansal and Yaron (2004)
ρ^e	loading on stochastic volatility	0.044	Bansal and Yaron (2004)

Table 8 presents the asset pricing moments implied by the model. Panel A displays the risk premium for individual portfolios in both the data and the model. For the model-implied risk premium, I further break down its components, including the long-run risk component x, *INT* level, *DOM* level, and the short-run component ϑ. Panel B shows the volatility for individual portfolios in both the data and the model. For the model-implied volatility, I further decompose it into the following sources: the long-run risk innovation e^x, *INT* innovation e^{INT}, *DOM* innovation e^{DOM}, the short-run innovation ϑ, and individual portfolio's idiosyncratic risk ϵ^i.

Table 8. Model Implied Asset Pricing Moments.
This table presents the asset pricing moments implied by the model. Panel A displays the risk premium for individual portfolios (including the market portfolio and factor-beta sorted portfolios) in both the data and the model. Panel A also includes the decomposition of the model-implied risk premium, breaking it down into the long-run risk component x, *INT* level, *DOM* level, and the short-run component ϑ. Panel B shows the volatility for individual portfolios in both the data and the model. Panel B further includes the decomposition of the model-implied volatility, sourced from the long-run risk innovation e^x, *INT* innovation e^{INT}, *DOM* innovation e^{DOM}, the short-run innovation ϑ, and individual portfolio's idiosyncratic risk ϵ^i.

	Market	Risk-Intensity Sorted			Risk-Dominance Sorted		
		1	2	3	1	2	3
Panel A: (Annualized) ERP decomposition							
Data (%)	16.10	12.91	10.72	9.13	8.91	10.32	13.52
Model (%)	16.11	12.23	10.83	10.02	8.51	10.20	12.12
x	14.87	9.13	9.12	9.25	10.15	9.30	8.95
INT	-0.04	-0.84	-0.39	-0.02	1.12	-0.07	-0.86
DOM	0.05	1.01	0.47	0.03	-1.34	0.09	1.03
ϑ	1.24	2.94	1.63	0.77	-1.42	0.88	3.00
Panel B: (Annualized) Volatility decomposition							
Data (%)	15.54	16.61	13.89	15.87	15.53	14.08	16.73
Model (%)	14.31	14.92	15.19	15.69	15.73	14.38	17.92
e^x	5.75	9.46	8.87	6.16	9.64	6.64	11.35
e^{INT}	0.35	1.62	1.56	0.37	2.52	0.76	1.92
e^{DOM}	0.20	0.93	0.90	0.21	1.45	0.44	1.11
ϑ	5.06	2.64	3.06	5.46	1.50	4.34	3.13
ϵ^i	2.94	0.27	0.80	3.49	0.62	2.21	0.41

Panel A shows that the model's calibration closely matches the risk premium of the market and each individual portfolio. Notably, the model delivers a return spread (-2.21% for *INT* and 3.61% for *DOM*) that closely mirrors the empirical data (-3.78% for *INT* and 4.61% for *DOM*). The decomposition reveals that the risk premiums are primarily driven by the long-run risk component

x. Panel B shows that the model-implied volatility for individual portfolios aligns well with the data. The decomposition shows that the volatility in individual portfolios is primarily driven by the volatility of the long-run risk innovation, along with the volatility of the *INT* and *DOM* innovations. The volatility of the long-run risk innovation is influenced by the levels of the network factors. This is consistent with the model's mechanism, where the two network factors are identified as volatility risk factors. The detailed calibration of the cross-section is specified in the Online Appendix B.2.

5 Conclusion

In this paper, I characterize the dynamics of idiosyncratic volatility spillovers using two network factors—*INT* and *DOM*—and demonstrate that they influence risk diversification across sectors and have a long-term impact on aggregate volatility. A long-short portfolio based on *INT*-beta delivers an annual return spread of -4%, as stocks more exposed to *INT* serve as hedges against rising marginal utility. Conversely, a long-short portfolio based on *DOM*-beta delivers an annual return spread of 5%, as stocks more exposed to *DOM* are riskier and require higher compensation.

This paper is the first to analyze network dynamics from a second-moment perspective and reveal the asset pricing implications of these dynamics. It offers a comprehensive approach to modeling and understanding network risk. The existing network literature studies firms' networks from a first-moment perspective—focusing on the connection of cash flows or returns—and relies heavily on input-output data, which is of annual frequency. In contrast, this paper adopts a novel perspective—specifically, a second-moment view—to analyze firms' networks. This perspective allows for the use of alternative high-frequency data to uncover more detailed and informative economic dynamics. Moreover, the findings in this paper elucidate the origins of aggregate volatility and shed light on why idiosyncratic volatility is priced—because its spillovers have a

significant and persistent aggregate impact.

While in this paper I trace idiosyncratic volatility spillovers back to input-output relationships, it is important to acknowledge that other mechanisms may also drive this spillovers. For instance, spillovers can occur through credit relationships, cross-holdings of assets, and other channels.[49] Future research could extend this paper by exploring spillover effects through these additional mechanisms and determining the relative contribution of each.

In addition, future studies could further examine the implications for co-movement of idiosyncratic volatilities. While in my model the co-movement is directly implied by the network structure, there has been no rigorous examination of how changes in the network structure affect the co-movement of idiosyncratic volatilities. Any theoretical implications could guide the construction of an alternative empirical measure for this co-movement.

Finally, as idiosyncratic risks evolve into systematic risks, there are potential policy implications that warrant further investigation. Policymakers should intervene with different sectors to prevent a fragile network structure and avoid cascading effects. Future research could decompose the formation of network structures into stages, identifying which sectors trigger the initial wave of contagion, followed by subsequent waves. This approach could inform more targeted intervention strategies for policymakers, allowing them to mitigate systematic risks from the outset.

[49] For a detailed enumeration of potential channels through which idiosyncratic volatility spillover may occur, please refer to the Online Appendix E.3.

References

Acemoglu, Daron, Ufuk Akcigit, and William Kerr, 2016, Networks and the macroeconomy: An empirical exploration, *NBER Macroeconomics Annual* 30, 273–335.

Acemoglu, Daron, Vasco M Carvalho, Asuman Ozdaglar, and Alireza Tahbaz-Salehi, 2012, The network origins of aggregate fluctuations, *Econometrica* 80, 1977–2016.

Acemoglu, Daron, Asuman Ozdaglar, and Alireza Tahbaz-Salehi, 2017, Microeconomic origins of macroeconomic tail risks, *American Economic Review* 107, 54–108.

Acharya, Viral, Robert Engle, and Matthew Richardson, 2012, Capital shortfall: A new approach to ranking and regulating systemic risks, *American Economic Review* 102, 59–64.

Adrian, Tobias, and Markus K Brunnermeier, 2011, Covar, Technical report, National Bureau of Economic Research.

Adrian, Tobias, and Joshua Rosenberg, 2008, Stock returns and volatility: Pricing the short-run and long-run components of market risk, *The Journal of Finance* 63, 2997–3030.

Ahern, Kenneth R, 2013, Network centrality and the cross section of stock returns, *Available at SSRN 2197370* .

Ahern, Kenneth R, and Jarrad Harford, 2014, The importance of industry links in merger waves, *The Journal of Finance* 69, 527–576.

Andersen, Torben G, Tim Bollerslev, Francis X Diebold, and Paul Labys, 2003, Modeling and forecasting realized volatility, *Econometrica* 71, 579–625.

Ang, Andrew, Robert J Hodrick, Yuhang Xing, and Xiaoyan Zhang, 2006, The cross-section of volatility and expected returns, *The Journal of Finance* 61, 259–299.

Ang, Andrew, Robert J Hodrick, Yuhang Xing, and Xiaoyan Zhang, 2009, High idiosyncratic volatility and low returns: International and further us evidence, *Journal of Financial Economics* 91, 1–23.

Bansal, Ravi, Dana Kiku, Ivan Shaliastovich, and Amir Yaron, 2014, Volatility, the macroeconomy, and asset prices, *The Journal of Finance* 69, 2471–2511.

Bansal, Ravi, Dana Kiku, and Amir Yaron, 2010, Long run risks, the macroeconomy, and asset prices, *American Economic Review* 100, 542–546.

Bansal, Ravi, and Amir Yaron, 2004, Risks for the long run: A potential resolution of asset pricing puzzles, *The Journal of Finance* 59, 1481–1509.

Belo, Frederico, 2010, Production-based measures of risk for asset pricing, *Journal of Monetary Economics* 57, 146–163.

Bianconi, Ginestra, 2007, The entropy of randomized network ensembles, *EPL (Europhysics Letters)* 81, 28005.

Bianconi, Ginestra, 2009, Entropy of network ensembles, *Physical Review E* 79, 036114.

Binsbergen, Jules H Van, 2016, Good-specific habit formation and the cross-section of expected returns, *The Journal of Finance* 71, 1699–1732.

Bloom, Nicholas, Max Floetotto, Nir Jaimovich, Itay Saporta-Eksten, and Stephen J Terry, 2018, Really uncertain business cycles, *Econometrica* 86, 1031–1065.

Bloom, Nick, Stephen Bond, and John Van Reenen, 2007, Uncertainty and investment dynamics, *The Review of Economic Studies* 74, 391–415.

Boguth, Oliver, and Lars-Alexander Kuehn, 2013, Consumption volatility risk, *The Journal of Finance* 68, 2589–2615.

Bonacich, Phillip, 1972, Factoring and weighting approaches to status scores and clique identification, *Journal of Mathematical Sociology* 2, 113–120.

Bonacich, Phillip, and Paulette Lloyd, 2001, Eigenvector-like measures of centrality for asymmetric relations, *Social Networks* 23, 191–201.

Branger, Nicole, Patrick Konermann, Christoph Meinerding, and Christian Schlag, 2021, Equilibrium asset pricing in directed networks, *Review of Finance* 25, 777–818.

Brownlees, Christian T, Robert Engle, et al., 2012, Volatility, correlation and tails for systemic risk measurement, *Available at SSRN* 1611229.

Burres, David, 1994, Homeomorphism between leontief and cobb-douglas input-output models, *Economics Letters* 44, 49–53.

Carvalho, Vasco, and Xavier Gabaix, 2013, The great diversification and its undoing, *American Economic Review* 103, 1697–1727.

Carvalho, Vasco M, 2008, *Aggregate fluctuations and the network structure of intersectoral trade* (The University of Chicago).

Chen, Hui, Winston Wei Dou, Hongye Guo, and Yan Ji, 2023, Feedback and contagion through distressed competition, Technical report, National Bureau of Economic Research.

Clara, Nuno, Alexandre Corhay, and Howard Kung, 2021, Firm product concentration and asset prices, *Available at SSRN 3488428* .

Cohen, Lauren, and Andrea Frazzini, 2008, Economic links and predictable returns, *The Journal of Finance* 63, 1977–2011.

Corhay, Alexandre, Howard Kung, and Lukas Schmid, 2020, Competition, markups, and predictable returns, *The Review of Financial Studies* 33, 5906–5939.

Croce, Mariano Massimiliano, 2014, Long-run productivity risk: A new hope for production-based asset pricing?, *Journal of Monetary Economics* 66, 13–31.

Demirer, Mert, Francis X Diebold, Laura Liu, and Kamil Yilmaz, 2018, Estimating global bank network connectedness, *Journal of Applied Econometrics* 33, 1–15.

Dew-Becker, Ian, 2023, Tail risk in production networks, *Econometrica* 91, 2089–2123.

Diebold, Francis X, and Kamil Yilmaz, 2012, Better to give than to receive: Predictive directional measurement of volatility spillovers, *International Journal of Forecasting* 28, 57–66.

Diebold, Francis X, and Kamil Yilmaz, 2014, On the network topology of variance decompositions: Measuring the connectedness of financial firms, *Journal of Econometrics* 182, 119–134.

Elliott, Matthew, Benjamin Golub, and Matthew O Jackson, 2014, Financial networks and contagion, *American Economic Review* 104, 3115–53.

Engle, Robert, and Bryan Kelly, 2012, Dynamic equicorrelation, *Journal of Business & Economic Statistics* 30, 212–228.

Fama, Eugene F, and Kenneth R French, 1993, Common risk factors in the returns on stocks and bonds, *Journal of Financial Economics* 33, 3–56.

Fama, Eugene F, and James D MacBeth, 1973, Risk, return, and equilibrium: Empirical tests, *Journal of Political Economy* 81, 607–636.

Farboodi, Maryam, and Péter Kondor, 2022, Heterogeneous global booms and busts, *American Economic Review* 112, 2178–2212.

Gabaix, Xavier, 1999, Zipf's law for cities: an explanation, *The Quarterly Journal of Economics* 114, 739–767.

Gabaix, Xavier, 2009, Power laws in economics and finance, *Annu. Rev. Econ.* 1, 255–294.

Gabaix, Xavier, 2011, The granular origins of aggregate fluctuations, *Econometrica* 79, 733–772.

Gabaix, Xavier, Parameswaran Gopikrishnan, Vasiliki Plerou, and H Eugene Stanley, 2003, A theory of power-law distributions in financial market fluctuations, *Nature* 423, 267–270.

Gaspar, José-Miguel, and Massimo Massa, 2006, Idiosyncratic volatility and product market competition, *The Journal of Business* 79, 3125–3152.

Gofman, Michael, Gill Segal, and Youchang Wu, 2020, Production networks and stock returns: The role of vertical creative destruction, *The Review of Financial Studies* 33, 5856–5905.

Gomes, Joao F, Leonid Kogan, and Motohiro Yogo, 2009, Durability of output and expected stock returns, *Journal of Political Economy* 117, 941–986.

Gomes, Joao F, and Lukas Schmid, 2012, Equilibrium credit spreads and the macroeconomy, *The Wharton School Research Paper* .

Grant, Everett, and Julieta Yung, 2019, Upstream, downstream & common firm shocks, *Globalization and Monetary Policy Institute Working Paper* .

Grigoris, Fotis, Yunzhi Hu, and Gill Segal, 2023, Counterparty risk: Implications for network linkages and asset prices, *The Review of Financial Studies* 36, 814–858.

Grigoris, Fotis, and Gill Segal, 2021, Investment under up-and downstream uncertainty, *Unpublished working paper. Indiana University* .

Herskovic, Bernard, 2018, Networks in production: Asset pricing implications, *The Journal of Finance* 73, 1785–1818.

Herskovic, Bernard, Bryan Kelly, Hanno Lustig, and Stijn Van Nieuwerburgh, 2016, The common factor in idiosyncratic volatility: Quantitative asset pricing implications, *Journal of Financial Economics* 119, 249–283.

Herskovic, Bernard, Bryan Kelly, Hanno Lustig, and Stijn Van Nieuwerburgh, 2020, Firm volatility in granular networks, *Journal of Political Economy* 128, 4097–4162.

Hou, Kewei, Haitao Mo, Chen Xue, and Lu Zhang, 2019, Which factors?, *Review of Finance* 23, 1–35.

Irvine, Paul J, and Jeffrey Pontiff, 2009, Idiosyncratic return volatility, cash flows, and product market competition, *The Review of Financial Studies* 22, 1149–1177.

Jackson, Matthew O, and Agathe Pernoud, 2021, Systemic risk in financial networks: A survey, *Annual Review of Economics* 13, 171–202.

Jermann, Urban J, 1998, Asset pricing in production economies, *Journal of Monetary Economics* 41, 257–275.

Jermann, Urban J, 2010, The equity premium implied by production, *Journal of Financial Economics* 98, 279–296.

Jermann, Urban J, 2013, A production-based model for the term structure, *Journal of Financial Economics* 109, 293–306.

Jurado, Kyle, Sydney C Ludvigson, and Serena Ng, 2015, Measuring uncertainty, *American Economic Review* 105, 1177–1216.

Khan, Aubhik, and Julia K Thomas, 2008, Idiosyncratic shocks and the role of nonconvexities in plant and aggregate investment dynamics, *Econometrica* 76, 395–436.

Kogan, Leonid, Dimitris Papanikolaou, and Noah Stoffman, 2013, Winners and losers: Creative destruction and the stock market, Technical report, National Bureau of Economic Research.

Kuehn, Lars-Alexander, 2009, Disentangling investment returns and stock returns: The importance of time-to-build, in *EFA 2007 Ljubljana Meetings Paper, AFA 2010 Atlanta Meetings Paper*.

Kuehn, Lars-Alexander, and Lukas Schmid, 2014, Investment-based corporate bond pricing, *The Journal of Finance* 69, 2741–2776.

Kung, Howard, and Lukas Schmid, 2015, Innovation, growth, and asset prices, *The Journal of Finance* 70, 1001–1037.

Lochstoer, Lars A, 2009, Expected returns and the business cycle: Heterogeneous goods and time-varying risk aversion, *The Review of Financial Studies* 22, 5251–5294.

Long Jr, John B, and Charles I Plosser, 1983, Real business cycles, *Journal of Political Economy* 91, 39–69.

Lucas, Robert E, 1995, Understanding business cycles, *Essential Readings in Economics* 306–327.

Menzly, Lior, and Oguzhan Ozbas, 2010, Market segmentation and cross-predictability of returns, *The Journal of Finance* 65, 1555–1580.

Newey, Whitney K, and Kenneth D West, 1987, A simple, positive semi-definite, heteroskedasticity and autocorrelation consistent covariance matrix, *Econometrica* 703–708.

Pástor, L'uboš, and Robert F Stambaugh, 2003, Liquidity risk and expected stock returns, *Journal of Political Economy* 111, 642–685.

Robert, Claudine, 1990, An entropy concentration theorem: applications in artificial intelligence and descriptive statistics, *Journal of Applied Probability* 27, 303–313.

Sharpe, William F, 1964, Capital asset prices: A theory of market equilibrium under conditions of risk, *The Journal of Finance* 19, 425–442.

Smirnyagin, Vladimir, and Aleh Tsyvinski, 2022, Macroeconomic and asset pricing effects of supply chain disasters, Technical report, National Bureau of Economic Research.

Yogo, Motohiro, 2006, A consumption-based explanation of expected stock returns, *The Journal of Finance* 61, 539–580.

Internet Appendix

A Model Proof **65**

A.1 Solve Firm's Problem . . . 65
A.2 Solve Household's Problem . . . 65
A.3 Sales Share . . . 67
A.4 Risk-less Claim . . . 68
A.5 Proof of Aggregate Output . . . 69
A.6 Proof of Proposition 1 . . . 70
A.7 Proof of Proposition 2 . . . 71
A.8 Proof of Proposition 3 . . . 74

B Structural Estimate **75**

B.1 Stochastic Discount Factor Derivation . . . 75
B.2 Calibration . . . 80

C Robustness of Network Factors **80**

C.1 Anomaly Portfolios in Fama-MacBeth Analysis . . . 80
C.2 Other Double-sorted Anomalies . . . 81
C.3 Fama-MacBeth Analysis with Input-output Network Factors . . . 82
C.4 Robustness of Double Sorting . . . 84
C.5 Robustness of Alternative Measurements . . . 86
C.6 Robustness of Different Parameters . . . 90

D Additional Empirical Analysis **90**

D.1 Are Network Factors Other Ways to Measure Systemic Risk? . . . 90
D.2 Other Mechanisms Behind the Network Dynamics . . . 93
D.3 Which Firms Are More Exposed to Network Factors? . . . 95
D.4 The Role of Intermediary Sectors . . . 96
D.5 Time Series Plots of Representative Sectors . . . 97
D.6 Return-based and Volatility-based Network Factors . . . 99

E Additional Conceptual Demonstration **101**

E.1 Why Use Negative Entropy to Measure Dominance? 101

E.2 Difference Between Input-Output Matrix and Volatility Spillover Matrix 103

E.3 Channels for Idiosyncratic Volatility Spillover 104

A Model Proof

A.1 Solve Firm's Problem

$$D_{i,t} = \max_{\{x_{ij,t}\},\{l_{i,t}\}} P_{i,t}y_{i,t} - \sum_{j=1}^{n} P_{j,t}x_{ij,t} - h_t l_{i,t}$$

s.t.

$$y_{i,t} = e^{z_{i,t}} \zeta_i l_{i,t}^{\eta} \prod_{j=1}^{n} x_{ij,t}^{(1-\eta)\omega_{ij,t}}$$

FOC with respect to $\{x_{ij,t}\}$ and $l_{i,t}$ yields that

$$\begin{cases} x_{ij,t} = \dfrac{(1-\eta)\,\omega_{ij,t} P_{i,t} y_{i,t}}{P_{j,t}} \\ l_{i,t} = \dfrac{\eta P_{i,t} y_{i,t}}{h_t} \end{cases}$$

A.2 Solve Household's Problem

The household maximization problem is

$$J_t\left(P_t, s_t, Q_t, h_t\right) = \max_{\{c_{i,t}, s_{i,t+1}\}} \left[(1-\psi)\, C_t^{1-\rho} + \psi \left(\mathbb{E}_t \left(J_{t+1}^{1-\gamma} \right) \right)^{\frac{1-\rho}{1-\gamma}} \right]^{\frac{1}{1-\rho}}$$

with respect to the intertemporal budget constraint:

$$\sum_{i=1}^{n} P_{i,t} c_{i,t} + \sum_{i=1}^{n} \left(V_{i,t} - D_{i,t} \right) s_{i,t+1} = \sum_{i=1}^{n} V_{i,t} s_{i,t} + h_t$$

The cum-dividend value of firm i, denoted as $V_{i,t}$, is computed recursively using Equation (7). Let λ_t be the Lagrange multiplier.

$$\max_{\{c_{i,t}, s_{i,t+1}\}} \left[(1-\psi)\, C_t^{1-\rho} + \psi \left(\mathbb{E}_t \left(J_{t+1}^{1-\gamma} \right) \right)^{\frac{1-\rho}{1-\gamma}} \right]^{\frac{1}{1-\rho}} - \lambda_t \left[\sum_{i=1}^{n} P_{i,t} c_{i,t} + \sum_{i=1}^{n} \left(V_{i,t} - D_{i,t} \right) s_{i,t+1} - \sum_{i=1}^{n} V_{i,t} s_{i,t} - h_t \right]$$

FOC with respect to $c_{i,t}$ yields $(1-\psi)\, J_t^{\rho} C_t^{-\rho} \frac{\partial C_t}{\partial c_{i,t}} = \lambda_t P_{i,t}$ where $\frac{\partial C_t}{\partial c_{i,t}} = \frac{\alpha_i}{c_{i,t}} C_t$. This further

leads to

$$\frac{\frac{\partial C_t}{\partial c_{i,t}}}{\frac{\partial C_t}{\partial c_{j,t}}} = \frac{P_{i,t}}{P_{j,t}}$$

$$c_{i,t} = \frac{\alpha_i \left(1-\psi\right) J_t^{\rho} C_t^{-\rho}}{\lambda_t P_{i,t}}$$

$$\frac{c_{i,t}P_{i,t}}{\alpha_i} = \frac{c_{j,t}P_{j,t}}{\alpha_j} \equiv \xi_t$$

$$\sum_i c_{i,t}P_{i,t} = (\sum_i \alpha_i)\xi_t = \xi_t$$

$$\therefore\ c_{i,t} = \frac{\alpha_i \xi_t}{P_{i,t}}$$

FOC with respect to $s_{i,t+1}$ yields $J_t^{\rho}\psi\mathbb{E}_t\left[J_{t+1}^{1-\gamma}\right]^{\frac{\gamma-\rho}{1-\gamma}}\mathbb{E}_t\left[J_{t+1}^{-\gamma}\frac{\partial J_{t+1}}{\partial s_{i,t+1}}\right] = \lambda_t Q_{i,t} = 0.$

Following the envelop theorem:

$$\begin{aligned}
\frac{\partial J_t}{\partial s_{i,t}} &= \frac{\partial J_t}{\partial s_{i,t+1}}\frac{\partial s_{i,t+1}}{\partial s_{i,t}} \\
&= \lambda_t Q_{i,t}\frac{V_{i,t}}{Q_{i,t}} \quad \text{(due to budget constraint)} \\
&= \lambda_t V_{i,t} \\
&= \left(1-\psi\right) J_t^{\rho} C_t^{-\rho}\frac{\partial C_t}{\partial c_{1,t}}\frac{1}{P_{1,t}}\left(D_{i,t}+Q_{i,t}\right)
\end{aligned}$$

Evaluate it one period ahead and plug it into the FOC:

$$\begin{aligned}
J_t^{\rho}\psi\mathbb{E}_t\left[J_{t+1}^{1-\gamma}\right]^{\frac{\gamma-\rho}{1-\gamma}}\mathbb{E}_t\left[J_{t+1}^{-\gamma}\left(1-\psi\right)J_{t+1}^{\rho}c_{t+1}^{-\rho}\frac{\partial C_{t+1}}{\partial c_{1,t+1}}\frac{1}{P_{1,t+1}}\left(D_{i,t+1}+Q_{i,t+1}\right)\right] &= \lambda_t Q_{i,t} \\
&= \left(1-\psi\right)J_t^{\rho}C_t^{-\rho}\frac{\partial C_t}{\partial c_{1,t}}\frac{1}{P_{1,t}}Q_{i,t}
\end{aligned}$$

Reorganizing the equation yields the pricing function:

$$\mathbb{E}_t\left[\underbrace{\psi\left(\frac{C_{t+1}}{C_t}\right)^{-\rho}\frac{\frac{\partial C_{t+1}}{\partial c_{1,t+1}}/P_{1,t+1}}{\frac{\partial C_t}{\partial c_{1,t}}/P_{1,t}}\left(\frac{J_{t+1}}{\mathbb{E}_t\left(J_{t+1}^{1-\gamma}\right)^{\frac{1}{1-\gamma}}}\right)^{\rho-\gamma}}_{\equiv M_{t+1}}\underbrace{\frac{D_{i,t+1}+Q_{i,t+1}}{Q_{i,t}}}_{\equiv R_{i,t+1}}\right]=1$$

Here I normalize the spot price: $\frac{\partial C_t}{\partial c_{i,t}}/P_{i,t}=1$. This normalization leads to the following relationship

$$\frac{\partial C_t}{\partial c_{i,t}}/P_{i,t}=\frac{\alpha_i}{P_{i,t}}\prod_{j=1}^{n}\left(\frac{\alpha_j P_{i,t}}{\alpha_i P_{j,t}}\right)^{\alpha_j}=\prod_{j=1}^{n}\left(\frac{\alpha_j}{P_{j,t}}\right)^{\alpha_j}=1$$

$$\therefore\ \prod_{j=1}^{n}P_{j,t}^{\alpha_j}=\prod_{j=1}^{n}\alpha_{j,t}^{\alpha_j}$$

$$\therefore\ C_t=\prod_{j=1}^{n}C_{j,t}^{\alpha_j}=\prod_{j=1}^{n}\left(\frac{\alpha_j}{P_{j,t}}\right)^{\alpha_j}\xi_t=\xi_t$$

Under the first-order condition, the firm share $s_{i,t+1}$ is chosen such that the pricing equation holds for each asset i.

A.3 Sales Share

I plug in the market clearing condition (11) into the expression for ξ_t:

$$y_{i,t}=\frac{\alpha_i\xi_t}{P_{i,t}}+\sum_{j=1}^{n}\frac{(1-\eta)\,\omega_{ji,t}P_{j,t}y_{j,t}}{P_{i,t}}$$

$$\therefore\ \frac{P_{i,t}y_{i,t}}{\xi_t}=\alpha_i+(1-\eta)\sum_{j=1}^{n}\omega_{ji,t}\left(\frac{P_{j,t+1}y_{j,t+1}}{\xi_{t+1}}\right)$$

$$\therefore\ v_{i,t}\equiv\frac{P_{i,t}y_{i,t}}{\xi_t}=\sum_{j=1}^{n}\alpha_j\tilde{l}_{ji,t}$$

where $\tilde{L}_t \equiv \left[\tilde{l_{ij}}\right]_t = \left(\mathbf{I} - (1-\eta)\,\mathbf{W}_t'\right)^{-1}$ is the Leontief inverse. All sales shares sum up to 1.

$$\sum_{i=1}^{n} v_{i,t} = 1$$

$$\therefore \xi_t = \sum_{i=1}^{n} P_{i,t} y_{i,t} = C_t$$

A.4 Risk-less Claim

The risk-free rate of return is sensitive to the chosen price normalization. For instance, if good 1 is defined as the numeraire, then the risk-free rate of return is the return on a claim to one unit of good 1. However, since all relative prices may change in the next period, this claim remains risky as one unit of good 1 may purchase different quantities of other goods. Consequently, when the household buys such a claim, its payoff (in terms of aggregator utility) is random, as the household will substitute consumption goods to maximize utility.

To address this issue, I define the risk-free rate as the return on a riskless bundle—specifically, a bundle that negates this substitution effect, thereby keeping the aggregator utility constant.

The risk-less claim is a claim to the aggregator utility:

$$\left(\frac{\alpha_1}{P_{1,t}}, \frac{\alpha_2}{P_{2,t}}, \cdots, \frac{\alpha_n}{P_{n,t}}\right)$$

This claim satisfies the intra-period first-order condition and the price of the bundle is 1. It is also a claim to the consumption aggregator due to the price normalization condition. If we purchase m unites of the claim, the return is equal to the consumption aggregator amount.

$$C_t = m \prod_{j=1}^{n} \left(\frac{\alpha_j}{P_{j,t}}\right)^{\alpha_j} \xi_t = m$$

A.5 Proof of Aggregate Output

FOC for firms yields

$$\begin{cases} x_{ij,t} = \dfrac{(1-\eta)\,\omega_{ij,t} v_{i,t} y_{j,t}}{v_{j,t}} \\ \\ l_{i,t} = \eta v_{i,t} \end{cases}$$

Substitute them into the production function:

$$\ln y_{i,t} = z_{i,t} + \ln v_i - (1-\eta) \sum_j \omega_{ij,t} \ln v_j + (1-\eta) \sum_j \omega_{ij} \ln y_{j,t}$$

I write it into matrices:

$$\ln \mathbf{y}_t = \tilde{\mathbf{L}} \mathbf{z_t} + \ln \mathbf{v}_t$$

$$\begin{aligned}
&\because \xi_t v_i = P_{i,t} y_{i,t} \\
&\therefore \ln \xi_t = \ln P_{i,t} + \ln y_{i,t} - \ln v_i \\
&\therefore \sum_i \alpha_i \ln \xi_t = \sum_i \alpha_i \ln P_{i,t} + \sum_i \alpha_i \ln y_{i,t} - \sum_i \alpha_i \ln v_i \\
&\therefore \ln \xi_t = \sum_i \alpha_i \ln \alpha_i + \sum_i \alpha_i \ln y_{i,t} - \sum_i \alpha_i \ln v_i \\
&\therefore \ln \xi_t = \sum_i \alpha_i \ln \alpha_i - \sum_i \alpha_i \ln v_i + \sum_i \alpha_i \left[\sum_k \tilde{l}_{ik,t} z_{k,t} + \ln v_i \right] \\
&\therefore \ln \xi_t = \sum_i \alpha_i \ln \alpha_i + \sum_i \alpha_i \sum_k \tilde{l}_{ik,t} z_{k,t}
\end{aligned}$$

Then I write it into matrices:

$$\begin{aligned}
\ln \xi_t &= \alpha' \ln \alpha + \alpha' \tilde{\mathbf{L}}_t \mathbf{z_t} \\
&= \alpha' \ln \alpha + \mathbf{v}_t' \mathbf{z_t}
\end{aligned}$$

A.6 Proof of Proposition 1

From the production function (1) and the firms' FOC, I can derive the following:

$$\ln y_{i,t} = z_{i,t} + \ln \zeta_i + \eta \ln l_{i,t} + (1-\eta) \sum_{j=1}^{n} \omega_{ij,t} \ln x_{ij,t}$$

$$\ln y_{i,t} = z_{i,t} + \ln \zeta_i + \eta \ln \eta + \eta \ln P_{i,t} + \eta \ln y_{i,t} - \eta \ln h_t + (1-\eta) \sum_{j=1}^{n} \omega_{ij,t} \left[\ln (1-\eta) + \ln \omega_{ij} + \ln P_{i,t} + \ln y_{i,t} - \ln P_{j,t} \right]$$

$$\ln \zeta_i \equiv -\eta \ln \eta - (1-\eta) \ln (1-\eta)$$

$$\therefore \ln P_{i,t} = (1-\eta) \sum_{j=1}^{n} \omega_{ij,t} \ln P_{j,t} - z_{i,t} + \eta \ln h_t - (1-\eta) \sum_{j=1}^{n} \omega_{ij,t} \ln \omega_{ij,t}$$

Write both sides as matrices and use the fact that the sales shares sum to 1, which can be derived from Equation (2). We can have the following expression:

$$\ln \mathbf{P}_t = \tilde{\mathbf{L}}_t \left[\underbrace{-ln\eta^{\eta} (1-\eta)^{1-\eta}}_{constant} \quad \underbrace{-\mathbf{z}_t}_{firm-specific} \quad \underbrace{- (1-\eta) \sum_{i=1}^{n} v_{i,t} \sum_{j=1}^{n} \omega_{ij,t} \ln \omega_{ij,t} + \eta \ln h_t}_{common} \right]$$

The idiosyncratic shock originates from the idiosyncratic productivity shock, denoted as $\mathbf{z}_t$. The final two components—the aggregate market wage ($\ln h_t$) and the average (i.e. sales-share weighted average) of concentration of input ($\sum_{i=1}^{n} v_{i,t} \sum_{j=1}^{n} \omega_{ij,t} \ln \omega_{ij,t}$)—concurrently influence the cross-sectional variation in prices. According to Herskovic (2018), the average Concentration of input is referred to as the Sparsity Factor for the input-output network. The underlying rationale for the Sparsity Factor is that firms adjust their input allocations in response to exogenous demand shocks, such as those from innovations. A higher Sparsity indicates a more concentrated input channel (a more efficient input reallocation) on average. Empirically the author showed that from the input-output data, this factor innovation follows an i.i.d. normal distribution over time. Following Herskovic (2018), I also assume that this Sparsity factor is i.i.d. normal. Consequently, both changes in the market wage and innovations in Sparsity emerge as common shocks affecting the

cross-section of prices, whereas the productivity shock remains uniquely idiosyncratic.

If we hold a claim on the final goods, we can approximate the idiosyncratic equity return and conditional idiosyncratic equity volatility as follows.

$$\Delta \ln \mathbf{P}^*_{t\to t+1} = \tilde{\mathbf{L}}_t \left[\mathbf{z}_t - \mathbf{z}_{t+1}\right]$$
$$Cov_t \left(\Delta \ln \mathbf{P}^*_{t\to t+1}\right) = \sigma^2_{z,t} \tilde{\mathbf{L}}_t \tilde{\mathbf{L}}'_t$$

The second equation comes from the fact that the conditional variation of the idiosyncratic return is determined by the diagonal element of the var-cov matrix. Because all of the eigenvalues of $(1-\eta)\mathbf{W}'_t$ lie within the unit circle, I can write the Leontief inverse as follows:

$$\left(\mathbf{I} - (1-\eta)\,\mathbf{W}'_\mathbf{t}\right)^{-1} = \mathbf{I} + (1-\eta)\,\mathbf{W}'_\mathbf{t} + (1-\eta)^2\,\mathbf{W}'^{\mathbf{2}}_\mathbf{t} + (1-\eta)^3\,\mathbf{W}'^{\mathbf{3}}_\mathbf{t} + \ldots$$

I then use $\mathbf{I} + (1-\eta)\,\mathbf{W}'_t$ as a first-order approximation of the Leontief inverse. For each firm i, the conditional idiosyncratic volatility can be expressed as follows:

$$Var_t \left(\Delta \ln P_{i,t\to t+1}\right) = \sigma^2_z \left[\sum_{k=1}^{i-1} \left((1-\eta)\,\omega_{ik,t}\right)^2 + \left(1 + (1-\eta)\,\omega_{ii,t}\right)^2 + \sum_{k=i+1}^{n} \left((1-\eta)\,\omega_{ik,t}\right)^2\right]$$

From this result, we know that for each sector i, its idiosyncratic equity volatility is not only explained by its own idiosyncratic shock (i.e. $\left(1 + (1-\eta)\,\omega_{ii,t}\right)^2$), but also explained by spillover of other sectors' idiosyncratic shocks (i.e. $\left((1-\eta)\,\omega_{ij,t}\right)^2$).

A.7 Proof of Proposition 2

In the following proof, I omit unnecessary constants. All limitations (lower or upper bounds) are derived under the condition that $n \to \infty$ while time t remains fixed.

$$\Delta \ln \xi_{t\to t+1} = \mathbf{v}' \left(\mathbf{z_{t+1}} - \mathbf{z_t}\right)$$
$$Var_t \left(\Delta \ln \xi_{t\to t+1}\right) = \Theta\left(\|v\|_2^2\right)$$

Conditional on time t, the following proof always holds for the economies $\left\{\mathcal{E}^n_t\right\}_{n\in\mathbb{N}}$. Therefore,

I am going to drop the subscript t for convenience. By assuming $\alpha_i = \frac{1}{n}$, I have

$$\begin{aligned}
\mathbf{v} &= \frac{1}{n}\left[I - W\right]^{-1} \\
&= \frac{1}{n}\left[I + W + ...\right] \\
\|\mathbf{v}\|_2^2 &\geq \frac{1}{n^2}\mathbf{1}'\left[I + W\right]\left[I + W\right]'\mathbf{1} \\
&= \Theta\left(\frac{1}{n^2}\sum_{i=1}^{n} d_i^2\right) \quad \left(\because \frac{1}{n^2}\sum_{i=1}^{n} d_i^2 \text{ dominates } \frac{1}{n} \text{ when n is large}\right)
\end{aligned}$$

Define $\hat{P}_n(k) \equiv \frac{1}{n}\left|\left\{i \in \mathcal{I}_n : d_i^2 > k\right\}\right|$ as the empirical counter-cumulative distribution function of the d_i^2 of economy $\{\mathcal{E}_n\}$. Therefore, by definition $\hat{P}_n(k) = P_n(\sqrt{k})$. I further define $B = \{b_1, ..., b_m\}$ as the set of values that the d_i^2 take, where $b_{k+1} > b_k$ for all k. Then I have

$$\begin{aligned}
\sum_{i=1}^{n} d_i^2 &= n\sum_{k=1}^{m} b_k\left[\hat{P}_n\left(b_{k-1}\right) - \hat{P}_n\left(b_k\right)\right] \\
&= n\sum_{k=0}^{m-1}\left(b_{k+1} - b_k\right)\hat{P}_n\left(b_k\right) \\
&= n\int_0^{b_m} \hat{P}_n(\iota)d\iota \;\; (\text{setting} b_0 = 0) \\
&= 2n\int_0^{d_{max}^n} \iota P_n(\iota)d\iota
\end{aligned}$$

Since I assume there exists a slowly varying function $\mathcal{F}(\cdot)$ such that $\lim_{\iota\to\infty}\mathcal{F}(\iota)\iota^{\delta} = \infty$ for any positive δ, I can derive the lower bound as follows.

$$\begin{aligned}
&\sum_{i=1}^{n} d_i^2 \geq n\hat{c}_n\int_0^{d_{max}^n} \iota^{1-\beta-\delta}d\iota \\
&\therefore Var_t\left(\Delta\ln\xi_{t\to t+1}\right) = \Theta\left(\|v\|_2^2\right) = \Omega\left(n^{\frac{2-2\beta-\delta}{\beta}}\right) \\
&\therefore \sqrt{Var_t\left(\Delta\ln\xi_{t\to t+1}\right)} = \Omega\left(n^{\frac{1-\beta-\frac{1}{2}\delta}{\beta}}\right)
\end{aligned}$$

I derived a lower bound for the conditional aggregate volatility, which is similar to the lower bound of a static model in Acemoglu et al. (2012). It holds for all $\beta \in (1, 2)$ and any positive δ.

Next, I focus on the distribution of our network factors. To be more specific, I analyze the limit of $\frac{DOM}{\sqrt{n}INT}$. By definition,

$$\Delta = \Theta\left(W \odot W\right)$$

Additionally,

$$\begin{aligned}
d_i &\equiv \sum_{j=1}^{n} \omega_{ji} \\
Out_i &\equiv \sum_{j=1}^{n} \omega_{ji}^2 \\
DOM &\equiv \sum_{i} Out_i \ln Out_i \\
INT &\equiv \frac{1}{n} \sum_{i=1}^{n} \sum_{j=1}^{n} \omega_{ij}^2 \ln \omega_{ij}^2
\end{aligned}$$

The DOM and INT are all negative values (i.e. negative entropy) by design. I compute $\frac{DOM}{\sqrt{n}INT}$ as $\frac{-DOM}{-\sqrt{n}INT}$ below in order to avoid any sign confusion. Also, by convention, I will leave out some constants for simplicity. The derivations follow from an argument similar to the proof above.

$$\begin{aligned}
-\frac{1}{\sqrt{n}} DOM &= \frac{1}{\sqrt{n}} \sum_{i} \left(\sum_{j=1}^{n} \omega_{ji}^2 \right) \ln \frac{1}{\left(\sum_{j=1}^{n} \omega_{ji}^2 \right)} \\
&= \mathcal{O}\left(\frac{1}{\sqrt{n}} \sum_{i} \left(\sum_{j=1}^{n} \omega_{ji}^2 \right) \frac{1}{\left(\sum_{j=1}^{n} \omega_{ji} \right)} \right) \\
&= \mathcal{O}\left(n^{\frac{1-\frac{3}{2}\beta+\delta}{\beta}} \right)
\end{aligned}$$

When $1 < \beta \leq \frac{6}{5}$, I have

$$\begin{aligned} -INT &= \frac{1}{n}\sum_i \sum_j \left(\omega_{ij}^2 \ln \frac{1}{\omega_{ij}^2}\right) \\ &= \Omega\left(\frac{1}{n}\sum_i \sum_j \omega_{ij}^3\right) \\ &= \Omega\left(\frac{1}{n} n^2 \omega_{col,min}^3\right) \\ &= \Omega\left(n \cdot n^{\frac{3-3\beta}{\beta}}\right) = \Omega\left(n^{\frac{1}{2}}\right) \end{aligned}$$

Therefore, when $1 < \beta \leq \frac{6}{5}$, I derive a limit infimum for the conditional aggregate volatility using our network factors.

$$Var_t\left(\Delta \ln \xi_{t\to t+1}\right) = \Omega\left(\frac{DOM}{\sqrt{n} INT}\right)$$

$$\therefore \sqrt{Var_t\left(\Delta \ln \xi_{t\to t+1}\right)} = \Omega\left(\frac{1}{n^{\frac{1}{4}}\sqrt{\frac{INT}{DOM}}}\right)$$

A.8 Proof of Proposition 3

I omit unnecessary constants in the following proof. Assume there are two representative sectors ($n = 2$) and that from t to $t + 1$, the change in the network matrix, dL_{t+1}, is minimal. Thus, I have:

$$\Delta\xi_{t+1} = \alpha'[\rho_z dL_{t+1} z_t + L_{t+1}\sigma_z \epsilon^z]$$

Given that ϵ^z is independent and under the assumption that $\omega_{ij,t+1} \approx \omega_{ij,t}$, I can approximate the aggregate volatility using the first approximation of the Leontief inverse as follows:

$$\begin{aligned} Var_t(\Delta \ln \xi_{t+1}) &= \sigma_z^2 \alpha'[I + (1-\eta)W_t'][I + (1-\eta)W_t]\alpha \\ &= \sigma_z^2 \alpha'[I + (1-\eta)(W_t + W_t') + (1-\eta)^2 W_t' W_t]\alpha \end{aligned}$$

In a two-sector scenario, one sector is assumed to dominate the economy's output according to the power law assumption. Let us assume sector 1 dominates the output. Since each row of W_t sums to 1, it follows that $\omega_{11,t}$ and $\omega_{21,t}$ are close to 1, while $\omega_{12,t}$ and $\omega_{22,t}$ are close to 0.

Assuming equal consumption preferences, i.e. $\alpha = [\frac{1}{2}, \frac{1}{2}]'$, the aggregate volatility can be approximated as follows:

$$Var_t(\Delta \ln \xi_{t+1}) \approx \frac{1}{2}\sigma_z^2 + \frac{1}{2}\sigma_z^2(1-\eta)(\omega_{11,t} + \omega_{21,t}) + \frac{1}{4}\sigma_z^2(1-\eta)^2(\omega_{11,t}^2 + \omega_{21,t}^2)$$

Next, I approximate the two network factors to understand how they affect the terms in this simplified case. For INT_t, since $INT_t \approx \sum_{ij} \omega_{ij,t}^2 \ln \omega_{ij,t}$, performing a first-order Taylor expansion of each element around its nearest value (0 or 1), I can approximate INT_t as the sum of $\omega_{11,t}$ and $\omega_{21,t}$. For DOM_t, it is defined as $\sum_i Out_{i,t} \ln Out_{i,t}$. Given that $Out_{i,t}$ is around 1 in the two-sector case, a first-order expansion around 1 allows us to approximate DOM_t as $-(\omega_{11,t}^2 + \omega_{21,t}^2) + O(\omega_{ij,t}^4)$.

Therefore, in the simplified two-sector case, aggregate volatility can be expressed as a linear function of INT_t and DOM_t.

$$Var_t(\Delta \ln \xi_{t+1}) \approx \frac{1}{2}\sigma_z^2 + \frac{1}{2}\sigma_z^2(1-\eta)INT_t - \frac{1}{4}\sigma_z^2(1-\eta)^2 DOM_t$$

B Structural Estimate

B.1 Stochastic Discount Factor Derivation

In this section, I present the detailed derivations for the SDF, market return, and portfolio returns. The unlevered consumption claim is specified as follows:

$$\begin{aligned}
\Delta \ln \xi_{t+1} &= x_t + \sigma_t \vartheta_{t+1} \\
x_{t+1} &= \rho^x x_t + \rho^e \sigma_t e_{t+1}^x \\
\sigma_t^2 &= \nu_0 + \nu_1 \mathcal{N}_t^{INT} + \nu_2 \mathcal{N}_t^{DOM}
\end{aligned}$$

where

$$\begin{aligned}
\mathcal{N}_{t+1}^{INT} &= \rho^{INT} \mathcal{N}_t^{INT} + \sigma^{INT} e_{t+1}^{INT} \\
\mathcal{N}_{t+1}^{DOM} &= \rho^{DOM} \mathcal{N}_t^{DOM} + \sigma^{DOM} e_{t+1}^{DOM}
\end{aligned}$$

and ϑ_{t+1}, e_{t+1}^x, e_{t+1}^{SPC}, e_{t+1}^{INT} and e_{t+1}^{DOM} are $i.i.d$ standard normal random variables.

The first order approximation of the return on total wealth is given by

$$r^w_{t+1} = \kappa^c_0 + \Delta \ln \xi_{t+1} + \kappa^c_1 wc_{t+1} - wc_t$$

where $\kappa^c_0 = \ln\left(\exp\left(\mu_{wc}\right) + 1\right) - \frac{\exp(\mu_{wc})}{\exp(\mu_{wc})+1}\mu_{wc}$, $\kappa^c_1 = \frac{\exp(\mu_{wc})}{\exp(\mu_{wc})+1} < 1$ and μ_{wc} is the unconditional average of the wealth consumption expenditure ratio. I guess that the wealth-consumption expenditure ratio is linear on the long-run risk component and the two long run network factors:

$$wc_t = \mu_{wc} + A_0 x_t + A_1 \mathcal{N}^{INT}_t + A_2 \mathcal{N}^{DOM}_t$$

Substituting the wealth-consumption ratio in the unlevered return approximation yields:

$$r^w_{t+1} = r^c_0 + \beta_x x_t + \beta_I \mathcal{N}^{INT}_t + \beta_D \mathcal{N}^{DOM}_t + \beta_{\varepsilon,e}\sigma_t e^x_{t+1} + \beta_{\varepsilon,\vartheta}\sigma_t \vartheta_{t+1} + \beta_{\varepsilon,I}\sigma^{INT} e^{INT}_{t+1} + \beta_{\varepsilon,D}\sigma^{DOM} e^{DOM}_{t+1}$$

where

$$\begin{aligned}
r^c_0 &= \kappa^c_0 + \mu_{wc}\left(\kappa^c_1 - 1\right) \\
\beta_x &= 1 + A_0(\kappa^c_1 \rho^x - 1) \\
\beta_I &= A_1(\kappa^c_1 \rho^{INT} - 1) \\
\beta_D &= A_2(\kappa^c_1 \rho^{DOM} - 1) \\
\beta_{\varepsilon,e} &= A_0 \kappa^c_1 \rho^e \\
\beta_{\varepsilon,\vartheta} &= 1 \\
\beta_{\varepsilon,I} &= \kappa^c_1 A_1 \\
\beta_{\varepsilon,D} &= \kappa^c_1 A_2
\end{aligned}$$

Define $\theta = \frac{1-\gamma}{1-\rho}$. When the consumption aggregator is homogenous of degree one, under our price normalization, the SDF can be written as[50]

$$m_{t+1} = \theta \ln d - \rho\theta \Delta w_{t+1} + (\theta - 1) r^w_{t+1}$$

[50] see Herskovic (2018) as well for a similar derivation

The SDF can be derived based on unlevered consumption claim and it's given by

$$m_{t+1} = \lambda_0 + \lambda_x x_t + \lambda_I \mathcal{N}_t^{INT} + \lambda_D \mathcal{N}_t^{DOM} + \lambda_{\varepsilon,e}\sigma_t e_{t+1}^x + \lambda_{\varepsilon,\vartheta}\sigma_t \vartheta_{t+1} + \lambda_{\varepsilon,I}\sigma^{INT} e_{t+1}^{INT} + \lambda_{\varepsilon,D}\sigma^{DOM} e_{t+1}^{DOM}$$

where

$$\begin{aligned}
\lambda_0 &= \theta \ln d + (\theta - 1) r_0^c \\
\lambda_x &= -\rho\theta + (\theta - 1)\beta_x \\
\lambda_I &= (\theta - 1)\beta_I \\
\lambda_D &= (\theta - 1)\beta_D \\
\lambda_{\varepsilon,e} &= (\theta - 1)\beta_{\varepsilon,e} \\
\lambda_{\varepsilon,\vartheta} &= (\theta - 1)\beta_{\varepsilon,\vartheta} - \rho\theta \\
\lambda_{\varepsilon,I} &= (\theta - 1)\beta_{\varepsilon,I} \\
\lambda_{\varepsilon,D} &= (\theta - 1)\beta_{\varepsilon,D}
\end{aligned}$$

The Euler equation for the return on total wealth is given by

$$\begin{aligned}
&\mathbb{E}_t\left[m_{t+1} + r_{t+1}^w\right] + \frac{1}{2} Var_t\left(m_{t+1} + r_{t+1}^w\right) = 0 \\
\therefore 0 &= (\lambda_0 + r_0^c) + (\lambda_x + \beta_x) x_t + (\lambda_I + \beta_I)\mathcal{N}_t^{INT} + (\lambda_D + \beta_D)\mathcal{N}_t^{DOM} \\
&+ \frac{1}{2}\left[(\beta_{\varepsilon,e} + \lambda_{\varepsilon,e})^2 + (\beta_{\varepsilon,\vartheta} + \lambda_{\varepsilon,\vartheta})^2\right]\left[\nu_0 + \nu_1 \mathcal{N}_t^{INT} + \nu_2 \mathcal{N}_t^{DOM}\right] \\
&+ \frac{1}{2}\left[(\beta_{\varepsilon,I} + \lambda_{\varepsilon,I})^2 (\sigma^{INT})^2 + (\beta_{\varepsilon,D} + \lambda_{\varepsilon,D})^2 (\sigma^{DOM})^2\right]
\end{aligned}$$

Setting the constant and coefficients before x_t, $\mathcal{N}_t^{INT}$ and $\mathcal{N}_t^{DOM}$ to zero yields:

$$\begin{aligned}
A_0 &= \frac{1 - \rho}{1 - \kappa_1^c \rho^x} \\
A_1 &= \frac{\nu_1 \theta\left[(\kappa_1^c A_0 \rho^e)^2 + (1 - \rho)^2\right]}{2(1 - \kappa_1^c \rho^{INT})} \\
A_2 &= \frac{\nu_2 \theta\left[(\kappa_1^c A_0 \rho^e)^2 + (1 - \rho)^2\right]}{2(1 - \kappa_1^c \rho^{DOM})}
\end{aligned}$$

Additionally, μ_{wc} solves the nonlinear equation:

$$0 = \theta \ln d + \theta\left(\kappa_0^c + \kappa_1^c \mu_{wc} - \mu_{wc}\right) + \frac{\nu_0 \theta^2}{2}\left[(\kappa_1^c A_0 \rho^e)^2 + (1-\rho)^2\right] + \frac{(\theta\kappa_1^c)^2}{2}\left[(\sigma^{INT} A_1)^2 + (\sigma^{DOM} A_2)^2\right]$$

Here, I assume each portfolio has a different leverage on consumption growth. I specify the dividend growth for the market dividend and individual portfolio dividends as follows:

$$\begin{aligned}\Delta d_{t+1}^m &= \varphi^m \Delta \ln \xi_{t+1} \\ \Delta d_{t+1}^i &= \varphi^i \Delta \ln \xi_{t+1} + \sigma^i \varepsilon_{t+1}^i\end{aligned}$$

I guess and verify that the log pd ratio for portfolio i is linear with respect to the long-run component and network terms:

$$pd_{i,t} = \mu_{i,pd} + A_{0,i} x_t + A_{1,i} \mathcal{N}_t^{INT} + A_{2,i} \mathcal{N}_t^{DOM}$$

The return of portfolio i is approximated by:

$$r_{i,t+1} = \Delta d_{t+1}^i + \kappa_0^i + \kappa_1^i pd_{i,t+1} - pd_{i,t}$$

where $\kappa_1^i = \frac{\exp(\mu_{i,pd})}{1+\exp(\mu_{i,pd})}$ and $\kappa_0^i = \log\left(1+\exp\left(\mu_{i,pd}\right)\right) - \kappa_1^i \mu_{i,pd}$ are the approximation constants. Substituting the price-dividend expression into the return approximation yields:

$$\begin{aligned}r_{i,t+1} = & r_0^i + \beta_x^i x_t + \beta_I^i \mathcal{N}_t^{INT} + \beta_D^i \mathcal{N}_t^{DOM} + \beta_{\varepsilon,e}^i \sigma_t e_{t+1}^x + \beta_{\varepsilon,\vartheta}^i \sigma_t \vartheta_{t+1} \\ & + \beta_{\varepsilon,I}^i \sigma^{INT} e_{t+1}^{INT} + \beta_{\varepsilon,D}^i \sigma^{DOM} e_{t+1}^{DOM} + \sigma^i \varepsilon_{t+1}^i\end{aligned}$$

where

$$
\begin{aligned}
r_0^i &= \kappa_0^i + (\kappa_1^i - 1)\mu_{i,pd} \\
\beta_x^i &= \varphi^i + A_{0,i}(\kappa_1^i \rho^x - 1) \\
\beta_I^i &= A_{1,i}(\kappa_1^i \rho^{INT} - 1) \\
\beta_D^i &= A_{2,i}(\kappa_1^i \rho^{DOM} - 1) \\
\beta_{\varepsilon,e}^i &= \kappa_1^i A_{0,i} \rho^e \\
\beta_{\varepsilon,\vartheta}^i &= \varphi^i \\
\beta_{\varepsilon,I}^i &= \kappa_1^i A_{1,i} \\
\beta_{\varepsilon,D}^i &= \kappa_1^i A_{2,i}
\end{aligned}
$$

The Euler equation for each portfolio i yields:

$$
\begin{aligned}
& \mathbb{E}_t \left[m_{t+1} + r_{i,t+1} \right] + \frac{1}{2} Var_t \left(m_{t+1} + r_{i,t+1} \right) = 0 \\
\therefore\ 0 =& \lambda_0 + \lambda_x x_t + \lambda_I \mathcal{N}_t^{INT} + \lambda_D \mathcal{N}_t^{DOM} + r_0^i + \beta_x^i x_t + \beta_I^i \mathcal{N}_t^{INT} + \beta_D^i \mathcal{N}_t^{DOM} \\
& + \frac{1}{2} \left[(\beta_{\varepsilon,e}^i + \lambda_{\varepsilon,e})^2 + (\beta_{\varepsilon,\vartheta}^i + \lambda_{\varepsilon,\vartheta})^2 \right] \left[\nu_0 + \nu_1 \mathcal{N}_t^{INT} + \nu_2 \mathcal{N}_t^{DOM} \right] \\
& + \frac{1}{2} \left[(\beta_{\varepsilon,I}^i + \lambda_{\varepsilon,I})^2 (\sigma^{INT})^2 + (\beta_{\varepsilon,D}^i + \lambda_{\varepsilon,D})^2 (\sigma^{DOM})^2 \right]
\end{aligned}
$$

Setting the constant and coefficients before x_t, $\mathcal{N}_t^{INT}$ and $\mathcal{N}_t^{DOM}$ to zero yields:

$$
\begin{aligned}
A_{0,i} &= \frac{\varphi^i + \lambda_x}{1 - \kappa_1^i \rho^x} \\
A_{1,i} &= \frac{\lambda_I + \frac{\nu_1}{2} \left[(\kappa_1^i A_{0,i} \rho^e + \lambda_{\varepsilon,e})^2 + (\varphi^i + \lambda_{\varepsilon,\vartheta})^2 \right]}{1 - \kappa_1^i \rho^{INT}} \\
A_{2,i} &= \frac{\lambda_D + \frac{\nu_2}{2} \left[(\kappa_1^i A_{0,i} \rho^e + \lambda_{\varepsilon,e})^2 + (\varphi^i + \lambda_{\varepsilon,\vartheta})^2 \right]}{1 - \kappa_1^i \rho^{DOM}}
\end{aligned}
$$

And $\mu_{i,pd}$ solves the nonlinear equation

$$
\begin{aligned}
0 =& \lambda_0 + r_0^i + \frac{\nu_0}{2} \left[(\beta_{\varepsilon,e}^i + \lambda_{\varepsilon,e})^2 + (\beta_{\varepsilon,\vartheta}^i + \lambda_{\varepsilon,\vartheta})^2 \right] \\
& + \frac{1}{2} \left[(\beta_{\varepsilon,I}^i + \lambda_{\varepsilon,I})^2 (\sigma^{INT})^2 + (\beta_{\varepsilon,D}^i + \lambda_{\varepsilon,D})^2 (\sigma^{DOM})^2 \right]
\end{aligned}
$$

B.2 Calibration

For the cross-section, only two parameters require calibration. I calibrate these parameters to match both the risk premium and the volatility of individual portfolios. The calibrated parameters are presented in Panel C of Table 8.

Table 9. Dividend Growth Parameters.
The table lists the parameters used to calibrate the cross-sectional dividend growth.

	Market	Risk-Intensity Sorted			Risk-Dominance Sorted		
		1	2	3	1	2	3
Panel C: Dividend Growth Parameters							
φ^i	0.90	3.81	2.00	0.90	-1.41	1.03	3.98
σ^i	0.04	0.03	0.04	0.04	0.04	0.04	0.05

C Robustness of Network Factors

C.1 Anomaly Portfolios in Fama-MacBeth Analysis

The test assets for Table 5 and Table 6 are organized into four groups as follows:

1. 80 Volatility-related Test Assets (VOL80): This group includes 10 Dollar Trading Volume sorted portfolios (Dtv10), 10 Market-beta sorted portfolios (Beta10), 10 Idiosyncratic volatility sorted portfolios (Idiovol10), 10 Realized volatility sorted portfolios (Realvol10), 10 Idiosyncratic skewness sorted portfolios (Idioskew10), 10 Aggregate Volatility sorted portfolios (Aggvol10), 10 DOM sorted portfolios (DOM10), and 10 INT sorted portfolios (INT10).

2. 70 Investment-related Test Assets (INV70): This group includes 10 Market Capitalization Sorted portfolios (SZ10), 10 Investment sorted portfolios (INV10), 10 Operating Profitability sorted portfolios (OP10), 10 Cashflow/Price sorted portfolios (CFP10), 10 Dividend/Price sorted portfolios (DP10), 10 Earnings/Price sorted portfolios (EP10), and 10 Accruals sorted portfolios (AC10).

3. 90 Investment-related Test Assets (INV90): An extension of INV70, this group adds 10 DOM sorted portfolios (DOM10) and 10 INT sorted portfolios (INT10) to the original 70 investment-related test assets.

4. ALL 150 Test Assets (ALL 150): A comprehensive set that merges the 80 Volatility-related Test Assets (VOL80) with the 70 Investment-related Test Assets (INV70).[51]

C.2 Other Double-sorted Anomalies

In order to further explore the pricing capabilities of network factors on other anomaly portfolios, I do an additional Fama-MacBeth analysis using four new groups of double-sorted anomaly portfolios. The sets of test assets are specified as follows:

1. Set 1 includes 60 portfolios: 15 size and market-beta double sorted porfolios, 15 size and dollar trading volume double sorted portfolios, 15 size and idiosyncratic skewwness double sorted portfolios, 15 size and aggregate volatility double sorted portfolios.

2. Set 2 includes 70 portfolios: 25 size and idiosyncratic volatility double sorted portfolios, 25 size and realized volatility double sorted portfolios, 10 *DOM*-beta sorted portfolios, 10 *INT*-beta sorted portfolios.

3. Set 3 includes 62 portfolios: 25 size and investment double sorted portfolios, 25 size and accruals double sorted portfolios, 6 size and cashflow/price double sorted portfolios, 6 size and earnings/price double sorted portfolios.

4. Set 4 includes 70 portfolios: 25 book-to-market and investment double sorted portfolios, 25 book-to-market and operating profitability double sorted portfolios, 10 *DOM*-beta sorted portfolios, 10 *INT*-beta sorted portfolios.

Table 10 summarizes the findings. Across the four sets of double-sorted test assets, both *DOM* and *INT* are significantly priced. *DOM* earns a price or risk around 0.4 and *INT* has a price or risk around -0.5.

[51] Dtv10, Beta10, Idioskew10 and Aggvol10 are from Lu Zhang's website (Hou, Mo, Xue, and Zhang (2019)). SZ10, INV10, OP10, CFP10, EP10 and AC10 are from French's website.

Table 10. Fama-MacBeth with Double-sorted Anomalies
The table presents the estimated price of risk (λ) for the factors, along with their Newey-West standard errors (accounting for one lag), derived from the GMM framework. The time range is from 198304 to 201912 monthly. The set of test assets are combinations of double-sorted anomaly portfolios. For each test assets, two factor models are considered. One is Fama-French 5 factors and another is FF5 *+DOM+INT*. The last row reports the cross-sectional R^2 and the second to last row reports the mean absolute pricing error in percentage values.

	SZ*Beta15 +SZ*Dtv15 +SZ*IdioSkew15 +SZ*Aggvol15		SZ*Idiovol25 +SZ*Vol25 +DOM10 +INT10		SZ*INV25 +SZ*AC25 +SZ*CFP6 +SZ*EP6		BM*INV25 +BM*OP25 +DOM10 +INT10	
Const	0.89	0.99	1.52	1.57	0.75	0.95	1.45	1.58
t	(3.56)	(4.14)	(5.36)	(5.55)	(2.80)	(3.76)	(2.54)	(2.87)
Mkt.Rf	-0.10	-0.20	-0.65	-0.71	0.12	-0.08	-0.62	-0.75
t	(-0.32)	(-0.64)	(-1.86)	(-2.01)	(0.36)	(-0.23)	(-1.01)	(-1.26)
SMB	0.33	0.32	0.46	0.38	0.21	0.18	1.34	1.31
t	(2.31)	(2.29)	(3.03)	(2.59)	(1.54)	(1.31)	(4.82)	(4.65)
HML	-0.84	-0.81	-0.92	-0.73	-0.05	0.11	-0.04	-0.02
t	(-2.91)	(-2.67)	(-2.99)	(-2.20)	(-0.28)	(0.64)	(-0.23)	(-0.12)
RMW	0.72	0.69	0.95	0.93	0.31	0.17	0.61	0.57
t	(3.25)	(3.10)	(3.73)	(3.46)	(1.72)	(0.98)	(3.36)	(3.12)
CMA	0.05	-0.01	-0.73	-0.90	0.30	0.26	0.11	0.10
t	(0.22)	(-0.07)	(-2.37)	(-3.02)	(2.89)	(2.51)	(0.88)	(0.83)
DOM		**0.46**		**0.43**		**0.37**		**0.37**
t		**(2.38)**		**(2.30)**		**(2.04)**		**(2.02)**
INT		**-0.56**		**-0.47**		**-0.50**		**-0.42**
t		**(-2.80)**		**(-2.29)**		**(-2.49)**		**(-2.07)**
MAPE%	0.11	0.10	0.13	0.12	0.13	0.13	0.12	0.12
R^2	0.62	0.65	0.69	0.72	0.34	0.41	0.60	0.62

C.3 Fama-MacBeth Analysis with Input-output Network Factors

In Herskovic (2018), the author introduces first-moment network factors—the *Concentration* factor and the *Sparsity* factor—to capture changes in the structure of the production-based network. The *Concentration* factor reflects the extent to which output is dominated by a few key nodes. When *Concentration* is high, aggregate output decreases as the economy moves closer to a monopolistic state. Consequently, the *Concentration* (*CON*) factor is priced as a negative risk. Conversely, the *Sparsity* factor measures how sparse the input sources are. When firms substitute inefficient inputs with efficient ones to maximize their profits, the sparsity of input edges increases. When *Sparsity* is high, aggregate output increases, and thus the *Sparsity* (*SPC*) factor is expected to carry a positive price of risk.

To facilitate a direct comparison between my second-moment network factors and Herskovic's first-moment factors, I annualize my monthly mimicking factors and incorporate them alongside the annual production-based factors into the Fama-MacBeth analysis.[52] Table 11 demonstrates that the volatility-based *DOM* factor correctly exhibits a positive price of risk, while *INT* correctly exhibits a negative price of risk. In most cases, the production-based factors either become statistically insignificant or exhibit a reversal in their expected signs. Furthermore, the inclusion of our volatility-based factors significantly enhances the R^2 values, indicating a substantial improvement in the model's explanatory power.

Table 11. Annual Fama-MacBeth with Herskovic's Factors

The table presents the estimated price of risk (λ) for the factors, along with their Newey-West standard errors (accounting for one lag), derived from the GMM framework. The time range is from 1983 to 2014 annually. The set of test assets are ALL150 in columns 1-2, VOL80 in columns 3-4, INV70 in columns 5-6 and INV90 in columns 7-8. For each test assets, two factor models are considered. One is FF5+ Herskovic's factors and another is FF5+ Herskovic's factors+*DOM*+*INT*. The last row reports the cross-sectional R2 and the second to last row reports the mean absolute pricing error in percentage values.

	ALL150		VOL80		INV70		INV90	
Const	25.75	20.84	6.68	3.91	103.39	88.00	53.77	46.00
t	(3.25)	(4.42)	(2.70)	(1.46)	(3.61)	(3.69)	(3.56)	(3.70)
Mkt.Rf	1.33	0.62	1.88	0.31	1.00	0.36	1.05	0.40
t	(1.44)	(0.70)	(1.17)	(0.10)	(1.04)	(0.45)	(1.07)	(0.49)
SMB	-2.06	-1.92	-1.26	-1.15	-2.00	-1.86	-2.08	-1.93
t	(-2.16)	(-2.07)	(-1.43)	(-0.97)	(-2.08)	(-2.06)	(-2.09)	(-2.08)
HML	1.94	1.47	2.21	1.08	1.94	1.57	2.00	1.61
t	(2.48)	(2.42)	(2.52)	(0.90)	(2.47)	(2.41)	(2.47)	(2.43)
RMW	-0.13	0.35	-0.18	1.60	-0.37	-0.08	-0.38	-0.08
t	(-0.11)	(0.43)	(-0.13)	(0.81)	(-0.34)	(-0.09)	(-0.34)	(-0.09)
CMA	-1.04	-0.88	-1.33	-0.78	-1.05	-0.92	-1.09	-0.95
t	(-1.37)	(-1.26)	(-1.11)	(-0.47)	(-1.48)	(-1.48)	(-1.51)	(-1.49)
CON	**-1.26**	**1.30**	**-2.93**	**3.42**	**-3.17**	**-0.97**	**-3.19**	**-0.95**
t	**(-0.26)**	**(0.40)**	**(-0.57)**	**(0.48)**	**(-0.64)**	**(-0.32)**	**(-0.63)**	**(-0.31)**
SPC	**0.21**	**2.57**	**2.47**	**8.18**	**-1.90**	**0.10**	**-1.93**	**0.11**
t	**(0.04)**	**(0.73)**	**(0.49)**	**(1.48)**	**(-0.37)**	**(0.03)**	**(-0.38)**	**(0.03)**
DOM		**2.93**		**2.39**		**2.57**		**2.61**
t		**(2.48)**		**(3.41)**		**(2.12)**		**(2.11)**
INT		**-1.87**		**-2.07**		**-1.31**		**-1.35**
t		**(-2.30)**		**(-1.76)**		**(-1.86)**		**(-1.90)**
MAPE%	81.05	74.42	53.99	35.88	45.21	37.01	31.78	23.82
R^2	0.94	0.95	0.96	0.98	0.83	0.86	0.90	0.92

[52] Due to methodological constraints, the direct construction of annual volatility factors was not feasible given the limited length of the time series.

C.4 Robustness of Double Sorting

I double sort *INT* with *DOM*, as well as other network factors, to examine their combined effects. Table 12 reports the tercile-tercile sorted results for *INT* and *DOM*. The portfolios are value-weighted. Panel A presents the annualized average risk premium. Panel B reports the monthly α_{FF3}, which refers to the intercept obtained by regressing the sorted portfolios onto the Fama-French 3 factors. Panel C reports the monthly $\alpha_{4factor}$, referring to the intercept obtained by regressing the sorted portfolios onto four factors (FF3 plus Momentum). Panel D reports the monthly α_{FF5}, referring to the intercept obtained by regressing the sorted portfolios onto FF3 plus Momentum and Liquidity, as per Pástor and Stambaugh (2003). The results clearly indicate that both factors remain robust when subjected to double sorting.

Panel A: Average Excess Return

		INT				
		1	2	3	H-L	
DOM	1	0.102	0.087	0.077	-0.025	
	2	0.122	0.099	0.087	-0.035	
	3	0.155	0.128	0.122	-0.033	
	H-L	0.053	0.041	0.045		

Panel B: α_{FF3}

		INT				
		1	2	3	H-L	t-stat
DOM	1	0.002	0.001	-0.001	-0.003	-1.989
	2	0.003	0.002	0.000	-0.003	-2.385
	3	0.005	0.003	0.003	-0.002	-1.967
	H-L	0.003	0.002	0.004		
	t-stat	2.173	1.765	2.596		

Panel C: $\alpha_{4factor}$

		INT				
		1	2	3	H-L	t-stat
DOM	1	0.002	0.001	-0.001	-0.003	-2.332
	2	0.004	0.002	0.000	-0.003	-2.529
	3	0.006	0.004	0.003	-0.003	-1.917
	H-L	0.004	0.003	0.005		
	t-stat	2.727	2.614	3.246		

Panel D: $\alpha_{5factor}$

		INT				
		1	2	3	H-L	t-stat
DOM	1	0.002	0.001	-0.001	-0.003	-2.159
	2	0.004	0.002	0.000	-0.003	-2.466
	3	0.006	0.004	0.004	-0.003	-1.783
	H-L	0.004	0.003	0.005		
	t-stat	2.714	2.602	3.198		

Table 12. Double Sorting portfolios based on two network factors.

		Returns	α_{FF3}		$\alpha_{4factor}$		$\alpha_{5factor}$	
		H-L	H-L	t-stat	H-L	t-stat	H-L	t-stat
Mkt.RF	L	-0.032	-0.003	-2.007	-0.003	-2.340	-0.003	-2.247
	M	-0.044	-0.004	-2.498	-0.004	-2.986	-0.004	-2.859
	H	-0.040	-0.004	-2.268	-0.005	-2.869	-0.004	-2.710
SMB	L	-0.043	-0.004	-2.816	-0.005	-3.441	-0.004	-3.348
	M	-0.044	-0.004	-2.598	-0.004	-3.002	-0.004	-2.861
	H	-0.028	-0.002	-1.513	-0.003	-1.950	-0.003	-1.802
HML	L	-0.035	-0.002	-1.607	-0.004	-2.359	-0.003	-2.278
	M	-0.043	-0.004	-2.630	-0.004	-2.941	-0.004	-2.818
	H	-0.038	-0.004	-2.519	-0.004	-2.856	-0.004	-2.690

Table 13. Double Sorting portfolios based on INT and other factors. This Table reports the tercile-tercile sorted results for INT and other anomaly factor. The portfolios are formed via value-weighted. I reported the annualized High-Low risk premium, the monthly α_{FF3}, the monthly $\alpha_{4factor}$ and the monthly $\alpha_{5factor}$ for each category of the anomaly factors.

		Returns	α_{FF3}		$\alpha_{4factor}$		$\alpha_{5factor}$	
		H-L	H-L	t-stat	H-L	t-stat	H-L	t-stat
Mkt.RF	L	0.044	0.003	2.543	0.004	3.285	0.004	3.276
	M	0.046	0.003	2.222	0.004	2.930	0.004	2.854
	H	0.048	0.003	1.803	0.004	2.384	0.004	2.393
SMB	L	0.052	0.004	2.658	0.004	3.304	0.004	3.303
	M	0.043	0.003	1.913	0.004	2.687	0.004	2.726
	H	0.043	0.003	1.972	0.004	2.573	0.004	2.478
HML	L	0.044	0.003	2.263	0.004	2.592	0.004	2.543
	M	0.048	0.003	2.378	0.004	2.935	0.004	2.930
	H	0.047	0.003	1.788	0.004	2.865	0.004	2.849

Table 14. Double Sorting portfolios based on DOM and other factors. This Table reports the tercile-tercile sorted results for DOM and other anomaly factor. The portfolios are formed via value-weighted. I reported the annualized High-Low risk premium, the monthly α_{FF3}, the monthly $\alpha_{4factor}$ and the monthly $\alpha_{5factor}$ for each category of the anomaly factors.

C.5 Robustness of Alternative Measurements

Panel A: Average Excess Returns

		INT					DOM				
		1	2	3	H-L	t-stat	1	2	3	H-L	t-stat
1	$DOM_{herfout}$	0.134	0.106	0.086	-0.048	-2.698	0.083	0.100	0.123	0.040	2.011
2	$DOM_{eigvec1}$	0.128	0.105	0.094	-0.034	-2.534	0.087	0.105	0.134	0.046	2.032
3	$DOM_{eigvec2}$	0.126	0.103	0.097	-0.029	-2.001	0.101	0.102	0.123	0.022	1.974
4	Squared sum measurement	0.124	0.104	0.098	-0.026	-1.602	0.090	0.102	0.133	0.043	2.542
5	Benchmark controls+MOM+LIQ	0.129	0.105	0.093	-0.036	-2.535	0.093	0.102	0.132	0.039	2.001
6	Benchmark controls+ΔMktVol	0.130	0.102	0.094	-0.036	-2.537	0.088	0.103	0.135	0.046	2.202
7	Control Prev Levels	0.134	0.101	0.091	-0.043	-2.600	0.089	0.102	0.134	0.045	2.032
8	No Control	0.122	0.102	0.101	-0.021	-1.985	0.103	0.103	0.126	0.023	1.985
9	All CRSP stocks	0.143	0.098	0.085	-0.058	-2.996	0.081	0.095	0.151	0.069	2.236
10	PC5 Idio Vol	0.130	0.106	0.090	-0.040	-2.598	0.089	0.103	0.134	0.044	2.228
11	NAICS2digit	0.095	0.090	0.056	-0.039	-2.591	0.070	0.084	0.098	0.029	1.998
12	SIC3digit	0.107	0.080	0.058	-0.050	-2.701	0.067	0.083	0.098	0.032	2.000

Panel B: α_{FF3}

		INT					DOM				
		1	2	3	H-L	t-stat	1	2	3	H-L	t-stat
1	$DOM_{herfout}$	0.004	0.002	-0.001	-0.004	-3.229	0.001	0.001	0.003	0.001	1.963
2	$DOM_{eigvec1}$	0.003	0.002	0.000	-0.003	-2.461	0.000	0.002	0.003	0.003	1.962
3	$DOM_{eigvec2}$	0.003	0.002	0.000	-0.003	-1.969	0.002	0.001	0.002	0.001	1.927
4	Squared sum measurement	0.003	0.002	0.001	-0.002	-1.313	0.001	0.001	0.003	0.002	1.630
5	Benchmark controls+MOM+LIQ	0.003	0.002	0.000	-0.003	-2.152	0.001	0.001	0.003	0.003	2.063
6	Benchmark controls+ΔMktVol	0.003	0.002	0.000	-0.003	-2.099	0.002	0.001	0.002	0.000	2.225
7	Control Prev Level	0.004	0.001	0.000	-0.005	-3.099	0.001	0.001	0.003	0.002	2.532
8	No Control	0.003	0.002	0.000	-0.003	-2.033	0.002	0.002	0.002	0.000	1.949
9	All CRSP stocks	0.004	0.001	-0.001	-0.005	-2.533	-0.001	0.001	0.004	0.005	2.122
10	PC5 Idio Vol	0.004	0.002	0.000	-0.004	-2.774	0.001	0.001	0.003	0.003	2.169
11	NAICS2digit	0.002	0.002	-0.002	-0.004	-2.665	-0.001	0.001	0.002	0.003	2.654
12	SIC3digit	0.002	0.001	-0.002	-0.004	-2.270	-0.001	0.001	0.002	0.003	1.499

Panel C: $\alpha_{4factor}$

		INT					DOM				
		1	2	3	H-L	t-stat	1	2	3	H-L	t-stat
1	$DOM_{herfout}$	0.005	0.002	0.000	-0.005	-3.423	0.002	0.002	0.004	0.002	2.003
2	$DOM_{eigvec1}$	0.005	0.002	0.000	-0.004	-2.952	0.001	0.002	0.004	0.003	2.064
3	$DOM_{eigvec2}$	0.004	0.002	0.001	-0.003	-2.192	0.002	0.002	0.003	0.000	2.310
4	Squared sum measurement	0.004	0.002	0.001	-0.003	-1.833	0.001	0.002	0.004	0.003	2.490
5	Benchmark controls+MOM+LIQ	0.004	0.002	0.001	-0.003	-2.187	0.001	0.002	0.004	0.003	2.381
6	Benchmark controls+ΔMktVol	0.004	0.002	0.001	-0.003	-2.218	0.003	0.002	0.003	0.000	2.112
7	Control Prev Level	0.005	0.002	0.000	-0.005	-3.521	0.001	0.002	0.004	0.003	1.985
8	No Control	0.004	0.002	0.001	-0.003	-2.225	0.002	0.002	0.003	0.000	1.917
9	All CRSP stocks	0.006	0.002	0.000	-0.006	-3.018	0.001	0.001	0.006	0.005	2.287
10	PC5 Idio Vol	0.005	0.002	0.000	-0.004	-3.163	0.001	0.002	0.004	0.003	2.509
11	NAICS2digit	0.002	0.002	-0.002	-0.004	-2.337	0.000	0.001	0.002	0.002	2.262
12	SIC3digit	0.003	0.001	-0.002	-0.005	-2.659	-0.001	0.001	0.002	0.002	1.267

Panel D: $\alpha_{5factor}$

		INT					DOM				
		1	2	3	H-L	t-stat	1	2	3	H-L	t-stat
1	$DOM_{herfout}$	0.005	0.002	0.000	-0.005	-3.233	0.002	0.002	0.004	0.002	2.374
2	$DOM_{eigvec1}$	0.004	0.002	0.001	-0.004	-2.686	0.001	0.002	0.004	0.003	2.137
3	$DOM_{eigvec2}$	0.004	0.002	0.001	-0.003	-1.974	0.002	0.002	0.003	0.001	2.675
4	Squared sum measurement	0.004	0.002	0.001	-0.002	-1.657	0.001	0.002	0.004	0.004	2.541
5	Benchmark controls+MOM+LIQ	0.004	0.002	0.001	-0.003	-1.944	0.001	0.002	0.004	0.003	2.398
6	Benchmark controls+ΔMktVol	0.004	0.002	0.001	-0.003	-2.018	0.002	0.002	0.003	0.001	2.383
7	Control Prev Level	0.005	0.002	0.000	-0.005	-3.230	0.001	0.002	0.004	0.003	1.952
8	No Control	0.004	0.002	0.001	-0.003	-1.972	0.002	0.002	0.003	0.001	1.966
9	All CRSP stocks	0.006	0.002	0.000	-0.006	-2.856	0.001	0.001	0.006	0.006	2.419
10	PC5 Idio Vol	0.004	0.002	0.000	-0.004	-2.918	0.001	0.002	0.004	0.003	2.483
11	NAICS2digit	0.002	0.001	-0.002	-0.004	-2.017	0.000	0.001	0.003	0.003	2.176
12	SIC3digit	0.003	0.001	-0.002	-0.004	-2.359	0.000	0.001	0.001	0.002	0.991

Table 15. Single sorted portfolios under alternative measurements or controls.

Table 15 reports the tercile-sorted results for *INT* and *DOM* using different measurements of factors, different controls, or different definitions of industries. The table is organized as follows:

- Lines 1-4: I consider different measurements for constructing the *CON* factor, discussed in detail in the next paragraph.
- Lines 5-8: I consider different controls in portfolio sorting.
  - Line 5 reports results by adding benchmark controls plus momentum and liquidity.
  - Line 6 reports results by adding benchmark controls plus market volatility innovation.
  - Line 7 reports results by adding previous factor levels as controls.
  - Line 8 reports results with no controls.
- Line 9: I consider sorting portfolios using all CRSP returns, including penny stocks.
- Line 10: I consider idiosyncratic volatility from PC5 factors.
- Line 11: I consider idiosyncratic volatility spillover for NAICS 2-digit sectors.
- Line 12: I consider idiosyncratic volatility spillover for 3-digit SIC codes.

It is evident that the return spread remains significant for both factors under different alternative measurements and controls. The anomaly αs are also significant, suggesting that the return spread cannot be explained by the factor models. An interesting observation is in line 12. Here, I retained the sectors with non-missing values, totaling 153 sectors from 1969 to 2019. The H-L α is significant for *INT* but not for *DOM*. This result is logical, as at a very granular level, the size difference between nodes becomes much smaller, making it harder to capture the concept of dominance. However, the intensity remains about the connection level across all sectors.

Here I elaborate the alternative measurements for the *DOM* factor (line 1-4).

Line 1: I use the negative entropy of out-Herfindahl degrees to capture the dominance. In graph theory, besides Outdegree, I can also use out-Herfindahl index to represent volatility spreading capacity.

$$
\begin{aligned}
Herfout &= \left[\frac{\sum_{i=1,i\neq 1}^{48} d_{i,1}}{\sum_{i=1}^{48} d_{i,1}} \quad \frac{\sum_{i=1,i\neq 2}^{48} d_{i,2}}{\sum_{i=1}^{48} d_{i,2}} \quad \cdots \quad \frac{\sum_{i=1,i\neq 48}^{48} d_{i,48}}{\sum_{i=1}^{48} d_{i,48}} \right] \\
&= \left[\frac{O_1}{\sum_{i=1}^{48} d_{i,1}} \quad \frac{O_2}{\sum_{i=1}^{48} d_{i,2}} \quad \cdots \quad \frac{O_{48}}{\sum_{i=1}^{48} d_{i,48}} \right]
\end{aligned}
$$

I normalize it and compute Negative Entropy of the out-Herfindahl degrees for *DOM* Factor.[53]

Line 2 and line 3: I give a symmetric approximation of the asymmetric adjacency matrix (using two methods) and then capture the dominance using negative entropy of the eigenvector centrality.

In the network literature, it is attractive to construct 'undirected' or symmetric approximation for the original network structure. It is known that the 'direction' is an important part in the network: The shock from industry i to industry j is not equal to the shock from industry j to industry i, but only the thicker edge has important asset pricing implications for both i and j.

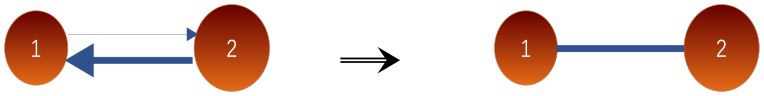


Figure 6. From directed to undirected

So naturally, the first symmetric approximation for A_0 is to assign each pair of diagonal-symmetric elements to be the larger one of them. i.e.

$$d^*_{i,j} = \max_{i,j}\{d_{i,j}, d_{j,i}\}$$

where$A_0 = \left[d_{i,j}\right]$ and $A^* = \left[d^*_{i,j}\right]$. This is also the method adopted by Ahern (2013).

Next, I construct a second symmetric approximation of A_0 from a statistical perspective. In network literature, we often require the adjacency matrix to be irreducible and positive (because we often want to apply Perron-Frobenius theorem to extract eigenvector centrality etc.) So the approximation must also be irreducible and positive.

For convenience, I construct a 1-dim symmetric approximation(instead of a 48-dim). It is reasonable as it still produces an irreducible matrix. In network language, 'irreducible' means that the network is strongly connected and every node is reachable by other nodes. This is guaranteed by the nature property of volatility spillover. Hence, I assume the symmetric approximation $A^* = xx'$ and try to find vector x to minimize the Frobenius-norm of $\|A_0 - xx'\|_F$. The solution is $x'H = \|x\|^2 x'$ where $H = \frac{A_0 + A_0'}{2}$ (the Hermitian matrix of A_0). Then I find all largest eigenvalue λ and the corresponding eigenvector μ and set x as $\pm\frac{\lambda^{1/2}}{\|\mu\|}\mu$.

[53] Since each row is already normalized in the benchmark. I do not have an alternative ratio measurement for the *INT* factor.

The solution is derived as follows. I assume $Y = A_0 - xx'$ and J as the Frobenius norm of Y.

$$\begin{aligned}
dY &= -dxx' - xdx' \\
dJ &= tr(Y + dY)'(Y + dY) - trY'Y \\
&= tr(Y - dxx' - xdx')'(Y - dxx' - xdx') - trY'Y \\
&= tr(-Y'dxx' - Y'xdx' - xdx'Y - dxx'Y) \\
&= tr(-x'Y'dx - x'Ydx - x'Y'dx - x'Ydx) \\
&= tr(-2x'(Y + Y')dx) \\
J'(x) &= -2x'(Y + Y') \\
&= -2x'(A_0 + A_0' - 2xx') \\
&= -2x'(A_0 + A_0') + 4\|x\|^2x'
\end{aligned}$$

I set $J'(x)$ to be 0 to solve for x. Or alternatively, if one directly realizes that

$$\begin{aligned}
J(x) &= tr(A_0 - xx')'(A_0 - xx') \\
&= tr(A_0A_0' - xx'A_0 - A_0'xx' + xx'xx') \\
&= \|A_0\|^2 - 2tr(x'\frac{A_0 + A_0'}{2}x) + \|x\|^2
\end{aligned}$$

The solution is then $x'H = \|x\|^2x'$ where $H = \frac{A_0+A_0'}{2}$ (the Hermitian matrix of A_0). Then I find all largest eigenvalue λ and the corresponding eigenvector μ and set x as $\pm\frac{\lambda^{1/2}}{\|\mu\|}\mu$.

In the following empirical results, I denote the statistical approximation as A_1^* and the approximation using Ahern's method as A_2^*. Since the two alternative adjacency matrices implicitly unite indegree and outdegree, both degree can be represented using the eigenvector centrality degree and I am going to construct an alternative measurement of *DOM* factor through Negative Entropy of normalized eigenvector centrality. Eigenvector centrality degree is constructed according to Bonacich (1972) and Bonacich and Lloyd (2001). If I have a symmetric and nonnegative adjacency matrix, then I can do the Perron-Frobenius-type eigenvector decomposition(EVD) and eigenvector centrality is simply defined as the eigenvector corresponding to the absolutely largest eigenvalue. All of the elements in the eigenvector centrality are nonnegative (according to Perron-Frobenius

theorem).[54][55]

Line 4: I learn from the HHI measure, and construct the dominance using the sum of the squared spillover outdegree, and the *INT* using the cross-sectional average of the sum of the squared shock-receiving proportions.

C.6 Robustness of Different Parameters

I show the portfolio sorting is robust by change different parameter choices: trailing window for sorting portfolio, rolling window for constructing dynamic network and forecasting period for estimating VAR forecasting error.

In table 16, in line 1-5, I use different trailing window length to sort portfolio. In line 6-9, I use different rolling window length to construct the dynamic network. In line 10-13, I use different forecasting period for doing generalized variance decomposition of the forecasting error. The portfolio sorting results are very robust under different parameter choices.

D Additional Empirical Analysis

D.1 Are Network Factors Other Ways to Measure Systemic Risk?

This paper demonstrates that a sector's risk exposure depends on its position in the network, and this exposure can predict its stock returns. A related question to explore is whether sectors' factor loadings can reflect their positions in the network. If this is the case, factor betas could serve as an alternative measure of systemic risk.

One approach is to examine the correlation between factor betas and established systemic risk measures. Diebold and Yilmaz (2014) establish that Outdegree and Indegree are systemic risk metrics, where Outdegree is defined as the column sum of the adjacency matrix (excluding the diagonal), and Indegree is defined as the row sum (excluding the diagonal). Each sector has its own

[54]The Perron-Frobenius theorem says that there exists an eigenvector with only non-negative components. The Perron-Frobenius theorem also says that the non-negative eigenvector is associated with the absolutely largest eigenvalue (called the spectral radius) which is also non-negative. The eigenvectors related to all other eigenvalues must contain negative entries.

[55]Since the symmetric approximation makes the shock receiving channel (i.e. each row) obscure, it is difficult to construct an alternative measurement for the intensity factor. So I keep the *INT* factor the same for line 1-3 of table 15.

Outdegree and Indegree at each time point, which can reveal its position, or importance, within the market.

I sort FF-48 industry portfolios based on their exposures to the network factors. I then plot the time series of the cross-sectional distribution of Outdegree, Indegree, and factor betas, followed by an analysis of their correlations.

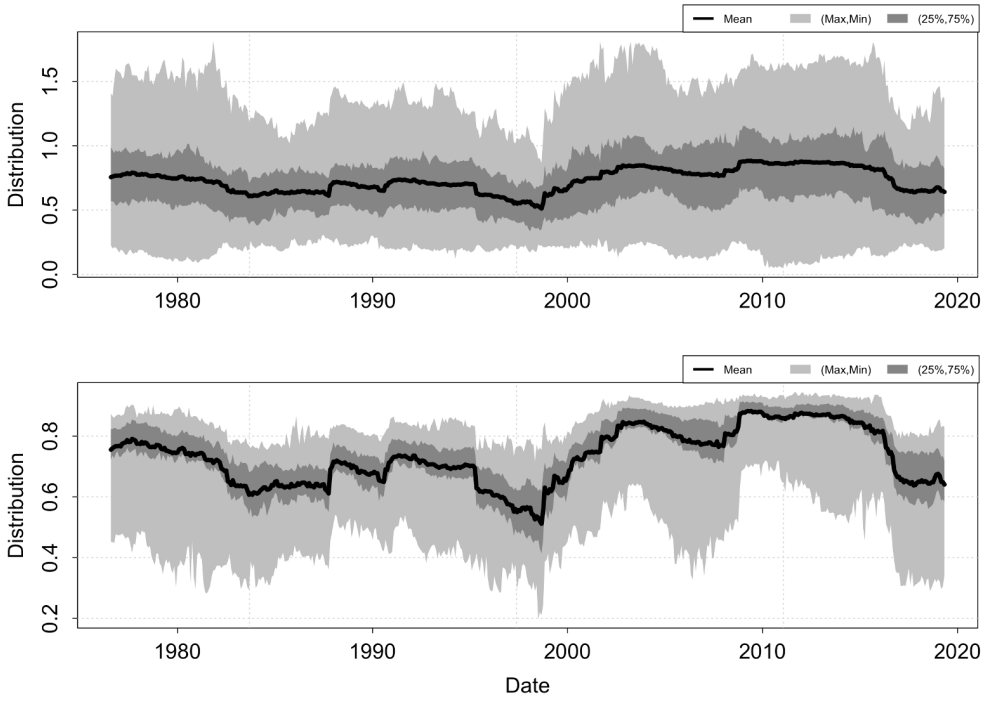


Figure 7. Cross-sectional distribution of systemic risk measurements. This figure shows the cross-sectional distribution for Outdegree and Indegree. The bold line represents the cross-sectional mean, while the shaded areas indicate the minimum/maximum and 25th/75th percentiles. The first panel displays the distribution of industry-level Outdegree, and the second panel shows the distribution of industry-level Indegree.

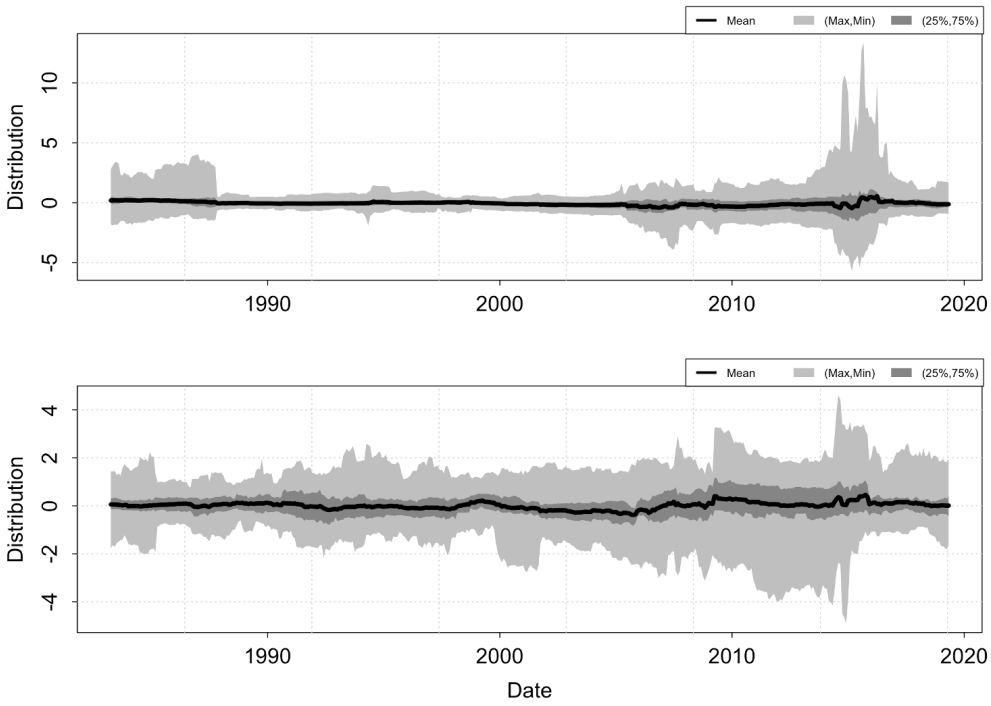


Figure 8. Cross-sectional distribution of beta measurements. This figure shows the cross-sectional distribution for *INT*-beta and *DOM*-beta. The bold line represents the cross-sectional mean, while the shaded areas indicate the minimum/maximum and 25th/75th percentiles. The first panel displays the distribution of industry-level *INT*-beta, and the second panel shows the distribution of industry-level *DOM*-beta.

During crisis periods, the Outdegree distribution exhibits slight right-skewness, while the Indegree distribution shows slight left-skewness. This suggests that some industries are transmitting more risk than they are receiving. However, the variation in Outdegree and Indegree is relatively small, as indicated by the limited range on the y-axis.

In contrast, the beta distributions show significantly larger variations. The *INT*-beta ranges from -5 to +10, while the *DOM*-beta ranges from -4 to +4. During 2008, the *INT*-beta exhibits slight left-skewness, indicating that many sectors had negative exposures to the *INT* factor. Since stocks with greater exposure to *INT* earn a lower risk premium, this suggests that many sectors were riskier and demanded higher returns during the crisis. Additionally, the *INT*-beta shows even larger variation in 2015, coinciding with the emergence of innovation and AI. During this period, firms faced challenges and were not fully prepared to absorb the new shocks, making them more sensitive to the *Risk-Intensity* factor. This new AI-driven phase is captured by the factor beta but not by the

traditional Outdegree and Indegree measurements. The *DOM*-beta is slightly left-skewed during 2008, indicating that many sectors had increased exposure to the *DOM* factor. Since stocks more exposed to *DOM* earn a higher risk premium, this suggests that many sectors demanded higher returns during 2008.

I further examine the correlations among the four measures. Specifically, I compute two sets of correlations: (1) the cross-sectional means of Outdegree, Indegree, and factor betas; and (2) the cross-sectional standard deviations of Outdegree, Indegree, and factor betas.

Correlation between systemic risk measurements

Cross-sectional Mean					Cross-sectional Std				
	Outdegree	Indegree	INT	DOM		Outdegree	Indegree	INT	DOM
Outdegree	1.00	0.63^{***}	-0.37^{***}	0.74^{***}	Outdegree	1.00	-0.48^{***}	0.54^{***}	0.42^{***}
Indegree	0.63^{***}	1.00	-0.57^{***}	0.74^{***}	Indegree	-0.48^{***}	1.00	-0.32^{***}	-0.49^{***}
INT	-0.37^{***}	-0.57^{***}	1.00	-0.30^{***}	INT	0.54^{***}	-0.32^{***}	1.00	0.67^{***}
DOM	0.74^{***}	0.74^{***}	-0.30^{***}	1.00	DOM	0.42^{***}	-0.49^{***}	0.67^{***}	1.00

Table 17. Correlation between four measurements.

Based on Table 17, Outdegree, Indegree, and the two factor betas are significantly correlated with one another in terms of both cross-sectional mean and cross-sectional standard deviation. This suggests that factor exposures can serve as alternative measures of systemic risk.

D.2 Other Mechanisms Behind the Network Dynamics

In this paper, the dynamics of network factors are taken as given, and the focus is on exploring their corresponding implications. However, we briefly discuss potential mechanisms driving these dynamics in each period, although a detailed investigation lies outside the scope of this paper.

The *INT* Factor:

- **1981-1982:** The Federal Reserve implemented aggressive monetary tightening, eliciting varied responses from firms. Companies with higher leverage or interest-rate-sensitive business

models experienced increased firm-specific risks, leading to higher idiosyncratic volatility. Additionally, stagflation (high inflation combined with stagnating economic growth) disproportionately affected certain industries.

- **1990-1991:** A broad-based economic contraction and credit crunch occurred following the Gulf War and rising oil prices. This led to more synchronized firm behavior, exposing companies to macro factors and aggregate shocks, which diminished firm-specific risks.
- **1995-1998:** The rise of the internet and tech industries prompted many firms to adapt to new technologies and business models, creating a more heterogeneous environment and increasing firm-specific volatility. The late 1990s marked the beginning of the dot-com bubble, with speculative investment driving volatility in specific firms, particularly new, high-growth tech companies.
- **Around 2000:** Firms began to gain more market power, partially due to reduced product concentration and broader product ranges.
- **Around 2008:** The broad economic contraction led firms to become more exposed to aggregate shocks, reducing the prominence of idiosyncratic risks. Alternatively, this may be attributed to shifts in consumption preferences. During prosperous times, investors focus on consuming products from central sectors (such as financial sectors), while consuming less from peripheral sectors like transportation. In economic downturns, spending becomes more cautious, with a focus on necessary goods across all sectors. This shift in preferences may mitigate adverse conditions in peripheral sectors, potentially explaining the drop in the *INT* factor and the simultaneous decrease in the *DOM* degree during the 2008 recession.
- **2016:** The *INT* factor rose again, likely due to several factors. Heightened globalization, increasing trade tensions, and protectionist policies disrupted trade dynamics, making it harder for firms to diversify away from product-specific shocks. Rapid technological advancements also likely diminished the effectiveness of prior diversification strategies. Additionally, growing digitization introduced new risks, such as cybersecurity threats, which affect multiple sectors simultaneously.

The *DOM* Factor:

- This factor is highly procyclical, with a 0.15 correlation with the P/D ratio, and drops during every recession period. Intuitively, during normal times, sectors like intermediary and manufacturing dominate risk spillover. However, during recessions, peripheral sectors experience poor health, becoming ineligible for loans, leading to stronger risk spillover back to financial sectors. Consequently, the overall dominance degree within the economy decreases. Alternatively, this could be due to a shift in consumption patterns, where consumers redirect spending from products in central sectors to necessary goods across all sectors, including peripheral sectors like transportation, thus lowering the overall dominance degree.

D.3 Which Firms Are More Exposed to Network Factors?

Firms have time-varying factor exposures. One question arises: over the entire sample period, which firms are more exposed to network factors? Do these firms cluster within specific sectors, or are they spread across the broader market?

Table 18 lists the top 30 firms with the highest average exposure to the factors. The data shows that these firms are not confined to any particular industry. This observation emphasizes that network factors are shaped by the entire economy, rather than being driven by specific sectors.

	DOM	INT
1	Wholesale	Apparel
2	Apparel	Electrical Equipment
3	Defense	Business Services
4	Retail	Agriculture
5	Automobiles and Trucks	Construction Materials
6	Steel Works Etc	Business Services
7	Trading	Retail
8	Retail	Aircraft
9	Transportation	Business Supplies
10	Retail	Computers
11	Machinery	Agriculture
12	Petroleum and Natural Gas	Insurance
13	Consumer Goods	Banking
14	Petroleum and Natural Gas	Steel Works Etc
15	Chemicals	Banking
16	Personal Services	Retail
17	Chemicals	Restaurants, Hotels, Motels
18	Insurance	Apparel
19	Aircraft	Printing and Publishing
20	Automobiles and Trucks	Aircraft
21	Chemicals	Business Supplies
22	Electrical Equipment	Consumer Goods
23	Steel Works Etc	Wholesale
24	Business Services	Electronic Equipment
25	Electronic Equipment	Trading
26	Steel Works Etc	Coal
27	Electrical Equipment	Utilities
28	Business Supplies	Construction
29	Machinery	Construction Materials
30	Electronic Equipment	Coal

Table 18. Top 30 exposures to the network factors.

D.4 The Role of Intermediary Sectors

From the static plot, it is evident that financial sectors play a central role in the network structure. One might wonder whether the results would still hold if the financial sectors were excluded. The answer is affirmative; the results are not solely driven by the intermediary sectors. I excluded the financial sectors (banking, trading, and insurance) and presented the sorting portfolio results.

Value-weighted														
	INT							DOM						
	1	2	3	H-L	t	grs stat	grs p	1	2	3	H-L	t	grs stat	grs p
Ave.Exc.Ret	0.131	0.102	0.093	-0.038	-2.331			0.092	0.105	0.129	0.037	2.215		
volatility	0.164	0.138	0.161	0.093				0.155	0.138	0.171	0.094			
Sharpe ratio	0.799	0.734	0.577	-0.414				0.595	0.758	0.755	0.393			
α_{CAPM}	0.005	0.003	0.002	-0.003	-2.189	4.791	0.029	0.002	0.003	0.004	0.002	1.777	3.156	0.076
α_{FF3}	0.004	0.002	0.000	-0.003	-2.394	5.730	0.017	0.001	0.002	0.003	0.002	1.651	2.726	0.100
$\alpha_{4factor}$	0.004	0.002	0.001	-0.004	-2.677	7.168	0.008	0.001	0.002	0.004	0.003	2.290	5.245	0.023
$\alpha_{5factor}$	0.004	0.002	0.001	-0.003	-2.399	5.755	0.017	0.001	0.002	0.004	0.003	2.197	4.829	0.029

Table 19. Single Sorted Portfolios by excluding intermediary sectors.

In the table 19, the H-L return spreads for both both factors drop a little but they are still significant. The H-L α for both factors are still not explained by the factor models (at 0.1 significance for *DOM* Factor and at 0.05 significance for *INT* Factor), indicating our results are not solely driven by the intermediary sectors, but by all sectors.[56]

D.5 Time Series Plots of Representative Sectors

I plot the production-based outdegree, indegree, and netdegree for several representative sectors. It is evident that during financial crises, sectors such as Insurance and Trading exert substantial influence on the rest of the economy. Additionally, the Computers sector has been increasingly influential in recent years. Interestingly, the Precious Metals sector neither spread nor received significant shocks during the 2008 crisis. This aligns with the notion of gold as a 'safe haven' during the 2008 financial crisis. While gold initially fell during the initial shock of the crisis, unlike the S&P which continued to decline, gold rebounded and ended the year up 5.5 percent. Over the total 18-month stock market selloff, gold rose more than 25 percent.

[56]This is the reason why I consider a production-based multi-sector model instead of an intermediary model in the model section.

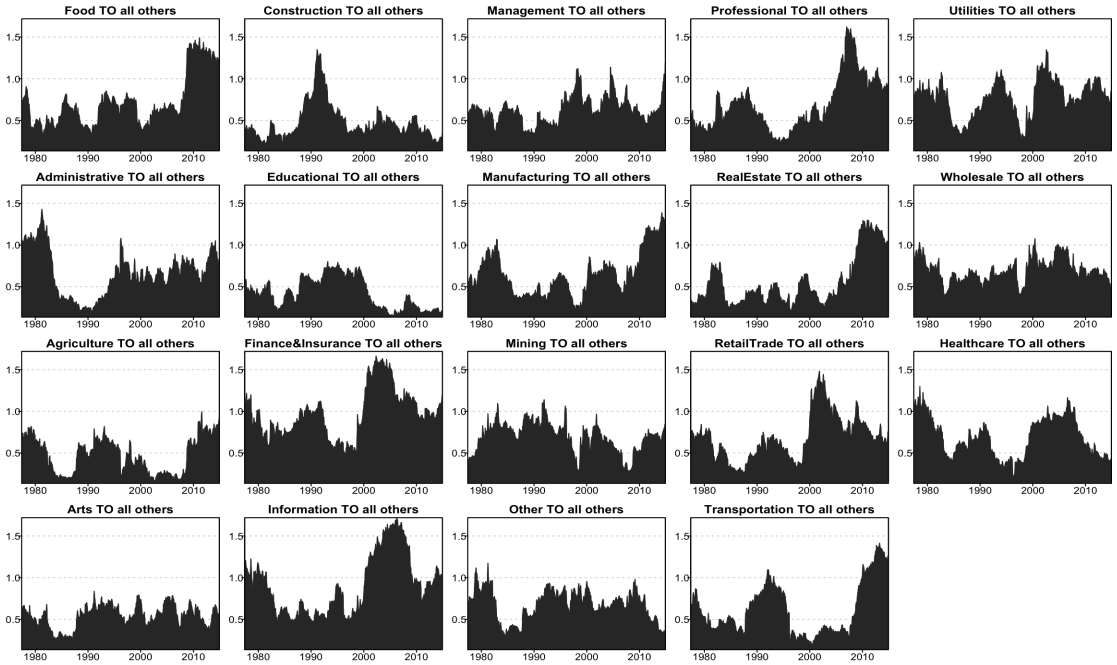


Figure 9. Time series of outdegree

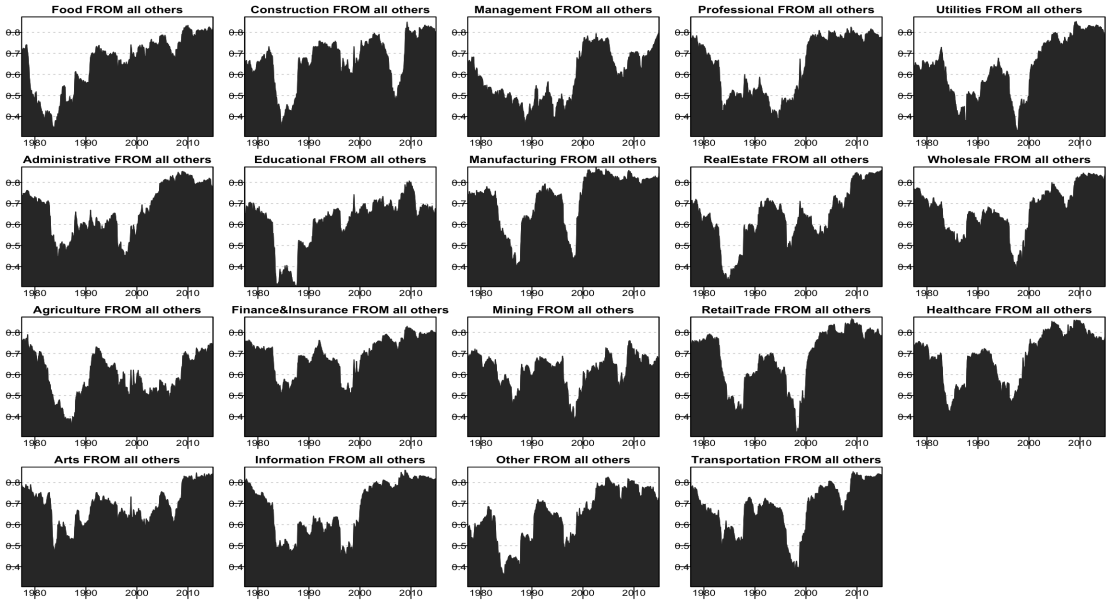


Figure 10. Time series of indegree

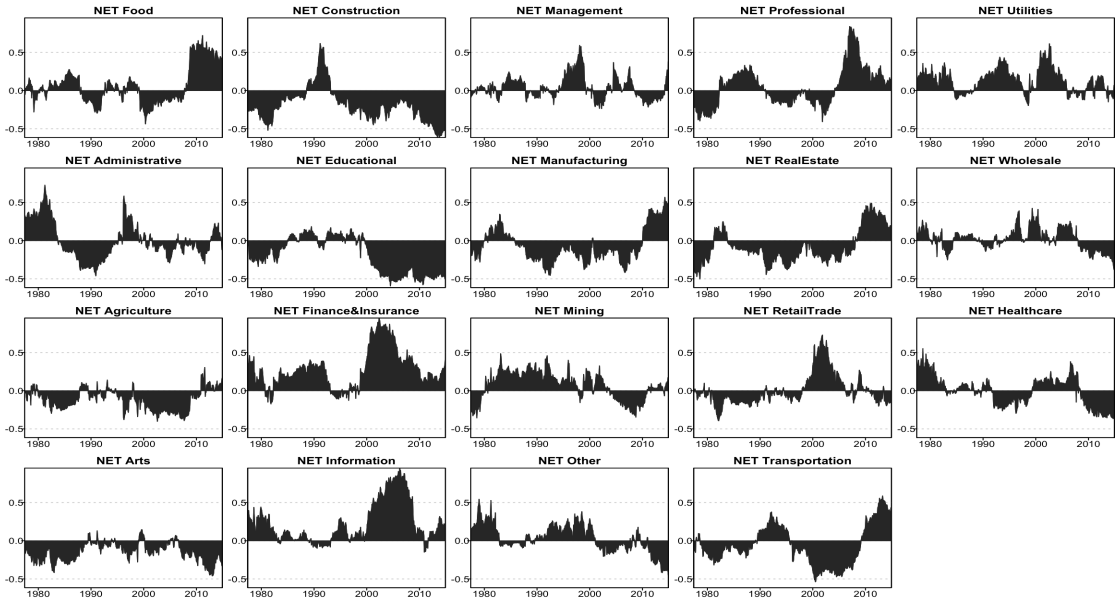


Figure 11. Time series of netdegree

D.6 Return-based and Volatility-based Network Factors

To justify why the volatility-based network is more insightful than the well-known return-based network, I compare the portfolio sorting results of return spillover factors with those of volatility spillover factors.

In this subsection, I directly construct the *DOM* and *INT* factors for the idiosyncratic return spillover network, as opposed to the idiosyncratic volatility spillover network.[57]

[57] I construct the idiosyncratic return matrix for FF48 industries and redo every step in the benchmark (i.e., rolling window GVD of the forecasting error) to construct the two network factors.

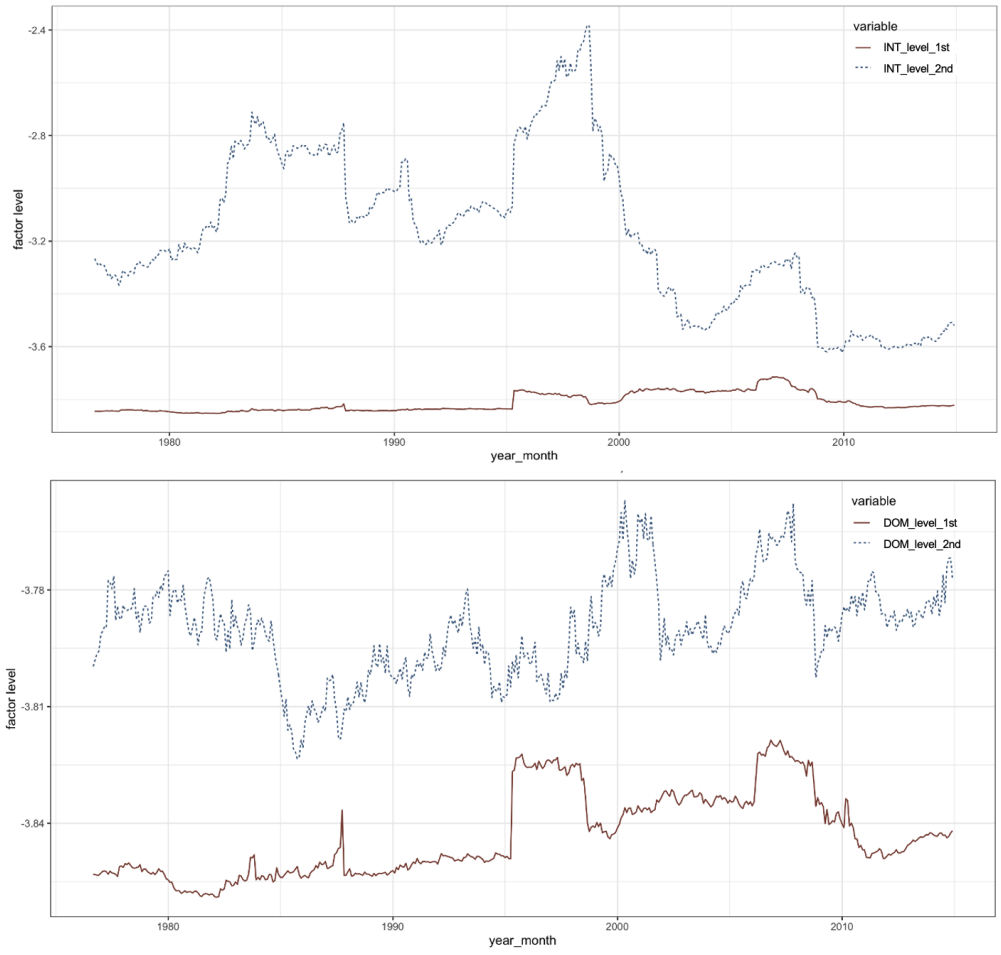


Figure 12. Time series plots of the return spillover and the volatility spillover network factors. The first panel plots both INT factors in level, with the red line denoting the return-based case and the blue line denoting the volatility-based case. The second panel plots both DOM factors in level.

Value-weighted portfolio for return spillover network factors														
	INT							DOM						
	1	2	3	H-L	t	grs stat	grs p	1	2	3	H-L	t	grs stat	grs p
Ave.Exc.Ret	0.103	0.102	0.121	0.018				0.113	0.101	0.112	-0.001			
volatility	0.162	0.141	0.163	0.098				0.163	0.142	0.164	0.107			
Sharpe ratio	0.636	0.726	0.742	0.186				0.693	0.714	0.682	-0.005			
α_{CAPM}	0.003	0.003	0.004	0.001	0.965	0.931	0.335	0.002	0.003	0.003	0.001	-0.043	0.002	0.966
α_{FF3}	0.001	0.002	0.003	0.001	0.996	0.992	0.320	0.002	0.001	0.002	0.000	-0.034	0.001	0.973
$\alpha_{4factor}$	0.002	0.002	0.003	0.001	0.750	0.563	0.454	0.002	0.002	0.003	0.001	0.237	0.056	0.813
$\alpha_{5factor}$	0.002	0.002	0.003	0.001	0.707	0.500	0.480	0.002	0.002	0.003	0.001	0.381	0.145	0.704

Table 20. Single Sorted Portfolios for return spillover factors.

From Figure 12, I observe that the two *INT* factors and the two *DOM* factors are not significantly correlated with each other. The *INT* and *DOM* factors derived from the volatility-based network exhibit much larger variations compared to those from the return-based network. I also sort portfolios using the return-based factors.

From Table 20, it is evident that the *INT* and *DOM* factors from the return-based network are fully explained by the CAPM. This is not surprising, as *INT* reflects the average magnitude of return comovement, which should be proportional to the market return. Additionally, as noted by Ahern (2013), in return connections, stocks in more central industries (higher DOM beta) exhibit greater market risk due to their increased exposure to sectoral shocks that propagate through intersectoral trade. Consequently, the *DOM* and *INT* factors from return connections do not appear to be as insightful as those derived from volatility connections.

E Additional Conceptual Demonstration

E.1 Why Use Negative Entropy to Measure Dominance?

In the field of information theory, the notion of "Negative Entropy" is employed to measure the degree of dominance within a network graph. A substantial body of research, including works by Bianconi (2007), Bianconi (2009) and Robert (1990), has demonstrated that a network's entropy

negatively correlates (i.e. negative entropy positively correlates) with the information content inherent in its defining constraints.

For instance, networks with Poisson degree distributions are known to possess higher entropy levels compared to scale-free networks, which adhere to power-law degree distributions. The latter typically exhibit a higher degree of dominance, characterized by a small number of nodes with significantly high degrees, while the majority of nodes have lower degrees (see Figure 13).

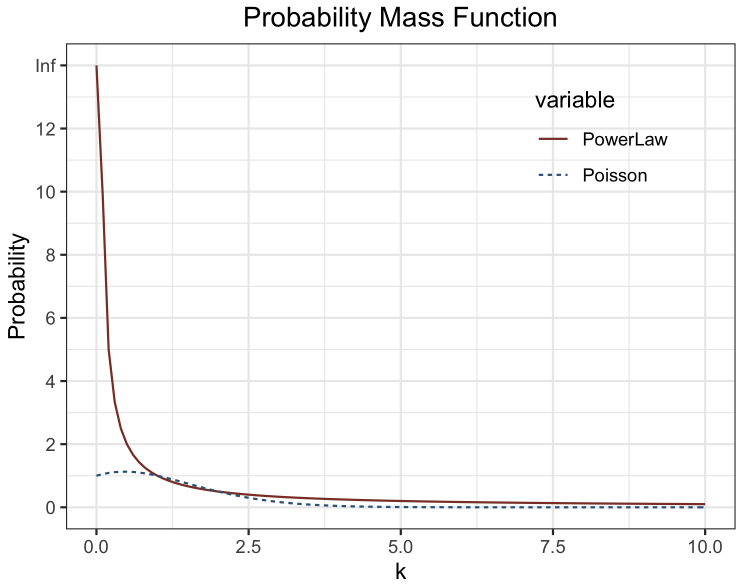


Figure 13. Degree Distribution under Poisson or Power-law.

To offer a more intuitive explanation, it is recognized that higher entropy signifies increased complexity, which can be interpreted as the challenge a Turing Machine faces in replicating a graph given specific properties such as node count and edge numbers. Within the context of network graphs, an increase in complexity implies a reduction in dominance. This principle can be illustrated through comparative figures.

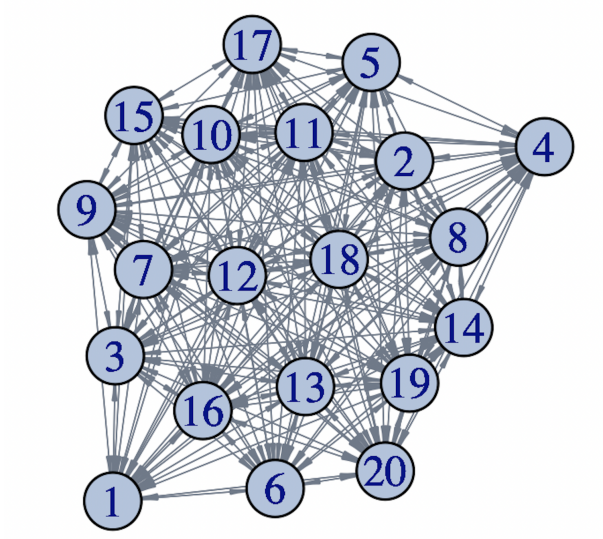


Figure 14. low Concentration

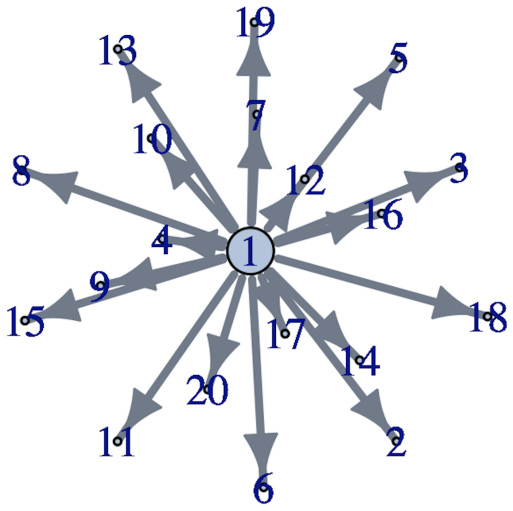


Figure 15. high Concentration

Consider a figure on the left with a total of 20 nodes, where each node holds equal importance, and every directed edge plays a crucial role in the network's structure. For a Turing Machine to replicate this network, it would need to simulate C_{20}^2 paths to identify a structure that closely resembles the figure on the left. Consequently, this figure is characterized by high complexity and negligible dominance. Conversely, the figure on the right depicts a scenario where only node 1 exerts influence over the remaining 19 nodes, with no additional edges present. This configuration is inherently simpler for reproduction, indicating lower complexity and higher dominance. Therefore, higher "negative entropy" captures higher dominance.

E.2 Difference Between Input-Output Matrix and Volatility Spillover Matrix

I demonstrate that this second-moment network exhibits a different structure when extended from the input-output network. At each time point t, the production-based network, denoted as $W = [\omega_{ij}]$, is determined exogenously. However, the idiosyncratic volatility spillover exists for the period from t to $t+1$ and is established after reaching equilibrium. This spillover network, represented by $\Delta = [\delta_{ij}]$, where δ_{ij} is a function of ω_{ij}, displays a distinct weight structure. For instance, consider at time t, sector 1 integrates 30% of goods from sector 2, 60% from sector 3, and 10% of its own goods into its production process. The production-based network at t is illustrated by $[0.1, 0.3, 0.6]$. As derived from the model (Equation (18)), the spillover network from t to $t+1$ is

characterized by:

$$[0.1, 0.3, 0.6] \xrightarrow{\text{apply function}} [(1+0.1)^2, 0.3^2, 0.6^2]$$
$$\xrightarrow{\text{normalize}} [0.73, 0.05, 0.22]$$

The term ω_{ij}^2, derived from the second moment, accentuates the disparity between critical and less critical suppliers. Particularly noteworthy is the addition of 1 in the diagonal ($(1+\omega_{ii})^2$). Given that ω_{ij} ranges between 0 and 1, this addition significantly alters the network's structure. This adjustment stems from the identity matrix in the Leontief inverse, representing the inherent demand from the representative household. In particular, the idiosyncratic shock to sector i impacts the production of good i and directly affects the household's consumption of good i. Should this shock transmit downstream to sector j, it directly affects the household's consumption of good j, and so on. Therefore, beyond trade-based transmission, the idiosyncratic shock of sector i affects total consumption and output through the household's direct demands, thereby creating a feedback loop on itself.

E.3 Channels for Idiosyncratic Volatility Spillover

In addition to the production-based relationship, there are several complex mechanisms that may facilitate the spillover of idiosyncratic volatility. This subsection briefly explores other potential channels.

First, there is a trade credit channel. This mechanism is rooted in the supplier-customer relationships across sectors but extends beyond direct transactions. For instance, sectors might have accounts payable or receivable with their partners, leveraging strong historical relationships for advance borrowing. Idiosyncratic shocks to one sector could render these future payments unrealized, impacting the financial health of another sector.

Second, idiosyncratic shocks can propagate through the activities of common investors. If two sectors produce complementary goods and share a customer base, a negative idiosyncratic shock to one sector that diminishes product quality could adversely affect the sales of the other sector's products. Investors might also have an indirect influence on these sectors through their reactions to limited information and uncertainty regarding the independence of the shock.

Third, the asset channel facilitates the transmission of idiosyncratic industry shocks. An industry-specific shock can influence the stock returns within that industry, which in turn may affect the returns of other firms with investment portfolios in that industry's assets. Since industry

market returns are calculated as the value-weighted returns of firms, the performance of other industries can be indirectly impacted, highlighting a broader transmission mechanism.

Fourth, there is household (labor) channel. As noted by Herskovic et al. (2016), idiosyncratic shocks directly impact labor income. A negative shock to one sector can reduce its productivity and profitability, leading to lower wages for its employees. Consequently, employees facing reduced labor income and personal wealth are likely to decrease their consumption of goods from other sectors.

Lastly, there is also a feedback and contagion channel through distressed competition. According to Chen, Dou, Guo, and Ji (2023), here is an illustration figure (figure 16).

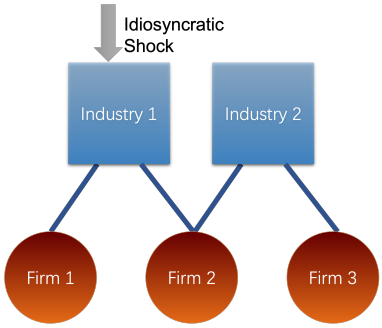


Figure 16. Feedback and contagion through distressed competition. This figure contains the possible idiosyncratic volatility spillover channel through feedback and contagion.

Consider a scenario where Firm 1 operates in Sector 1, Firm 2 in Sectors 1 and 2, and Firm 3 in Sector 3. An idiosyncratic shock to Sector 1 places Firm 1 under financial distress. This distress increases Firm 1's default probability, leading to a decrease in its willingness to collude and an increase in competitive aggression. This behavior results in reduced profit margins across all firms within the sector. Firm 2, facing these conditions, may engage in strategic competition, potentially lowering its profit margins to oust Firm 1 from the industry, especially if Sector 1 has high entry barriers. This strategy not only intensifies competition within Sector 1 but also in Sector 2, affecting Firm 3 by increasing its financial distress. Therefore, idiosyncratic shocks can propagate across sectors, with the transmission being more direct if Firm 2 is immediately impacted by a shock to Sector 1.

The five channels outlined above reveal the complexity of idiosyncratic volatility spillover mechanisms. This paper is motivated by the trade relationships to examine how idiosyncratic

volatility spillover dynamics affect the economy. In future researches, I also aim to individually explore these spillover channels.

Panel A: Average Excess Returns

		INT					DOM				
		1	2	3	H-L	t-stat	1	2	3	H-L	t-stat
1	trailing60	0.134	0.109	0.088	-0.046	-2.558	0.090	0.106	0.136	0.046	2.258
2	trailing70	0.140	0.107	0.094	-0.046	-2.562	0.096	0.109	0.136	0.040	2.166
3	trailing90	0.127	0.104	0.093	-0.033	-2.533	0.092	0.101	0.131	0.039	2.164
4	trailing95	0.129	0.107	0.101	-0.028	-2.388	0.094	0.106	0.137	0.043	2.230
5	trailing100	0.127	0.106	0.102	-0.025	-2.233	0.092	0.105	0.138	0.045	2.233
6	rolling80	0.133	0.111	0.110	-0.023	-2.232	0.100	0.112	0.142	0.042	2.226
7	rolling85	0.131	0.105	0.105	-0.036	-2.546	0.090	0.109	0.141	0.051	2.414
8	rolling95	0.126	0.099	0.096	-0.031	-2.565	0.090	0.100	0.132	0.042	2.173
9	rolling100	0.122	0.104	0.099	-0.024	-2.222	0.097	0.100	0.129	0.032	2.044
10	forecasting7	0.128	0.100	0.097	-0.032	-2.535	0.094	0.103	0.128	0.034	2.086
11	forecasting8	0.125	0.104	0.097	-0.029	-2.314	0.097	0.101	0.128	0.032	2.047
12	forecasting9	0.129	0.104	0.093	-0.036	-2.644	0.092	0.101	0.133	0.041	2.166
13	forecasting10	0.131	0.102	0.094	-0.037	-2.645	0.091	0.100	0.135	0.044	2.228

Panel B: α_{FF3}

		INT					DOM				
		1	2	3	H-L	t-stat	1	2	3	H-L	t-stat
1	trailing60	0.004	0.002	0.000	-0.004	-2.635	0.000	0.002	0.003	0.003	1.990
2	trailing70	0.004	0.002	0.000	-0.004	-2.986	0.001	0.002	0.003	0.002	1.989
3	trailing90	0.003	0.002	0.000	-0.003	-2.588	0.001	0.001	0.003	0.002	1.968
4	trailing95	0.003	0.002	0.000	-0.003	-2.245	0.001	0.002	0.003	0.003	1.963
5	trailing100	0.003	0.002	0.000	-0.003	-2.093	0.001	0.002	0.003	0.003	2.099
6	rolling80	0.003	0.002	0.001	-0.003	-1.967	0.000	0.002	0.004	0.004	2.658
7	rolling85	0.003	0.002	0.001	-0.003	-1.967	0.000	0.002	0.004	0.005	3.573
8	rolling95	0.003	0.002	0.001	-0.002	-2.047	0.000	0.001	0.004	0.003	2.311
9	rolling100	0.003	0.002	0.000	-0.003	-2.081	0.001	0.001	0.003	0.002	1.991
10	forecasting7	0.003	0.001	0.000	-0.003	-2.183	0.001	0.002	0.003	0.002	1.999
11	forecasting8	0.003	0.002	0.000	-0.003	-1.968	0.001	0.001	0.003	0.002	2.064
12	forecasting9	0.004	0.002	0.000	-0.004	-2.486	0.001	0.001	0.003	0.002	2.001
13	forecasting10	0.004	0.002	0.000	-0.004	-2.484	0.001	0.001	0.003	0.003	2.103

Panel C: $\alpha_{4factor}$

		INT					DOM				
		1	2	3	H-L	t-stat	1	2	3	H-L	t-stat
1	trailing60	0.005	0.003	0.000	-0.005	-3.127	0.001	0.002	0.005	0.004	2.436
2	trailing70	0.005	0.002	0.000	-0.005	-3.311	0.001	0.002	0.004	0.003	1.947
3	trailing90	0.004	0.002	0.000	-0.004	-2.978	0.001	0.002	0.004	0.003	2.053
4	trailing95	0.004	0.002	0.001	-0.003	-2.628	0.001	0.002	0.004	0.003	2.319
5	trailing100	0.004	0.002	0.001	-0.003	-2.459	0.001	0.002	0.004	0.003	2.459
6	rolling80	0.004	0.002	0.001	-0.002	-1.782	0.001	0.002	0.004	0.003	2.413
7	rolling85	0.004	0.002	0.001	-0.004	-2.467	0.000	0.002	0.005	0.005	3.619
8	rolling95	0.004	0.002	0.001	-0.003	-2.271	0.001	0.002	0.004	0.003	2.053
9	rolling100	0.004	0.002	0.001	-0.003	-2.289	0.001	0.002	0.004	0.003	2.196
10	forecasting7	0.005	0.002	0.001	-0.004	-2.686	0.001	0.002	0.004	0.003	2.376
11	forecasting8	0.004	0.002	0.001	-0.003	-2.386	0.002	0.002	0.004	0.002	2.032
12	forecasting9	0.005	0.002	0.000	-0.004	-3.033	0.001	0.002	0.004	0.003	1.989
13	forecasting10	0.005	0.002	0.001	-0.004	-2.759	0.001	0.002	0.005	0.004	2.544

Panel D: $\alpha_{5factor}$

		INT					DOM				
		1	2	3	H-L	t-stat	1	2	3	H-L	t-stat
1	trailing60	0.005	0.003	0.000	-0.005	-2.996	0.001	0.002	0.005	0.004	2.631
2	trailing70	0.005	0.002	0.000	-0.005	-3.122	0.001	0.002	0.004	0.003	2.106
3	trailing90	0.004	0.002	0.001	-0.004	-2.749	0.001	0.002	0.004	0.003	2.100
4	trailing95	0.004	0.002	0.001	-0.003	-2.409	0.001	0.002	0.004	0.003	2.351
5	trailing100	0.004	0.002	0.001	-0.003	-2.232	0.001	0.002	0.004	0.003	2.444
6	rolling80	0.004	0.002	0.002	-0.002	-1.719	0.001	0.002	0.005	0.004	2.478
7	rolling85	0.004	0.002	0.001	-0.003	-2.182	0.000	0.002	0.005	0.005	3.759
8	rolling95	0.004	0.002	0.001	-0.003	-2.049	0.001	0.002	0.004	0.003	2.170
9	rolling100	0.004	0.002	0.001	-0.003	-2.064	0.001	0.002	0.004	0.003	2.026
10	forecasting7	0.004	0.002	0.001	-0.003	-2.389	0.001	0.002	0.004	0.003	2.280
11	forecasting8	0.004	0.002	0.001	-0.003	-2.162	0.002	0.002	0.004	0.002	2.076
12	forecasting9	0.004	0.002	0.001	-0.004	-2.758	0.001	0.002	0.004	0.003	2.164
13	forecasting10	0.004	0.002	0.001	-0.004	-2.496	0.001	0.002	0.005	0.004	2.544

Table 16. Single sorted portfolios under different parameter choices.